ADDIS ABABA UNIVERSITY

COLLEGE OF NATURAL SCIENCES

SCHOOL OF EARTH SCIENCES

PALEOMAGNETIC INVESTIGATION OF SAHA AND SURROUNDING AREA VOLCANIC ROCKS, CENTRAL AFAR, NORTHEAST ETHIOPIA

Thesis submitted to School of Graduate studies of Addis Ababa University in Partial fulfillment for the requirements of the Degree of Master of Science in Earth Sciences (Structural Geology).

By: Temesgen Kendie

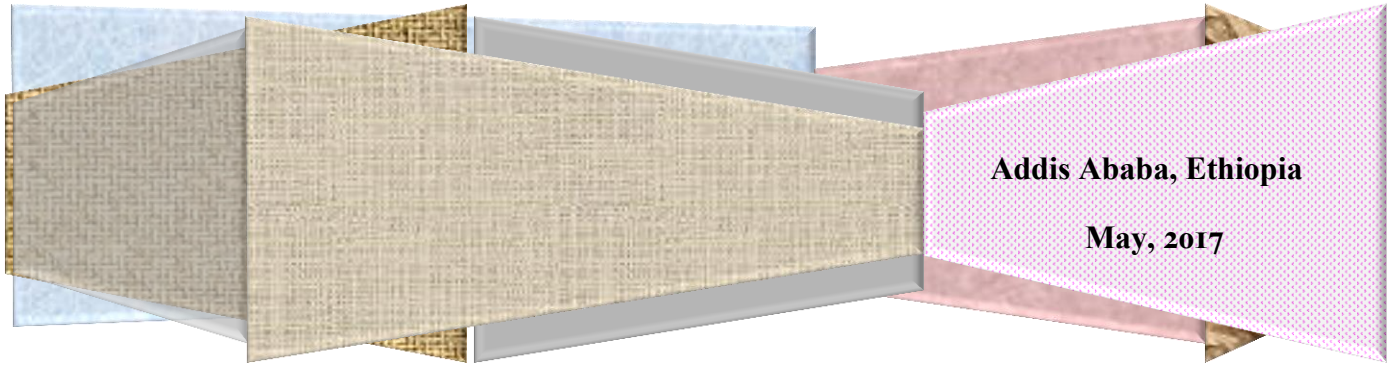

Addis Ababa University
School of Graduate Studies

This is to certify that the thesis prepared by **Temesgen Kendie**, entitled: *Paleomagnetic investigation of Saha and surrounding area Volcanic Rocks, Central Afar (Northeast Ethiopia)* and submitted in partial fulfillment of the requirement for the Degree of Master of Science (Structural Geology) complies with the regulations of the University and meets the accepted standards with respect to originality and quality.

Signed by the Examining Committee:

Examiner _____ Signature _____ Date _____

Examiner _____ Signature _____ Date _____

Advisor Prof. Tesfaye Kidane Signature _____ Date _____

Co-Advisor Dr. Ameha Atnafu Signature _____ Date _____

ABSTRACT

The paleomagnetic investigation was located in the area of Saha and surrounding area, central Afar. The paleomagnetic samples were collected from nine lava flow unit outcrop of basalt (Gulf basalt) which exposed Saha and surrounding area (Central Afar). Five to nine samples were collected from each lava flow. The specimens conducted to partial demagnetize by using Alternating field (AF) and Thermal (TH) demagnetization techniques, as well as magnetize by Impulse magnetizer techniques (IM). The paleomagnetic results were measured by using JR-6ASpinner Magnetometer from School of Earth Science paleomanetic laboratory in Addis Ababa University. The Natural Remenant magnetization (NRM) direction explains the specimens which display components of magnetizations were low stability component (secondary NRM) was removed by AF about 10mT- 30mT, by heating about 120°C- 300°C were as high stability components (primary NRM or characteristic remenant magnetization) above these steps and the vector straight line is directed towards the origin from orthogonal vector diagrams. The results of magnetization curve plots for magnetic rock analysis shows that magnetic mineralogy dominated by Ti- poor titanomagnetite, magnetite and few presence of maghemite. Principal component analysis and site mean direction calculated from both normal and reverse polarities. An overall mean direction was calculated from 9 individual site mean, the result obtained: D= 352.5°, I= 12.5°, K= 13.2, $\alpha 95$=14.7°, N= 9 and comparison with expected Geomagnetic Axial Dipole based on Apparent Polar Wander Path curve for 1Ma Mile- Gewane Ali Sabieh, (Kidane et al.,2003), as stable Africa plate Besse and Courtillot (2002). The mean paleomagnetic pole was calculated from the combined individual VGP, λ= 80.9°., ϕ =277.8°. , K = 22.8, $\alpha 95$ =11°. The declination difference which explains rotation of blocks about vertical axis was: =-7.2 ±6.6; difference in inclination was: = 3.9±3.2 obtained. This declination difference explains counter clock wise rotation about vertical axis due to the young propagation rift.

Contents **page**

List of figures

List of Plates

List of Tables

List of abbreviations

AD= Afar Depression

AF= Alternating Field

APWP= Apparent Polar Wander Path

ChRM= Characteristics Remnant Magnetization

D= Declination

EARS= East African Rift System

F=Flatting

GATZ= Gamarri–Alol Tear Zone

I= Inclination

IRM= Induced Remnant Magnetization

MAD= Maximum Angular Deviation

MD= Multi Domain

MER= Main Ethiopian Rift

MH =Manda Hararo

NRM= Natural Remnant Magnetization

PCA= Principal Component Analysis

R= Rotation

SD= Single Domain

SES = Shukra -el Sheik

TRM= Thermal Remnant Magnetization

VGP= Virtual Geomagnetic Polarity

VRM= Viscous Remnant Magnetization

1.0. INTRODUCTION

1.1. Tectonics Setting

Rifting between Africa and Arabia during the past ~30 Myr produced the ~300-km-wide Afar depression. The triple junction between the Red Sea, Gulf of Aden, and East African rifts (Figure. 1). The extensional developed within flood basalt province associated in the Afar plume (Schilling *et al.* 1992; Hofman *et al.* 1997).

These Depression (AD) considered as a triple rift junction that intersect both Gulf of Aden and Red Sea oceanic ridges described as East African continental rift (EAR) Audin (1999).

According to d'Acremont et al., (2010); Leroy et al., (2012) Oceanic spreading in the Gulf of Aden started around 18 Ma. Somalia and Nubia started to divergence around 11 Ma during the formation of a triple junction and opening of the MER (Wolfenden et al., 2004; Corti, 2009).

Rifting within the Red Sea and Gulf of Aden arms of the triple junction has progressed to oceanic spreading (Manighetti et al.1998), whereas the Main Ethiopian Rift (MER) is transitional from continental rifting to oceanic seafloor spreading (Hayward & Ebinger 1996). The Crustal thickness afar depression 18 km in the north to 24 km in the south (Berckhemer et al. 1975; Tiberi et al. 2005; Stuart et al. 2006). In the Afar, there has been a transition from extension by crustal-scale detachment faults to magma intrusion and minor faulting in the upper crust and magma injection zones. Within the southern Red Sea Rift and Afar, the initial development of border faults was roughly coincident with the 31–29 Ma flood basalt (Wolfenden et al. 2005). Strain transferred rift ward from 19 to 12 Ma (Wolfenden et al. 2005), and by ~5 Ma, an oceanic spreading ridge had developed in the south central Red Sea rift (Cochran 1983). Southward propagation of the ridge isolated the Danakil block between a truly oceanic rift branch to the northeast and a sub aerial rift zone to the southwest in the Afar depression. The southern Red Sea rift formed faulting and volcanism at around 3Ma (Barberi & Varet 1977).Both the Gulf Aden and red sea propagators reached the triple junction (20Ma; Courtillot et.al.1987), therefore, afar depression started to open. It seems two continental micro plates, Denkile and Ali Sabieh blocks were isolated and that the depressions start to stretch as these blocks begin rotating.

The Red Sea Ridge is propagating southeast towards the Afar depression (Courtillot et al., 1999) and developed the western boundary of an overlap zone and the Gulf of Aden rift is propagating

towards northwest (Courtillot et al., 1980; Manighetti, 1993). These two rift propagations developed dextral shear in the overlap zone and accommodated by bookshelf-style rotation as well as left lateral shear of NW-SE oriented blocks (Acton et al., 1991; Manighetti, 1993; Sigmundsson, 1992; Tapponnier et al., 1990). The details of the strain history of the blocks within the overlap zone based on vertical axis rotation are transient and the blocks (Manighetti et al., 2001). Bookshelf faults are distributed on northwest-southest striking normal faults between overlapping and active volcanic rifts (Manda Inakir-Asal and Manda Hararo Goba'ad rifts (Tapponnier et al., 990; Acton et al., 1991) respectively.

The central Afar has been dominated by a bookshelf faulting tectonic regime (2Ma) (Figure. 1; Tapponnier et al. 1990). Gulf of Aden rift has migrated inland along the western edge of the Danakil block and propagated towards north (Figure. 1). Towards the south terminate to Red Sea ridge system, defined at the Manda-Hararo rift (Figure. 1), towards the south propagated along western edge of the Afar depression arrived Ethiopian escarpment (Lahitte et al. 2003). These tectonic setting formed large overlap (Figure. 1; Courtillot et al. 1984; Manighetti et al. 2001; Kidane et al. 2003).

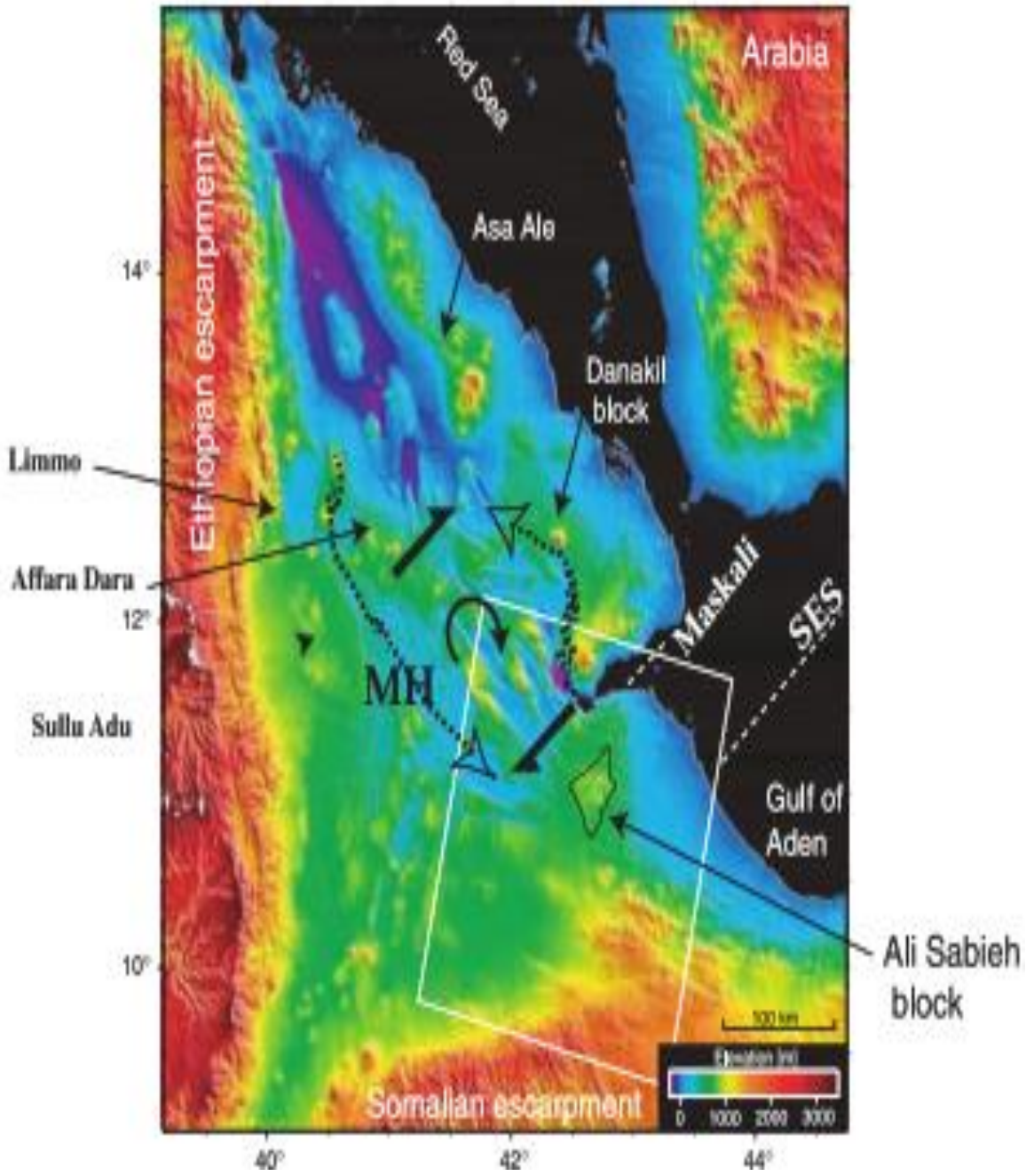

Figure 1.1.The Danakil and Ali Sabieh blocks show higher altitudes than the rest of the depression on this topographic map. The black arrows shear on the overlap zone (Tapponnier et al. 1990) Shukra -el Sheik discontinuity (SES), Manda Hararo rift zone (MH).

The two parts of the overlap are separated from each other by the Gamarri-Alol tear zone and northern extension of the East African rift (Figure 1. 2).

Strain migrate between the two rifts zones of Arabian and African plates, describes dextral shear, repose clockwise rotations of the northwest-southeast orientation. The normal faults bounding these crustal blocks activated with a significant component sinisterly shear (Manighetti, 1993 and Manighetti et al., 2001) and the quantitative values of block rotations (14° ± 7°; Courtillot et al., 1984) from overlap.

The overlap size is changed with time and propagation of the rifts: thus two distinct phases of deformation within two sequential overlaps separated by the Gamarri–Alol tear zone (GATZ) have been determined that record cause several block rotations (Acton et al., 2000; Kidane et al., 2003; Manighetti et al., 2001). The quantifying block rotations in this explained by Courtillot et al. (1984) measured result was 13°–17° by using paleomagnetic technique in the southeastern part of the overlap (first phase overlap). Further follow up work largely confirmed by paleomagnetic technique (Manighetti, 1993) and indicated small crustal block rotation 2°–3° in the northwestern overlap (second phase overlap) (Acton et al., 1991; Kidane et al., 1999, 2003; Manighetti, 1993) but, no rotation outside the overlap zone (Kidane et al., 2003).

The Afar depression is best field laboratories where the early stages of continental breakup and studied seafloor spreading in the field. The Gulf of Aden rift (Courtillot, 1980, 1982; Courtillot et al., 1980, 1987), and the finding that rather large block rotations due to rift propagation could be developed New paleomagnetic results (Kidane et al., 2003 describe that blocks surrounding the Galafi–Kadda Hawli area have not rotated significantly 2.4° ± 8.0°; Galafi–Kadda Hawli area, -1.3°± 7.8°) rotated clockwise (Data-Yager block, 10.0°± 8.3°) this quantitative interpretation by using measured paleomagnetic data (Courtillot et al., 1984).

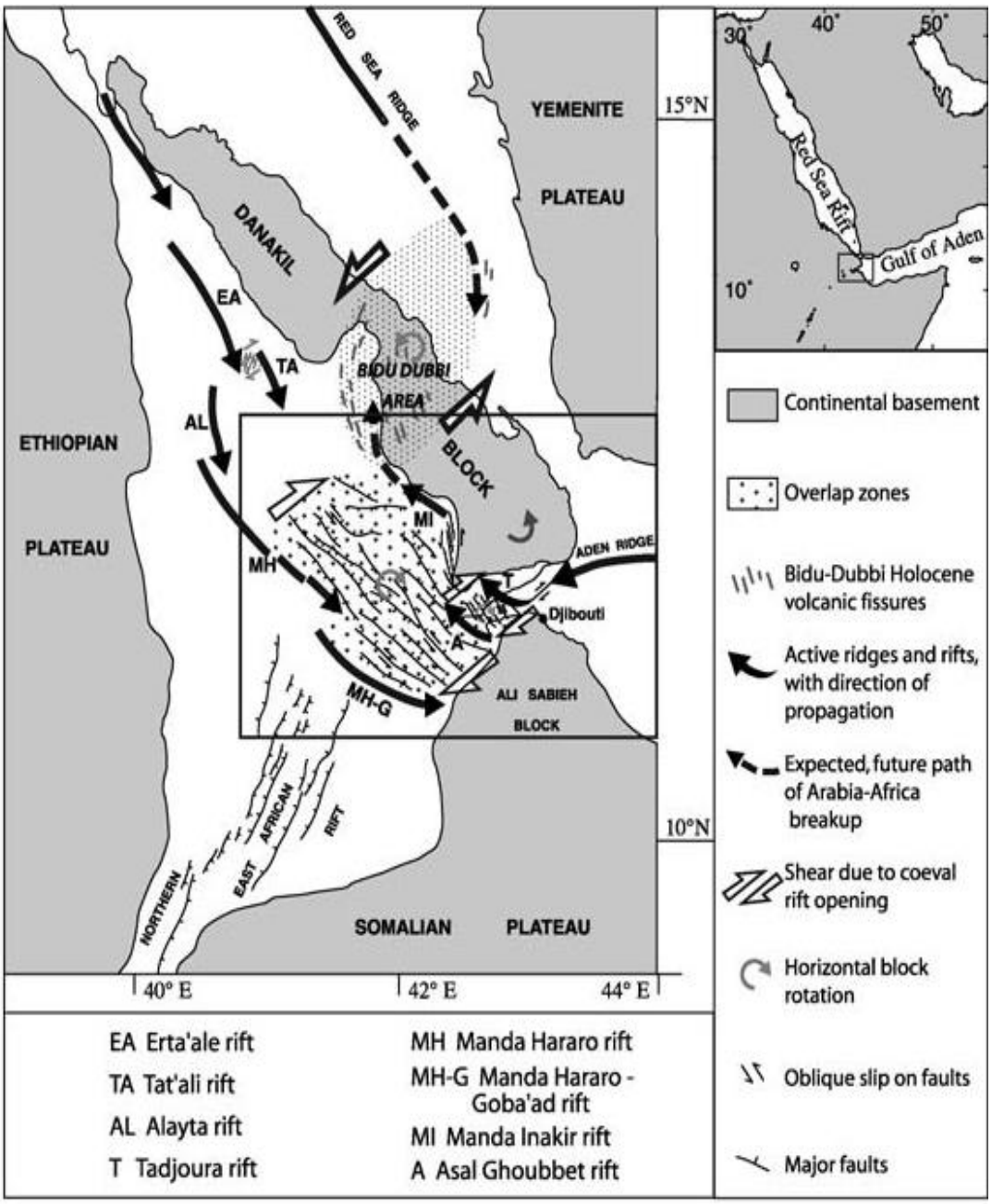

Figure 1.2.Tectonic map of Afar depression with propagating rifts (Manighetti et al., 2001).

1.2. Statement of problem

Earth is dynamic in nature so it's studied by the application of paleomagnetism. To determine deformational history and quantitative crustal block rotation link to the rift axis overlap

paleomagnetic investigation were carried out in central Afar. Hence these paleomagnetic investigations cannot show the same tectonic history of central Afar.

However, the application of paleomagnetism to tectonics in small scale it helps to determine the movement of crustal blocks rotation in continents, particularly about vertical axis rotation. The study area around saha and surrounding is found along the rift axis within central Afar. Where now tectonic activity are taking place which is responsible for the formation of different geological structure and numerous block rotation at the overlap of right stepping movement that form bookshelf fault. At this area pervious paleomagnetic investigation on outcropping rocks to the tectonic application have not been conducted, while it provides vital paleomagnetic information and tectonic history of the central Afar.

Paleomagnetic investigations tool for studying tectonic activity, due to this the study area structurally affected by tectonic force which is vertical rotation of the block. These structures were the extension of the blocks which is link to the rift. Due to this there is an expectation of declination difference with respect to the vertical axis.

Geologic and tectonic observations in the study area raise a number of scientific questions that I hope to address in my research, such as, what are the structures and possible tectonic setting of the area as well as what is the crustal block rotation and what is the magnitude of rotation? This research is assigned Saha and surrounding area to quantify the crustal block rotation which supports the overall counter clock wise rotation.

This research problem has been identified from previous researches because no research study ever conducted earlier around Saha to determine the tectonic activity through the use of paleomagnetic application. These conditions stimulate me to conduct my study area, therefore the proposed problem assign to make the data complete and to know the way of deformational activities in the study area.

1.3. Description of the study area

1.3.1. Location and accessibility

The study area is located in the north east part of Ethiopia in afar regional state in Awsi Rasu zone. It is located north east of Addis Ababa at distance of 659km geographically the area is bounded 11.84144° N to 12.75028° N and 41.08456°E to 41.44095°E. .

The area is accessed by asphalt, gravel and foot trials. It is found from Seha to Dichotto and from Afidera asphalt road, Serdo to Silsa. These asphalt and gravel roads which cross various part of the area were made the work easier but foot trials were not suitable in order to carry the instrument and in some site the accessibility difficult even the car tire burrowed due to the thick sand. The other day change to the site for collecting paleomagnetic samples.

This area is manifested faulted blocks with relatively gentle and steep scarps that form graben structure which are rugged topography.

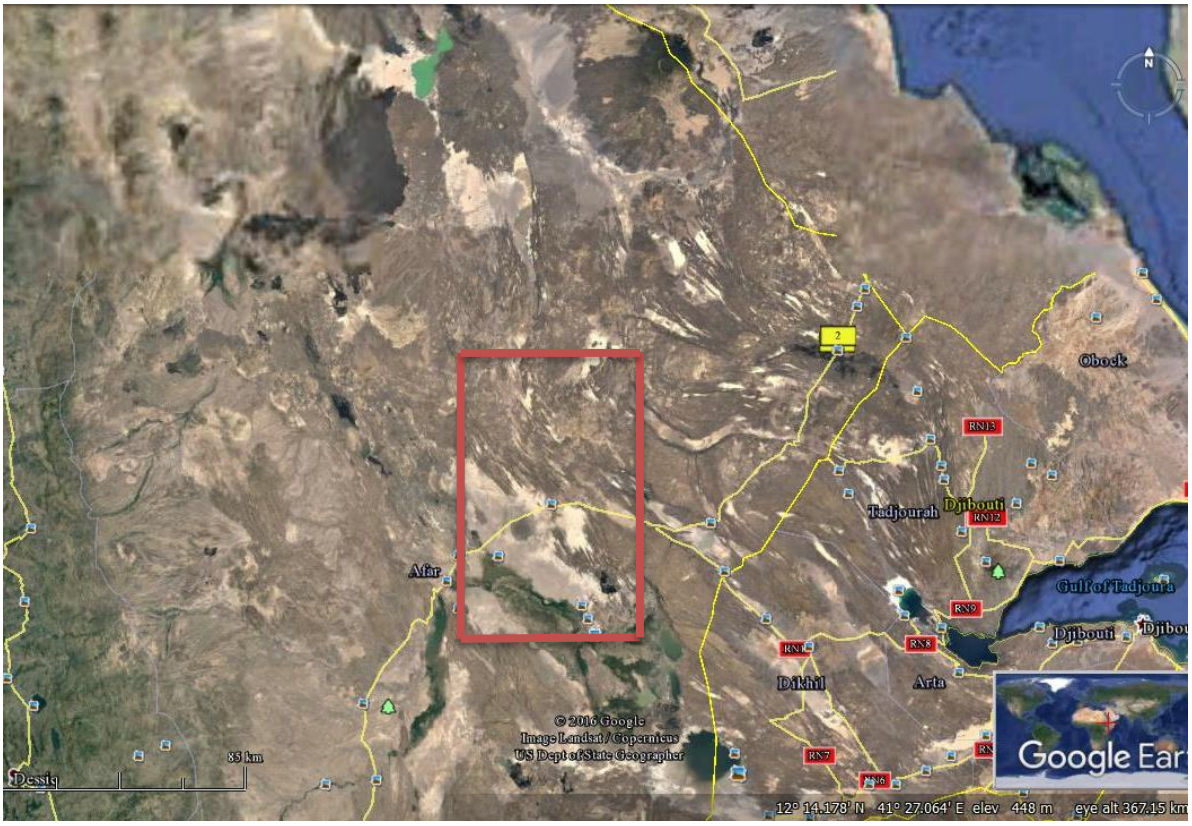

Figure 1.3.1a.location map of the central Afar and the rectangle symbol indicate the study area.

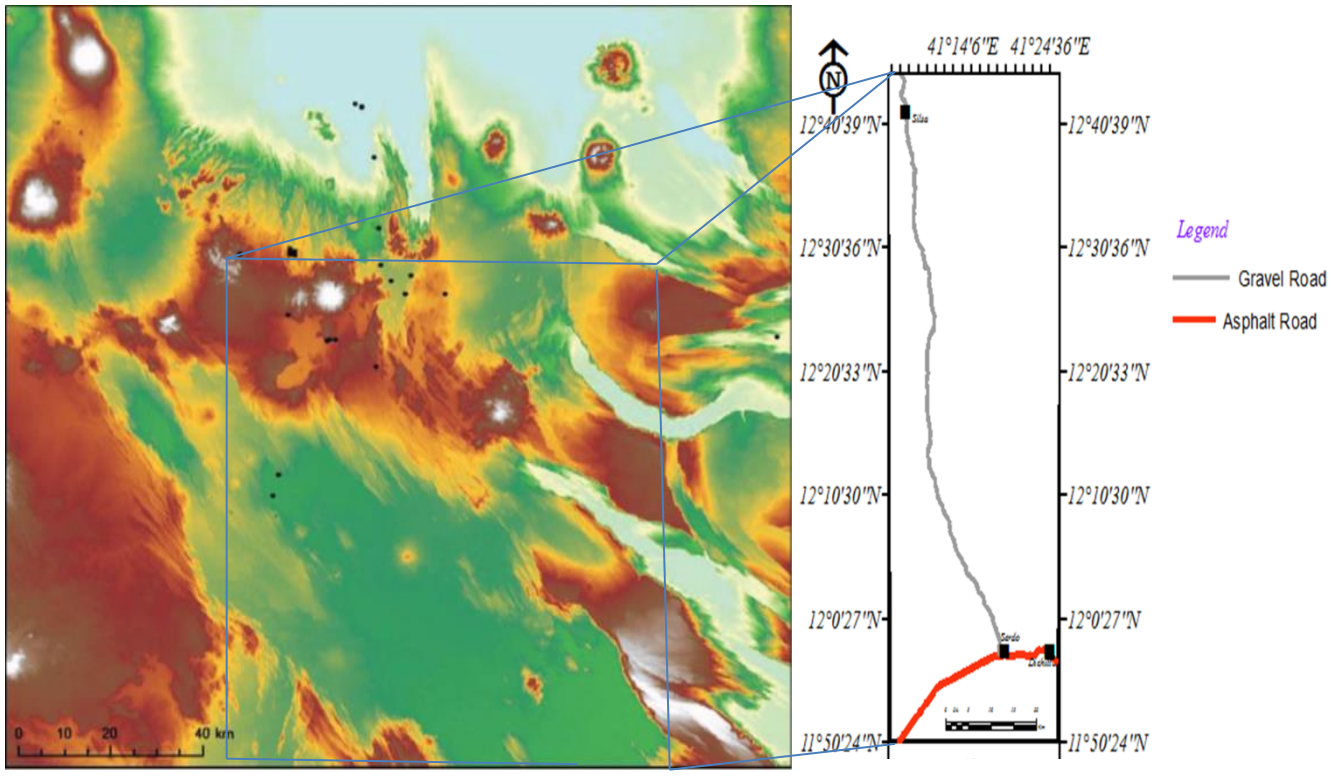

Figure 1.3.1b.Location map of the study area

1.3.2. Objective

The general objective of the study area is paleomagnetic investigations of the tectonic implications which quantify vertical axis rotation of crustal block in order to determine tectonic history from the paleomagnetic data.

The specific objective includes the following:

- To determine ferromagnetic minerals;
- To quantify crustal block rotation using paleomagnetism;
- To quantify the average paleomagnetic direction and pole;
- To map lithology and structures in the Saha and surrounding area.

2. METHODS, MATERIALS AND PROCEDURES

2.1. Sampling and laboratory treatment

Paleomagnetic samples were made during the afield work to Seha and surrounding area. A Total 55 oriented core samples from 9 paleomagnetic sites (plate 2.1.4). I collected samples as individual flows that safely reached from the sequences of volcanic flows which exposed along the fault scarps.

Routine laboratory started after specimen preparations then directional measurements were done in the paleomagnetic laboratory of School of Earth Sciences in Addis Ababa University.

The spinner magnetometer (JR–6A) was used for directional measurement and rock magnetic mineral identification by the demagnetization and magnetization process were done using LDA-3, Alternating field (AF) demagnetizer and MMTD80 furnace for thermal demagnetization (TH), Impulse magnetizer (IM-10) for ferromagnetic mineral determination. The specimens were demagnetized with AF technique, where the AF gave un removed results a specimen per site was treated using a TH technique. Therefore, a total of 87 specimens (from 55 oriented core samples) were obtained, which 40 were analyzed using AF, 41 using TH and 9 for mineralogy using Impulse magnetizer and TH(3 specimens added from AF demagnetizer). .

2.1.1. Principle of Collection and Measurement paleomagnetic Sample

First paleomagnetic survey was done in order to collect oriented cores with the information of each sample including coordinates, azimuth and dip. The goal of collectining samples was to average the errors, to assess the accuracy of the recording medium due to disturbance of nature. Therefore, there was conducted by paleomagnetic samples but, always not accurate in order to identify direction and magnetic intensity of paleomagnetic sample in the field. The cores samples were carfully oriented in the field by using both solar and magnetic compass (plate 2.1.1).

Logistics of sample collection dictate strategies for obtaining oriented samples. Basic attributes of the most common sampling methods were samples cored with portable drill, Block samples, and Lake-bottom or sea-bottom core samples. Out of these methods of sampling collections core sampling was used for this research.

The depth of cores and diameter is 6 to 12 cm, 2.5 cm respectively (Figure 2.1.1b), an orientation stage was put over the sample and attached to the rock at base (plate2.1.1). Orientation stage was

determining inclination by magnetic compass measured the core axis and or sun compass or both (plate 2.1.1).

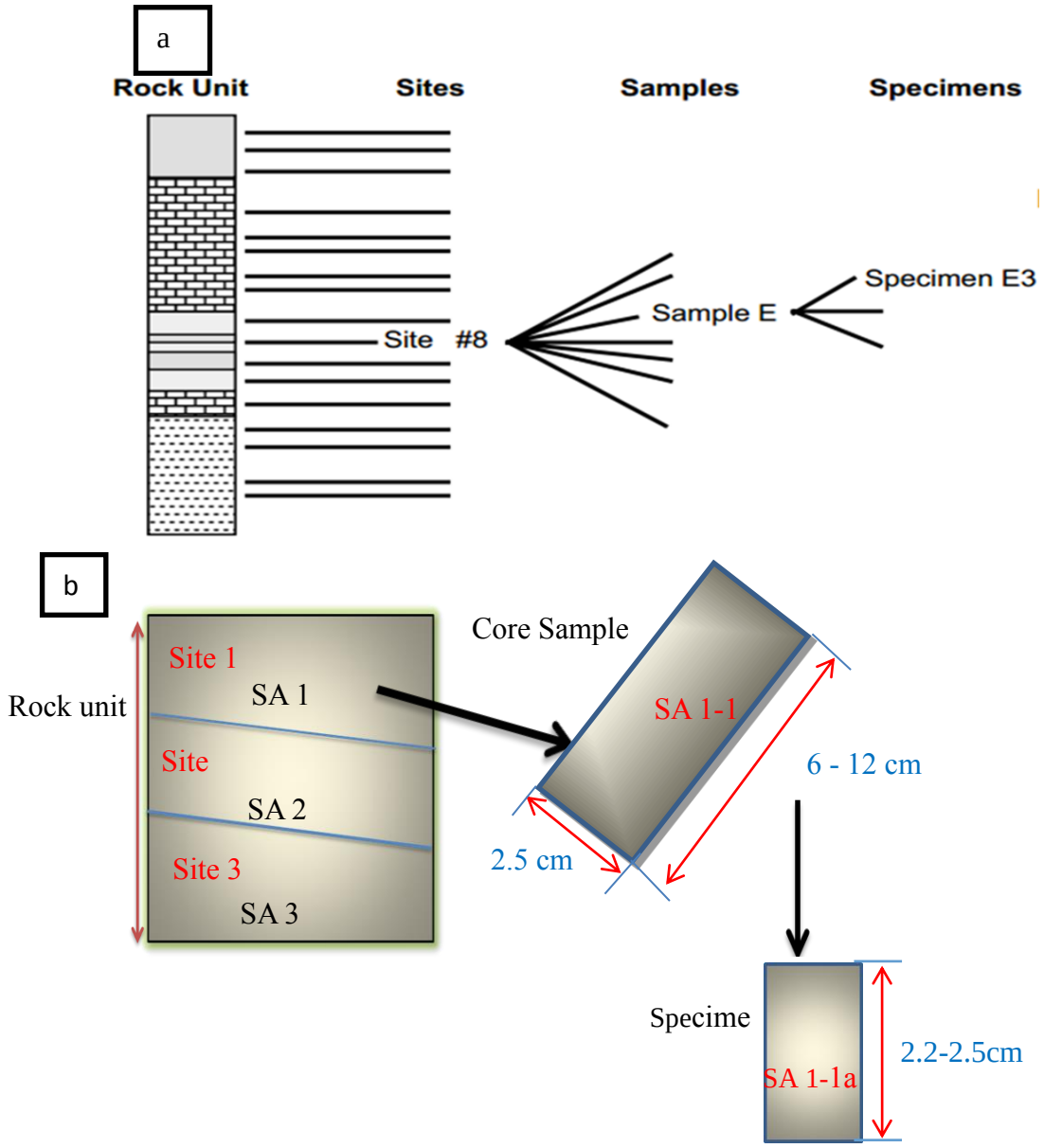

Figure 2.1.1.Generalized paleomagnetic sampling scheme, (a) several sites were collected from the rock unit; multiple samples were collected from each site; 3 specimens for laboratory measurements were prepared from each samples (Modified from Butler, 1992). (b) Several

samples were collected from each site, several specimens for laboratory measurement from each sample of the study area.

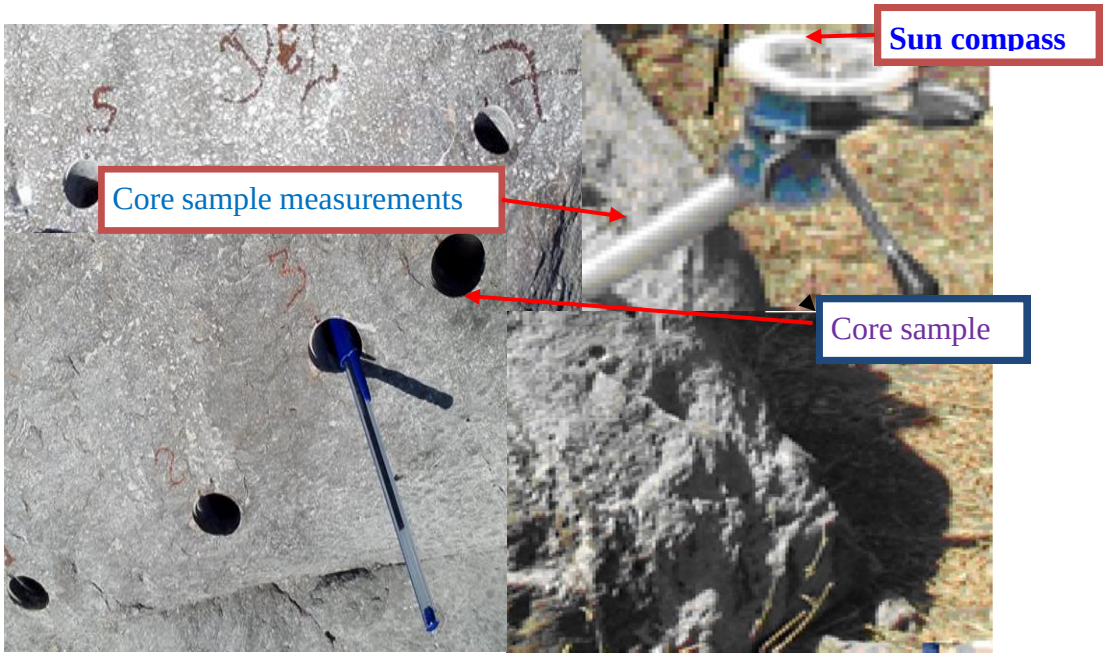

Plate 2.1.1.sampling Core measurement

2.1.2 Procedure of drilling and sample orientation technique

Sampling sites were collected to be representative of a single lava flow and location of site was known (figure 4.2).

The orientation of each sample was done (Butler, 1992). The sun compass recorded the time in order to know magnetic disturbances that might cause the magnetic compass record.

Actually there are 3 basic attribute of most common sampling method such as core, block and sea-bottom core sampling but for this research the most important one is core sampling. Each site consisted of a single lava flow and six to eight separately oriented samples were collected per site. Brunton compass is used to detect the presence of anomalously strong magnetization induced by lightning strikes. Therefore, to avoid lightning- strike regions, areas which are marked for sample collection where the needle deflection is small. Tectonic corrections were made for the paleomagnetic sites based on the assumptions that the flows were originally horizontal to sub horizontal and change of horizontal flow resulted from rotation. The samples

must be oriented before they were removed by orientation stage that consists of Brunton compass, and sun compass.

Care must be taken in moving of magnetic object far enough away so that they are not affecting the accuracy of brunton. There are many ways to orient a sample; the convenient one is used in this study were as shown:

1 core samples were drilled by using portable gasoline-powered drill with diamond drilling bit drilled;

2 insert sun compass;

3 rotate the slot to the top of the sample and note the azimuth and hade of the drill direction (into the outcrop) with a sun and or Burton compass, before this device was removed; a mark is scratched on the sample;

4 mark the sample through the slot with a brass;

5 The sun angle and local time were recorded in order to determine magnetic disturbances that might causes the magnetic compass record;

6 carefully extract sample; mark a fixed arrow on the side of the sample in the direction of the drilling and label the sample with the sample with local name;

7 make note orientation data in the field note book;

8 After the sample was broken, mark could be augmented.

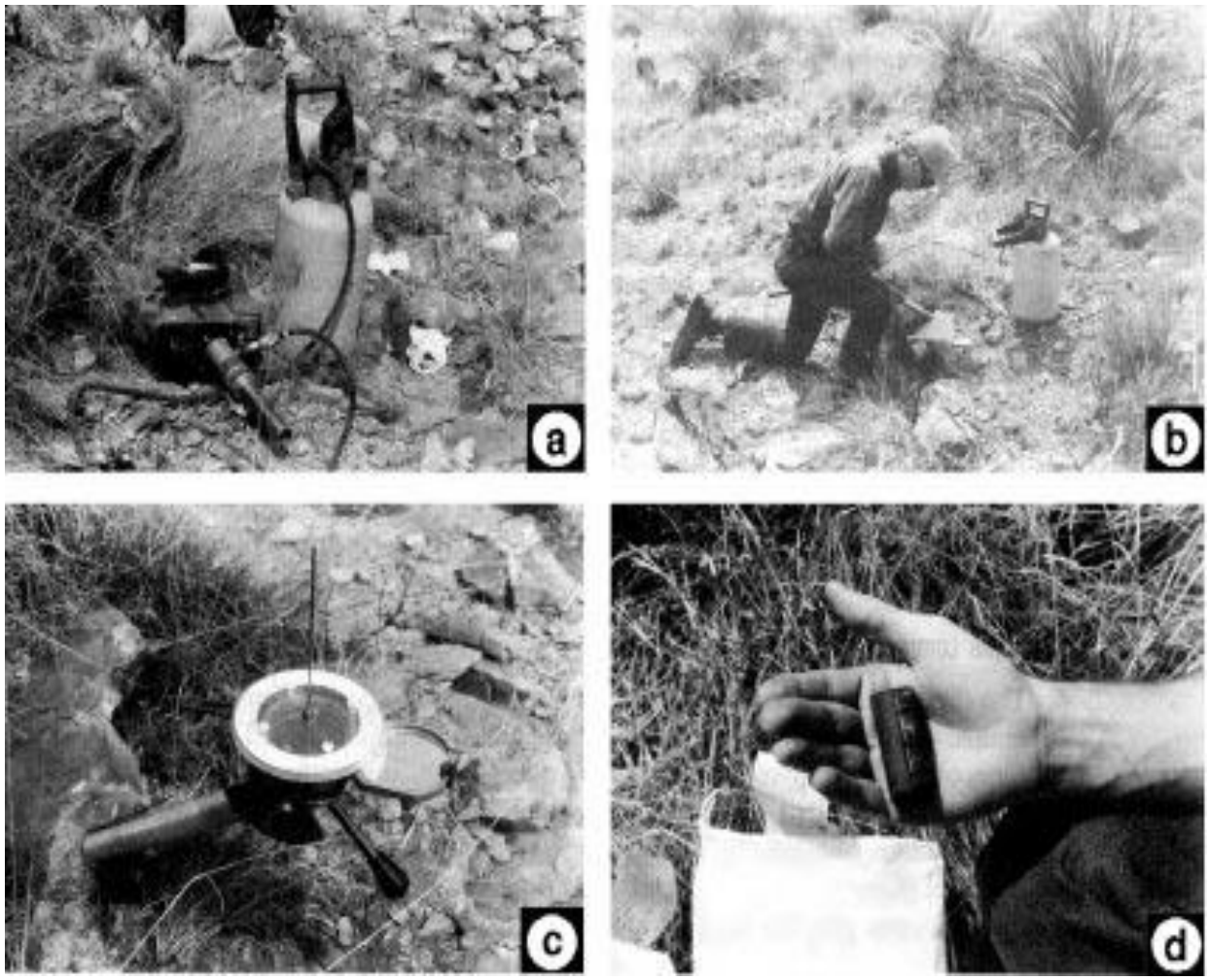

Plate 2.1.2 procedures for core sample collection, (a) drill with diamond drilling bit; (b) Unskilled laborer drilling a core. (c) Orientation stage put over in situ core sample. (d) Core sample with orientation markings (Butler, 1992).

2.1.3. Required instrument during field work

The sampling of geological units for paleomagnetic studies involves both removal of samples from their natural environments and marking them in such a way that their original orientation was known. Collecting of rock samples from the outcrop was field drilling with core drill.

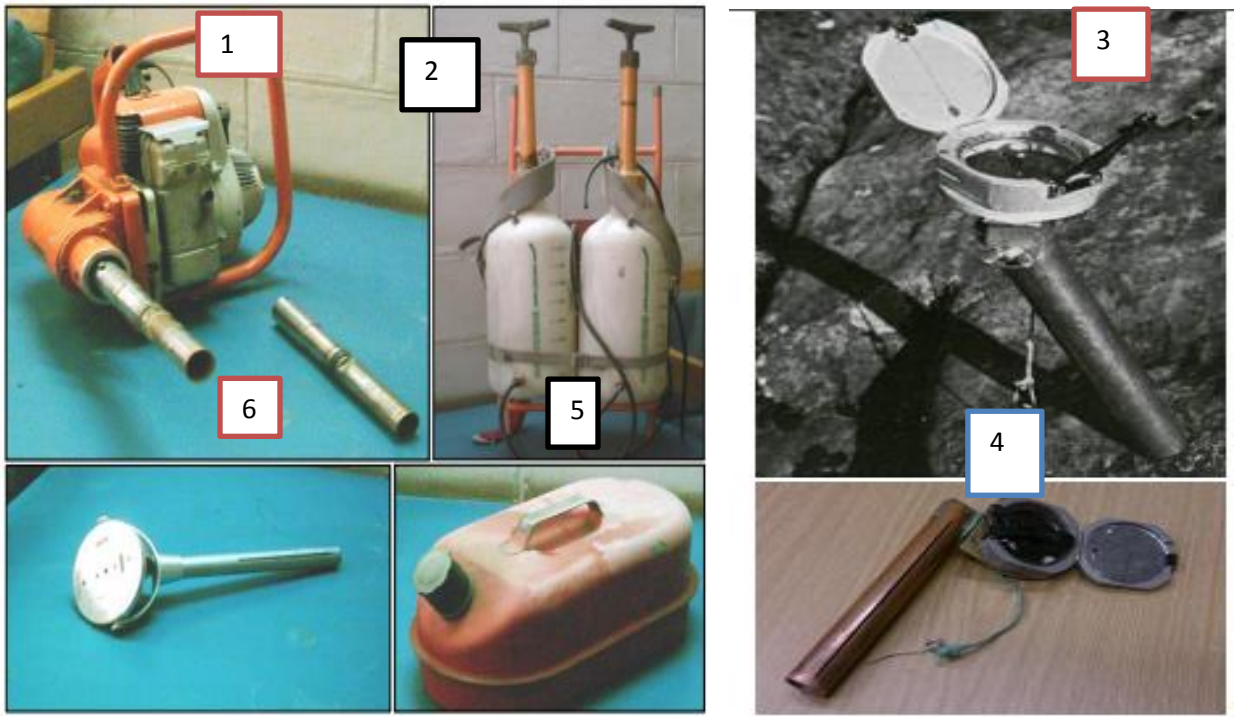

Plate 2.1.3.Instruments used in field for paleomagnetic core sampling, 1 drill with diamond Drilling bit 2 water pump 3 Orientation stage 4 magnetic compass 5 Tank for fuel 6 non-magnetic slotted tube , others were the metallic paleomagnetic pen and ruler, geologic hammer, Topographic map , GPS ,Digital camera ,Sample bag ,map scale, marker pen and note book Hand lenses.

2.1.4. Laboratory Activities (Post field work)

After collection of paleomagnetic samples from the paleomagnetic sites during field activities different paleomagnetic laboratory would be done. The laboratory activity started from collection and preparation of enough specimens from collected paleomagnetic sample. The cores samples cut into two cylindrical specimens (figure 2.1.1b). These activities were started from preparation of specimens for other partial demagnetization and magnetization laboratory techniques. Preparations of collected samples for laboratory, Compiling field information to generate paleomagnetic data analysis, synthesis, interpretations and discussions of results would be done.

The paleomagnetic analysis display determination of paleomagnetic direction. In paleomagnetic laboratory demagnetizations (alternating-Field Demagnetization, thermal demagnetization), and impulse magnetization techniques were used spinner magnetometer in order to measure magnetic saturation for each procedures.

Procedure in progressive demagnetization was step wise demagnetize a specimen at progressively higher levels, measuring remaining NRM following each demagnetization sequence.

A first step was determined and removed of secondary components of NRM. The NRMs of specimens from a rock unit were primary measured, the distribution of NRM which shows due to presence of secondary NRM. .

The principle AF demagnetization procedure was to expose a specimen to an alternating Magnetic field and conducted by AF (plate 2.2.5A).

The AF demagnetization was maximum 100mT magnetic fields, step by step from NRM measure each steps at 0mT, 5mT, 10mT, 15mT, 20mT, 25mT, 30mT, 40mT, 60mT, 80mT and 100mT. AF demagnetizing instruments by using tumbler apparatus that rotate the sample (plate 2.1.4A).

The tumbler was designed to present in sequence all axes of the specimen to the axis of the demagnetizing coil. The tumbler thus allows demagnetization of all axes of the specimen during the course of single demagnetization treatment. Paleomagnetic instrument that are available in school of earth science used for paleomagnetic analysis and preparing specimens were shown:

Plate 2.1.4A.Laboratory instruments available in school of earth science, Addis Ababa University in order to analysis Paleomagnetism, (a) cutter, cut sample into specimens, (b) LDA-3,AF. (c) MMTD 80TH. (d) ASC-IM for acquisition of IRM. (e) JR6-A spinner magnetometer which measure intensity of magnetization.

The thermal demagnetization is heating a specimen to an elevated temperature (Tdemag) below the Curie temperature which contains rock magnetic minerals. After cooling to room temperature was conduct to measured magnetization by spinner magnetometer. TH demagnetization temperature range steps were started from 0°C,120°C, 200°C,250°C, 300°C, 350°C, 400°C,430°C, 460°C, 520°C, 540°C, 560°C, 580°C, 600°C, 620°C and 640°C. The magnetization grains which TB ≤ Tdemag was scattered, as small hc grains during AF demagnetization.

Plate 2.1.4B.prepared paleomagnetic samples in order to analyze paleomagnetism in laboratory. (a) Collected field paleomagnetic samples. (b) Prepared specimens for Thermal demagnetization. (c) Prepared specimens for Alternating field demagnetization. (d) Prepared specimens for mineralogy.

2.1.5. Data analysis and synthesis

These activities were undertaken in the laboratory for paleomagnetic study to confirm field observations on rock compositions and laboratory progressive demagnetizations (AF, TH) and impulse magnetization techniques.

Determine rock magnetic minerals and analyzed from samples specimens when collected from the field.

Some specimen expose to Alternative magnetic field for removing secondary NRM and to isolate ChRM in rocks heating of specimen to an elevated temperature below curie temperature of content rock magnetic minerals, then cooling to room temperature.

Paleomagnetic Core sample preparation in to paleomagnetic specimens with appropriate dimensions in order to measure the Natural Remnant Magnetization (NRM).

Rock magnetic and paleomagnetic data analysis of remagnetization processes, Statistical analysis of paleomagnetic data using great circle and (PCA), Structural data plotting and analysis of best fit direction using zjidervld diagram.

Adequate define components of NRM, progressive Stepwise demagnetization technique for paleomagnetic Samples of specimen, identification of rock magnetic minerals using IM and TH from thermal demagnetation curves , display the Magnetic Moment to determine magnetic intensity of NRM, display AF, TH, IM and graphical representation of demagnetization data.

2.1.6. Interpretation and results

Based on the obtained result from stepwise demagnetization processes in Laboratory, field data and from reducing statistical uncertainty interpretation would be done.

In these stages the interpretations and discussions of the results of the analyzed samples were done.

The site-mean directions and paleomagnetic pole position determined from the paleomagnetic laboratory analyzed and interpreted by using Remasoft and Paleomac program. Comparison of determined mean direction with the expected direction then, interpreted the displacement of crustal block. Interpret stereographic projection, vector component diagrams were done by Thermal and Alternating Field demagnetization, the display of NRM directions and distribution from the result of progressive demagnetization.

3. GEOLOGY OF THE CENTERAL AFAR

3.1 Geology and Geochronology of the Central Afar

The Central Afar is wide zone of rifting and extends from the Ethiopian plateaus to the Gulf of Tadjoura (Wolfe den et al., 2005). Nubia and Arabia where separated during oblique rifting from Red Sea and Aden (Bellahsen et al., 2003; Faccenna et al., 2013). According to Stab et al., (2015) subdivided the volcanic products of the central Afar tectono magmatic chronozones were Oligocene to Pleistocene. These groups were described from the oldest to the youngest as the following:

3.1.1. Oligocene Flood Basalts

Traps formation is discovered from Sullu Adu area (29.7 ± 1.5 and 30.6± 1.5Ma) with strongly tilted rhyolites and present below the Miocene volcanic.

The Trap formation correlate in Sullu Adu to the Trap Basalts observed from Western Afar and on the plateaus.

3.1.2. Miocene Basalts and Rhyolites

The Miocene igneous rocks of the Afar region are divided into the peralkaline granites (26-22Ma), Trap Basalts (25-15Ma), Mabla rhyolite series (14-10Ma) and the Dahla series (8-6Ma) (Varet, 1978).

The marginal graben basalts near Dessie (24.40 ± 0.35 Ma) and formation correlates to other local marginal graben (Dessie and Kemise Formations). Late Miocene volcanic formations are found from Arabati and Sullu Adu zones.

In Arabati, Chifra series is bracketed between 22.9 ± 0.3Ma and 7.69 ± 0.50 Ma and 7.5± 0.4Ma. The base of the Finto series (23.5 ± 1.2 Ma) and ignimbrite layer lying conformably above a layer of green tuff, top of the Finto series (8.6 ± 0.4 Ma).

Correlate the Chifra and Finto series which argue erupted the same time.

Miocene formation can be correlated to the Burka, Aneno, and Bercha Formations.

3.1.3. Pliocene Flood Basalts

The Sullu Adu flat-lying basaltic formations located NE-SW Sullu Adu transect (5.39 ± 0.28 Ma) and determined same time (3.93 ± 0.06 Ma). South of Sullu Adu, correlates to the Pliocene flood basalts with the lower Stratoïd Formations. After emplacement of the Stratoïd Formation, the Sullu Adu area was uplifted while the Awra basin subsided and was filled with volcanic products Miocene Chifra series lie over the tilted Finto Miocene series.

3.1.4. Quaternary sedimentary rock

The Quaternary sedimentary rocks of the Afar Depression filled by fluvial/ lacustrine with thicknesses up to 200m (Varet, 1978).

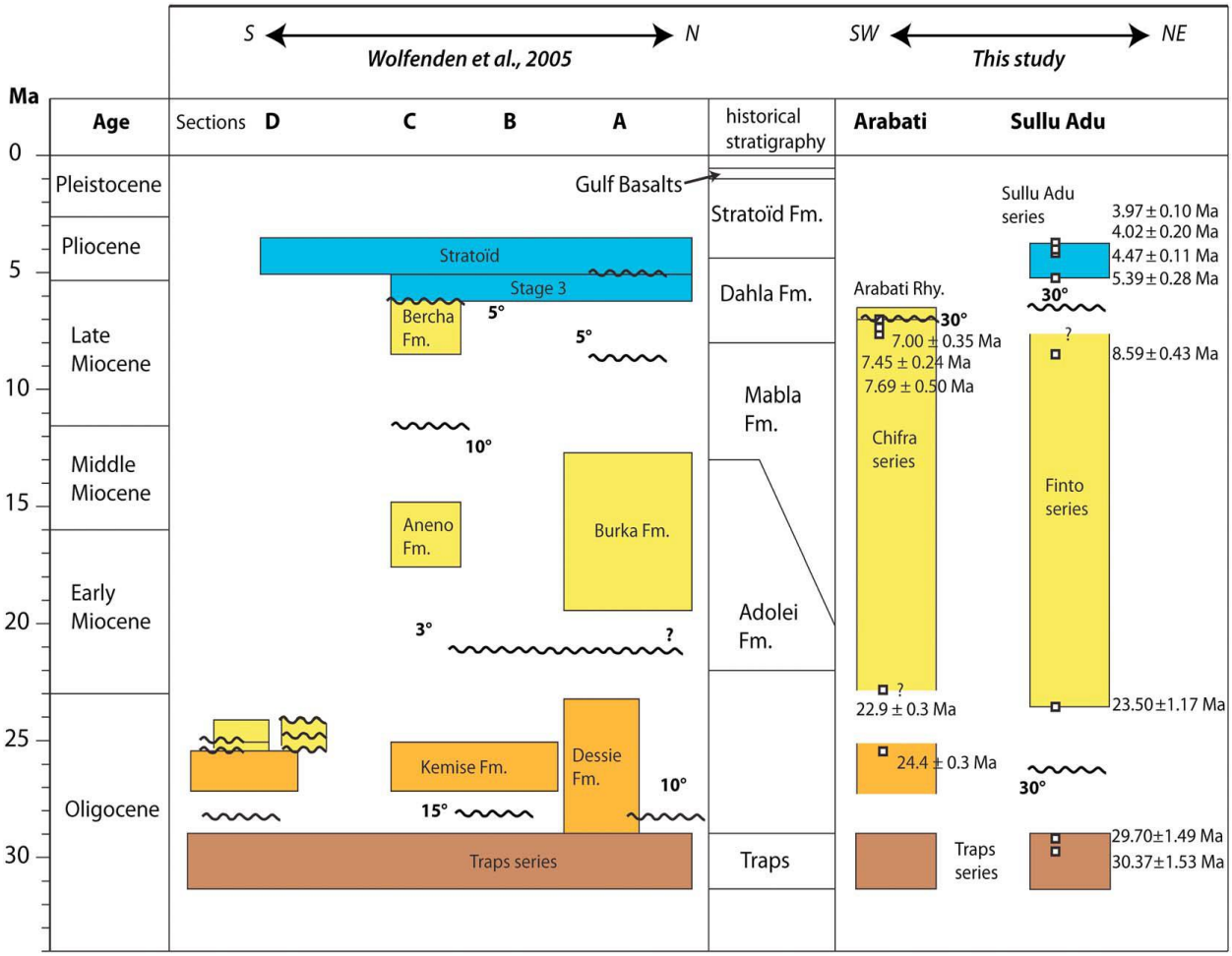

Figure 3.1.Volcano-stratigraphic chart of Central Afar. Left Compilation from Wolfenden et al. (2005) of local volcano-stratigraphic records mapped along four transects (A, B, C, and D) that show the along-strike N-S evolution of Western Afar and right compilation from Stab et al. (2015).

3.2 Structural Framework of Central Afar and Its Evolution

The East African Rift System (EARS) is an extensional system (Davidson and Rex, 1980). At Afar, the EARS join together the Gulf of Aden and Red Sea Rifts, both characterized by extension stage (Ebinger and Hayward, 1996).

According to Stab et al., (2015) two main Structural Style observations supported the presence of shear zone: (1) the same NE dip of tilted blocks separated by antithetic normal faulting and (2) wide distribution domino faulting style.

Because the tilted blocks developed by rotation (7 Ma) and normal faults have similar throws.

According Stab et al., 2015 rifting in Central Afar three main steps:

The first stretching phase (25Ma) occurred after emplacement of the Traps (30–29Ma).

The second phase of deformation (thinning phase) occurred after the emplacement of the Miocene series stopped at 7Ma (marking the end of Chifra and Finto series emplacement.

The other phase of deformation during the Quaternary is emplacement of the Stratoïd series (eruption of second pluse flood basalt at 4Ma).

According to Lister and Davis (1989) detachment faulting a thinning of the lower crust is focused on a single point, whereas extension at the surface is distributed. The stepping geometry of the Dôbi graben border indicate sinestral shear (stratoid series, locally 2 ±0.2 m. y Courtillot et al., 1984; Kidane et al., 2003). Locally, some third-order faults also tend to form dextral en echelon arrays parallel to the other faults indicate dextral shear and the northerly striking faults indicate sinistral en echelon arrays (Jacques et al., 1999).

Bookshelf faulting about the vertical axis shows strike-slip components of motion along the edges of small parallel blocks counterclockwise rotations of ~N110°E which develop strain transfer between NW-SE Dôbi and Hanle grabens (Jacques et al., 1999).

Paleomagnetic and tectonic studies (Manighetti et al., 2001; Kidane et al., 2003) show that this counterclockwise rotating inside the overlap between the Asal–Manda Inakir and Manda Hararo–Goba'ad rift axes.

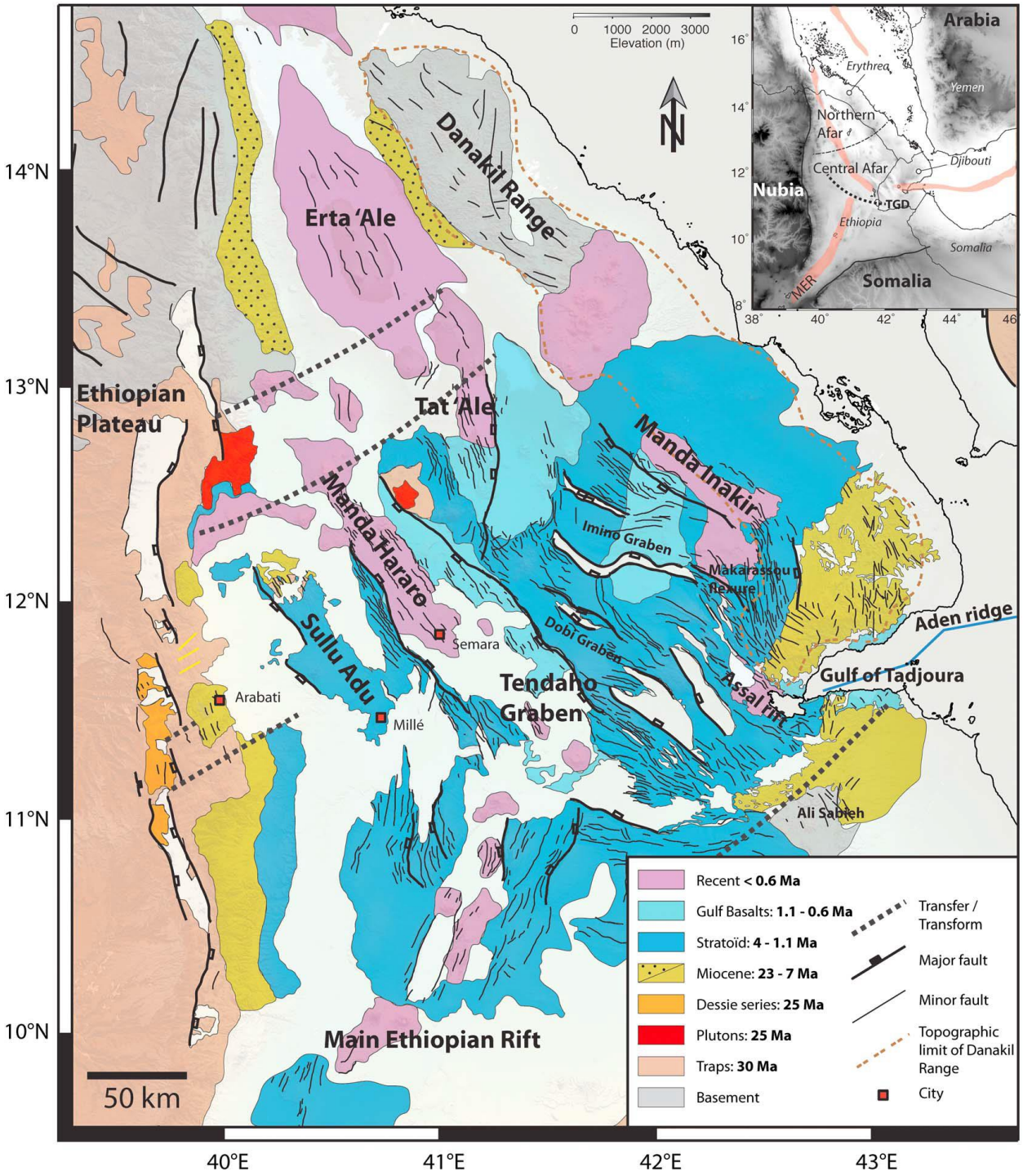

Figure 3.2a.Structural map of the Afar Depression Varet (1978) and Wolfenden et al. (2005).

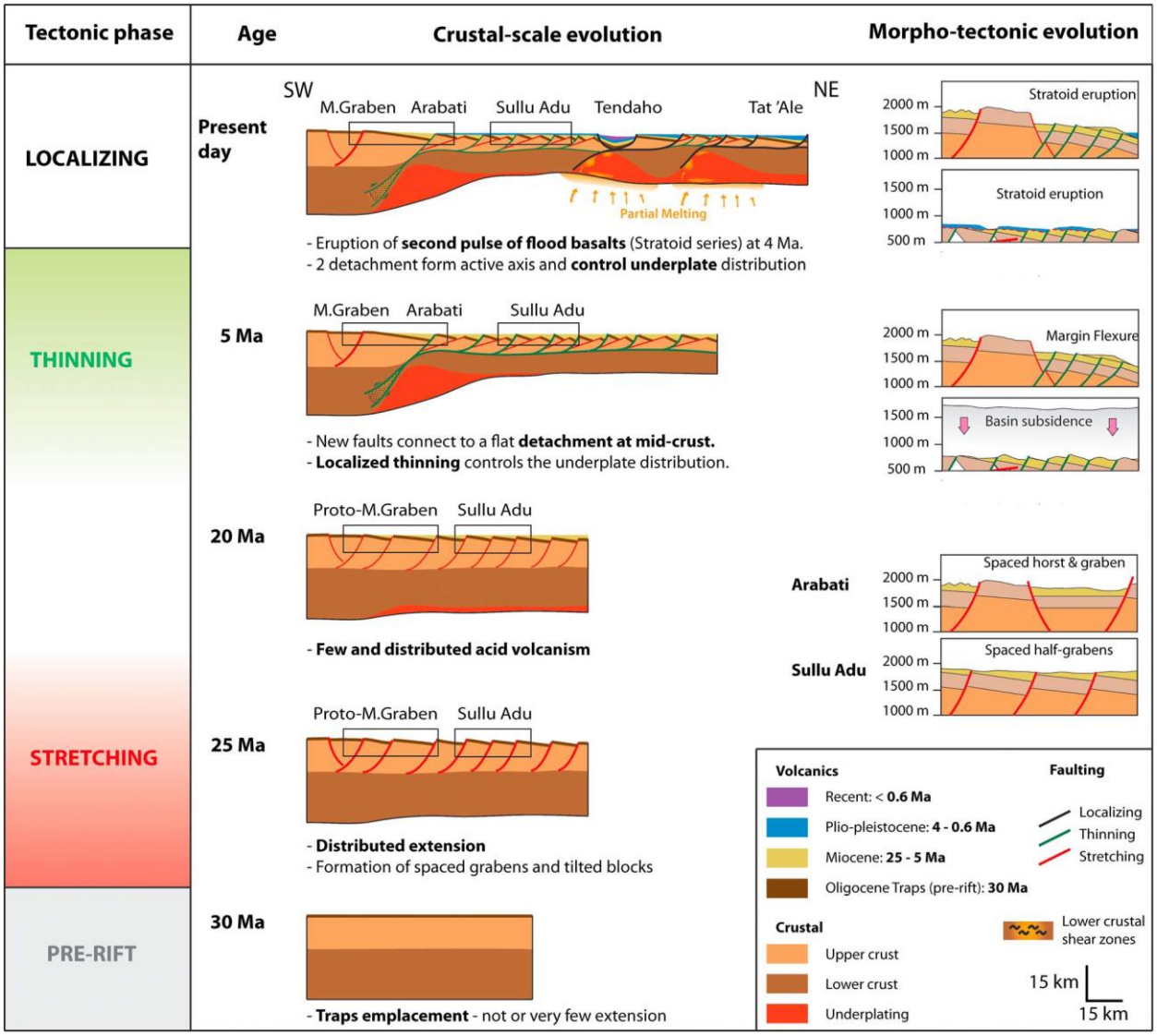

Figure 3.2b.Volcano-tectonic evolution of Central Afar Stab et al (2015). Table figure summarize the different tectonic phases that structured Central Afar. The stretching affected a wide area and was characterized by strong coupling between the brittle and ductile levels of the crust: NE dipping tilted blocks were created by the accommodation of extension on SW dipping faults. The Afar rift was already asymmetric at this point, with numerous half-grabens. The stretching phase was followed by a period of tectonic quiescence and the eruption of sparse acidic magmas.

4. GEOLOGY OF THE STUDY AREA

The study area mostly exposed igneous rock of plio-pleistocene Afar Stratoid Series with minimal Quaternary magmatism.

The major activities conducted during field work were identifications of lithology and geological structures with the scale of (1 to50, 000) and collected paleomagnetic samples from each paleomagnetic sites. The paleomagnetic samples were collected from the basalt, conducted as paleomagnetic sites, through paleomagnetic sampling schemes (figure 2.1.1). The followings were an identification and mapping of the lithology and structures of the study area.

4.1. Lithology

4.1.1. Basalt

This rock unit was outcropped mostly at the west north west of seha, north east of dechitoo and south east of silsa area, including vesicular basalts(vesicles formed by bubbling of gas and has vesicular texture) (plate 4.1.1). The lithology unite fissural type which exposed along road cut, quarry site and hill side. It has light grey fresh colour, dark grey and light redish weathered colour and aphonetic texture and the Composition of this lithological unit is mafic and its mode of formation is extrusive. The mineral assemblage of this lithology unite is plagioclase with some pyroxene and olivine which outcropped through NE trending open extension fractures, and outcropped north west trending fault which taken as paleomagnetic site to collect paleomagnetic core samples.

Plate 4.1.1.Basalt unit, (d) basaltic lava flows which have four basaltic lava flows exposed in Saha area with difference thickens of lava flow.

4.1.2. Rhyolites: This rock unit is out cropped at serdo, North West and south west of part of Silsa area. The rhyolite unit is exposed along hill side and road cut. It is highly weathered and around silsa area intercalated with the obsidian. This outcrop shows surface layering features (banding). The color of this rock unit is light grey fresh and reddish weathered color and flow banding texture.

Plate 4.1.2. Rhyolite unit

4.1.3. Lacustrine sediments: this sediment filled by incoming of different sediments deposited in the plain land as well as exposed on foot wall of the fault at seha area. The sediment includes weathered rock soil, fragment of gastropods bodies and different wild animal bodies deposited in saha plan land.

The sediment have light gray to light blackish colour which deposited saha, serdo and silsa plain land. Its texture is silt, sand gravel size in composition and the area is scarcely desert plant and grass vegetated and arid (plate 4.1).

Plate 4.1.lacustrine sediments exposed Saha plain area (a&b). (c) The light gray to yellowish color is layered sediments whereas the gray is fault scarps; dashed line is the contact of layered sediment and basalt.

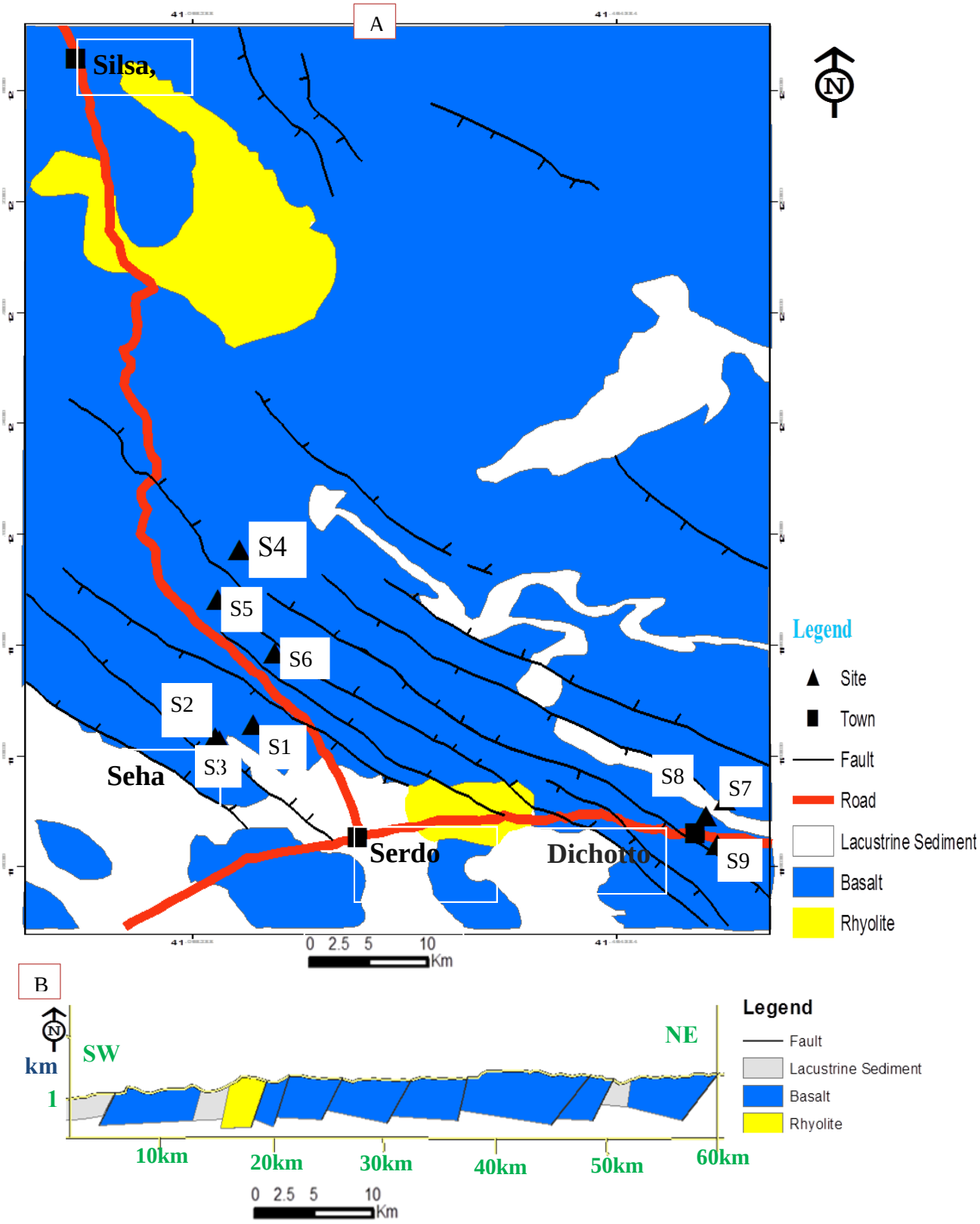

Figure 4.1 Geological (A) and cross section (B) map of the study area.

4.2. Structural interpretation of the study area

The movements of the Nubian, Arabian and Somalian plates have created a series of different tectonic regimes across the Afar region each with distinct structure style (Ebinger, 1996; Hofstetter & Beyth, 2003; Beyene & Abdelsalam, 2005).

On the study area different geological structures were observed which defined by different orientation (figure 4.2a, b) and mode of fracturing.

4.2.1. Faults

Faults are regular fracture of the rock which appreciable displacement of the blocks has taken place. The study area dominated by brittle deformation geological structures which propagated parallel to the Tendaho graben towards the red sea have North West and South East orientation. The extension direction of the faults North East and developed by mode III opening fracture. Normal faults are well developed geological structures in the youngest rift zone of the study area and they have full and half graben morphology. The rifts in rift structures are dominantly parallel to each other.

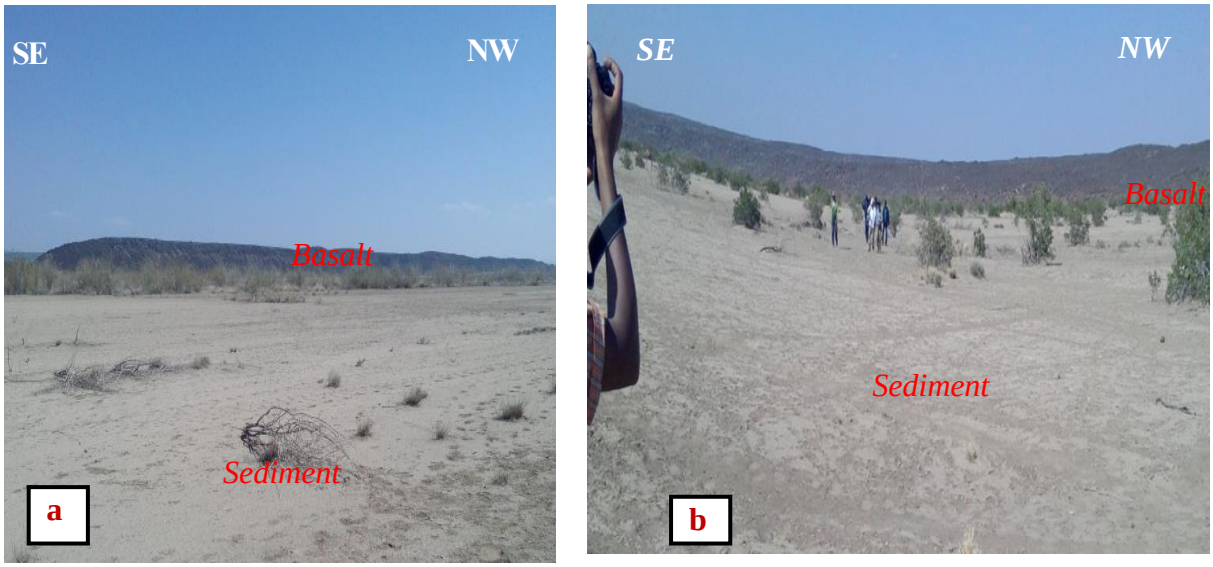

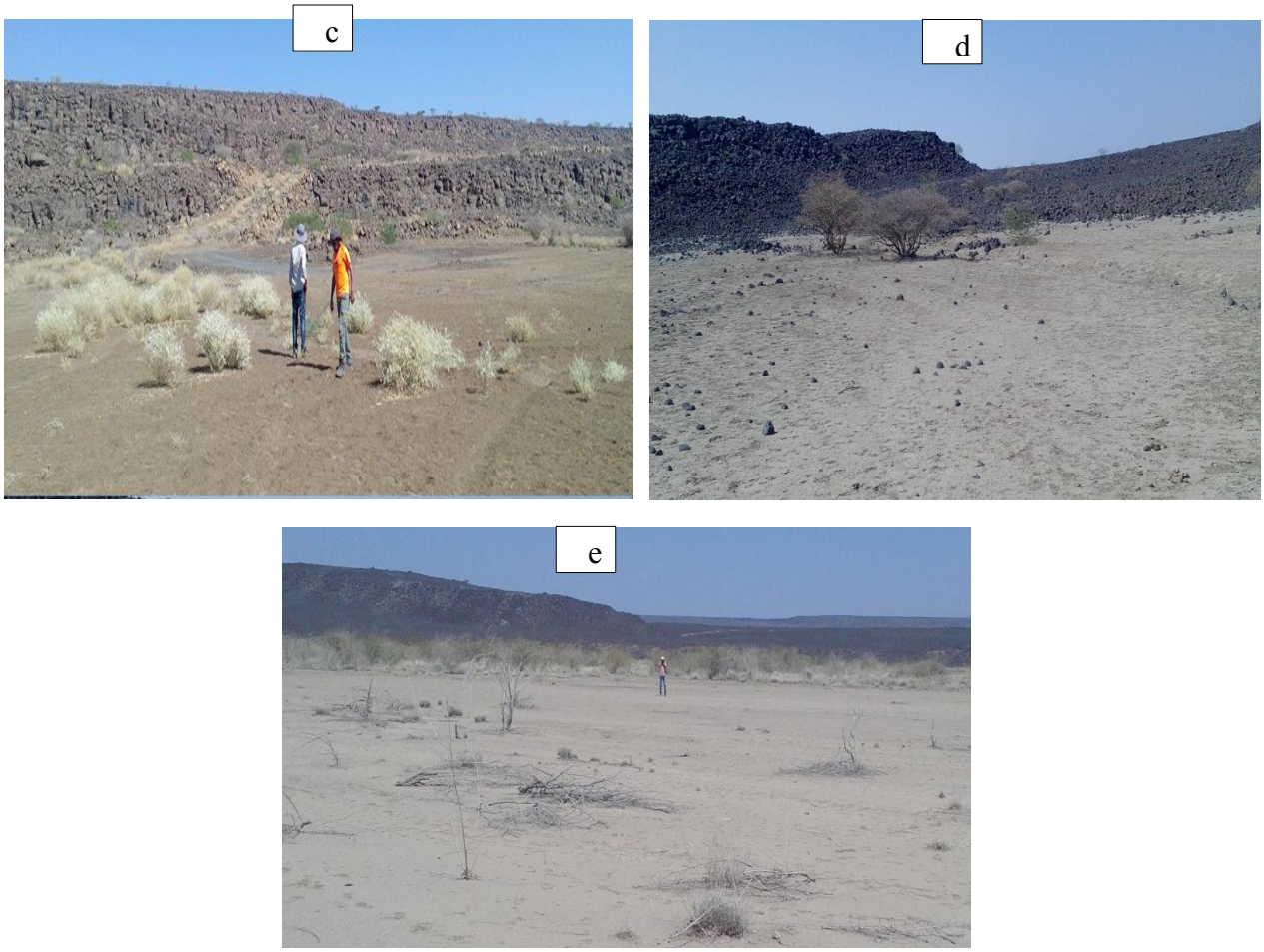

Plate 4.2.1.Fault, (a & b) open fault which is exposed at saha area (c, d & e) the individual fault topography features have different and die out which is off-set small fault is developed. The faults branched from the long fault, anastomosing and cut to that fault (figure 4.2).

4.2.2. Joints

Joints are regular fracturing that developed without displacement of the blocks and on the scale of meters to hundreds of meters in length.

The columnar joints exposed in basalt rock units which were located around silsa area (not well exposed). Columnar joints are occurred in volcanic rocks which formed by rapidly cooling and causing shrinkage crake to form commonly parallel polygonal or hexagonal pattern.

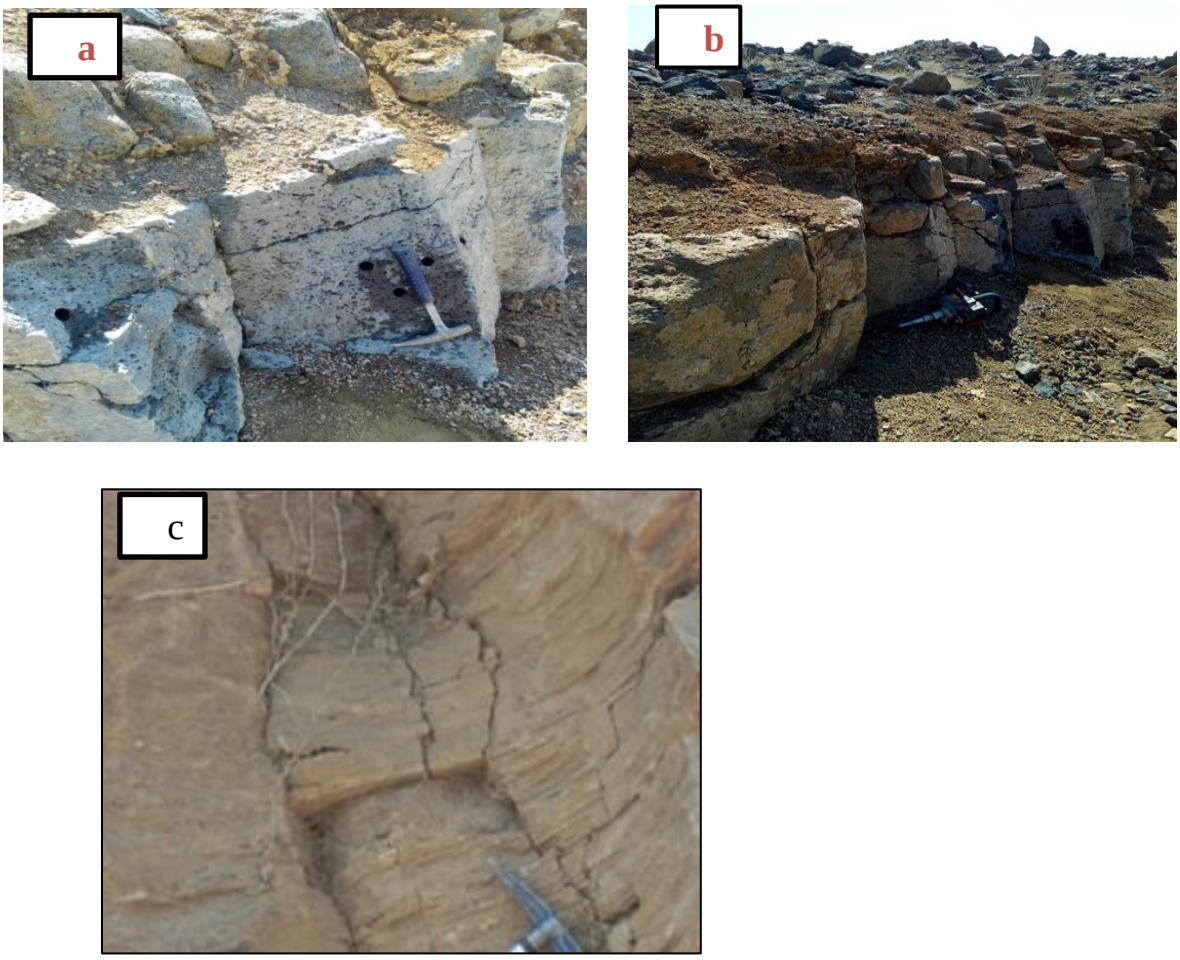

Plate 4.2.2.joint, (a, b) Columnar joints that exposed in basalt rock unit along road cut, (c) Joint intersection in Serdo area. Joints in the outcrop reveal a pattern which the traces of joints intersect and termination in the pre-existing joints .The joint terminated by branching and dying out .

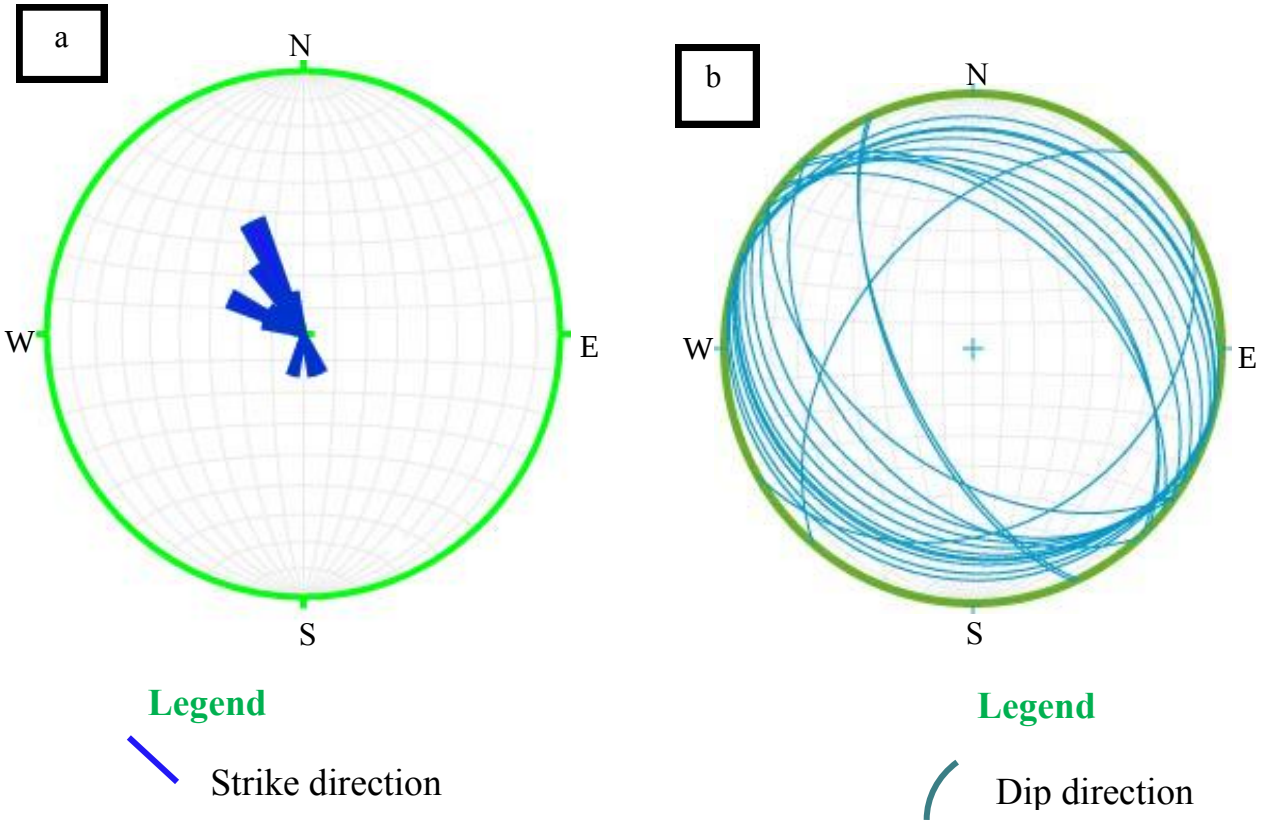
a
N
W
E
S
b
N
W
E
S
Legend
Strike direction
Legend
Dip direction

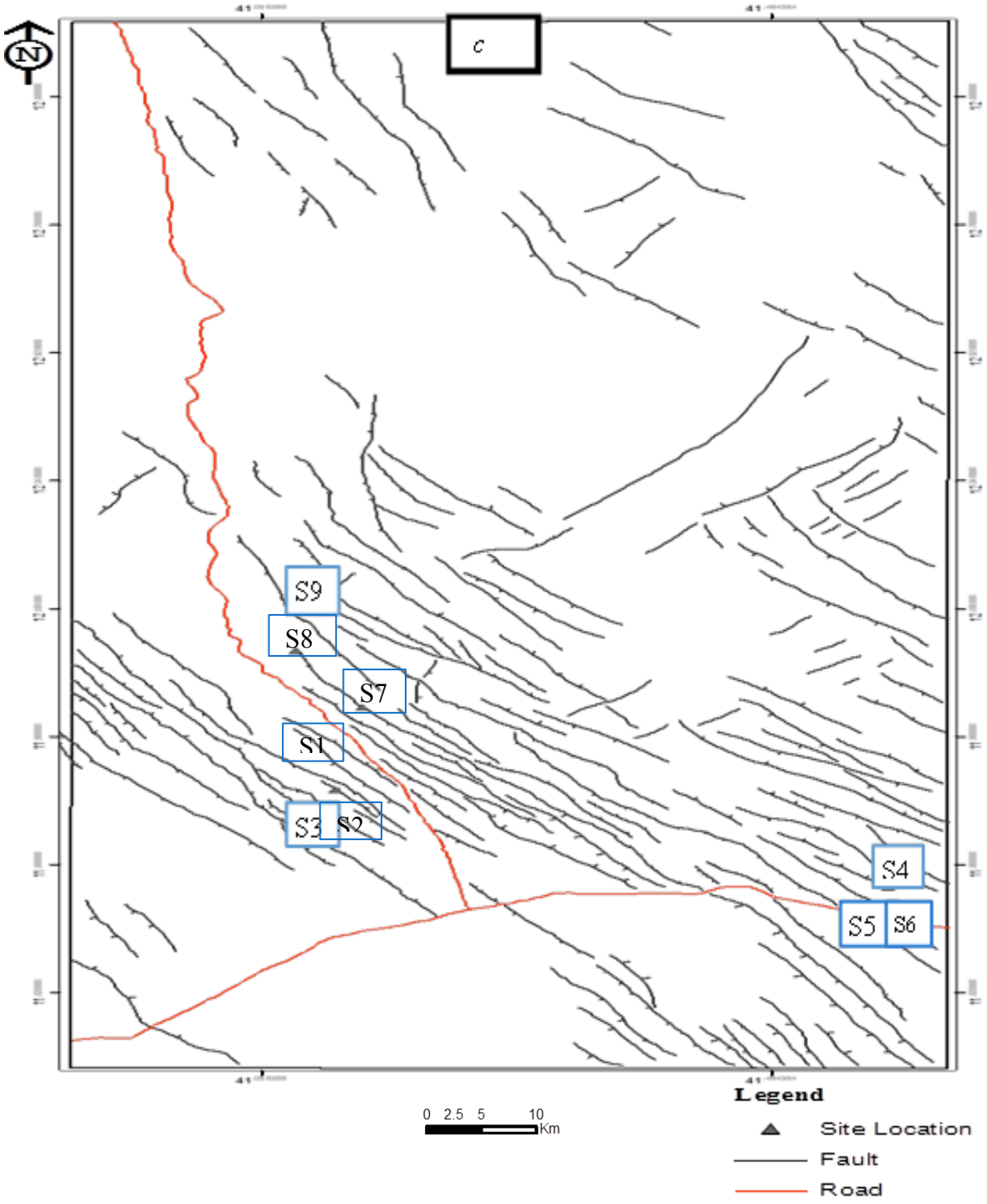

Figure 4.2.Geological structure, (a) Rose diagrams which shows the typical orientation of the fault strike directions, (b) Stereographic projections which show the orientation of faults. (c) Map of geological structure in the study area.

5. PALEOMAGNETIC RESULTS

From the central Afar in the north east of semera to Seha and surrounding area such as silsa, Dechotto 9 paleomagnetic sites selected and samples were collected in November, 2016. The Gulf and Stratoid basalts (mafic lava flow) were taken as paleomagnetic sites. The rocks unite cropped out along fault scarps and road cuts. From these rocks about 9 sites marked SA1-1 toSA3- 6, DE1-1 to DE3-6 and SS1-1 to SS3-5. A total of about 55 oriented core samples were collected and in laboratory about 87 specimens were prepared for paleomagnetic analysis (plate 2.2.5B). The samples were collected from horizontal to sub horizontal rock unites. For each core samples alpha- sun angle, alpha-magnetic and beta measurement were documented during the field work. After analysis determine natural remanent magnetization, rock magnetic minerals, paleomagnetic direction, tectonic rotation and pole of the study area were done.

5.1. Natural Remanent Magnetization (NRM)

Natural remanent magnetization (NRM) is magnetization present in a rock sample prior to laboratory results which depends on the geomagnetic field and geological processes during rock formation and during the history of the rock. However, NRM consist two components such as, primary (NRM acquired during rock formation) and secondary NRM (acquired subsequent to rock formation and can alter).

Samples were conducted to progressive AF demagnetization and TH demagnetization with 11 and 14-16 steps respectively. The Natural Remanent Magnetization of the measured specimens was between 0.4 A/m to 593 A/m, the smallest value observed from SA1-5, probably altered basalt, and the largest values which shows the intensity were due to the effect of lighting strike, this values from the resulted measured modules. The intensity of the NRM regionally shows a two modal distribution with an overall mean 3.6A/m and 15.8A/m obtained from Afar basalts (Courtillot et al. 1984, Pre´vot and Gromme´, 1975) and the declination was close to 180˚ and360˚ and scattered, inclination values small (Kidane et al., 1999).

The laboratory results indicate the components of remenant magnetization low and high stability components (secondary and primary NRM) isolation which have straight line segments respectively. However, isolation of high stability components refer to characteristics remenant

magnetization (primary NRM) with straight line segment directed to the origin of plot (figure 5.1b).

The removing of the secondary components (low stability components) observed by heating the temperature between 0-460°C and the primary components between temperature of 460°C-600°C which acquires ChRM during the rock formation), in the case of AF demagnetization the secondary components (low field components) removed between 0-20mT, some resist specimens 30mT to 60mT and primary (high field component) between 20mT, 30mT- 60mT to end of trajectory vector acquire ChRM (figure 5.1a). The trajectory vector end points are all most linear trend to the origin. When the trajectory vector trend from tail to end point is straight line isolates only the primary components (figure 5.1b).

Alternating Field demagnetization

a

Thermal demagnetization

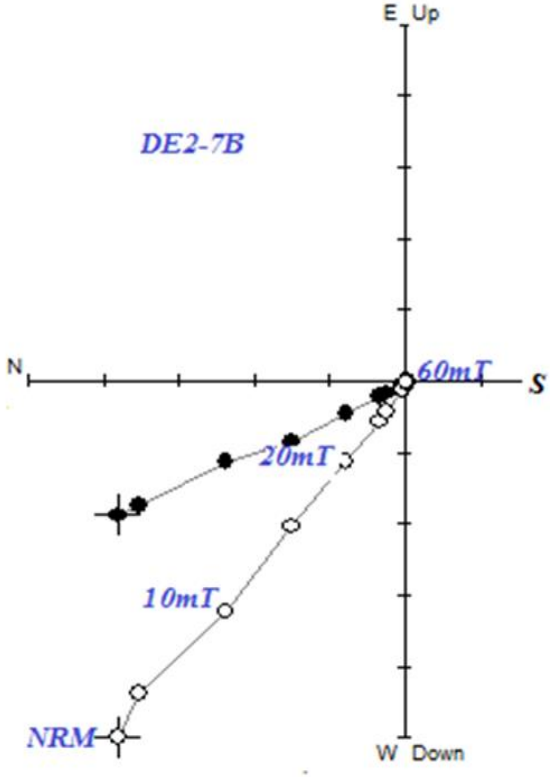

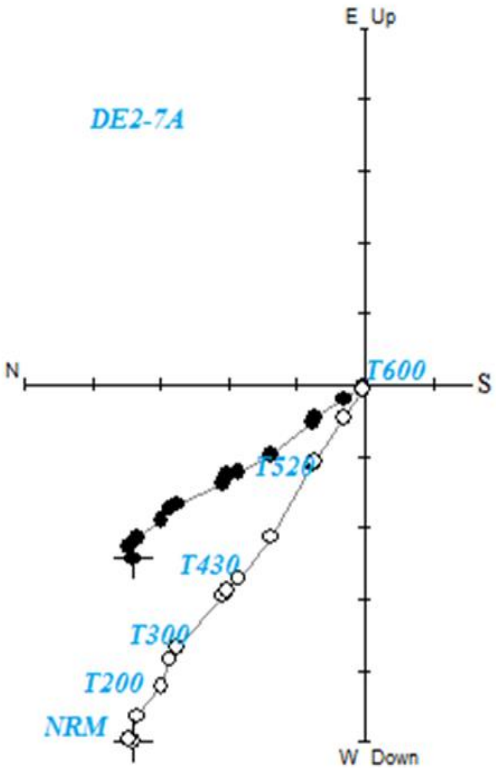

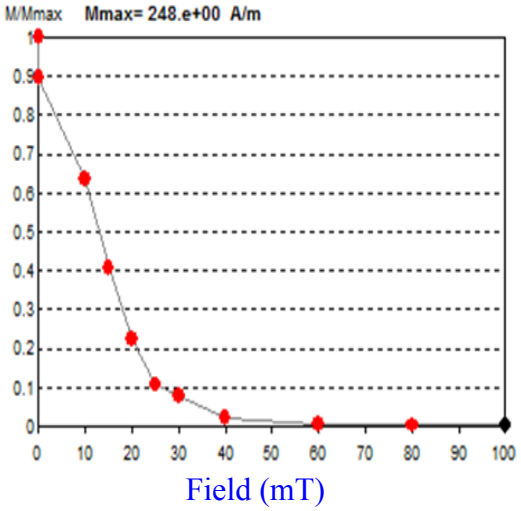

Field (mT)

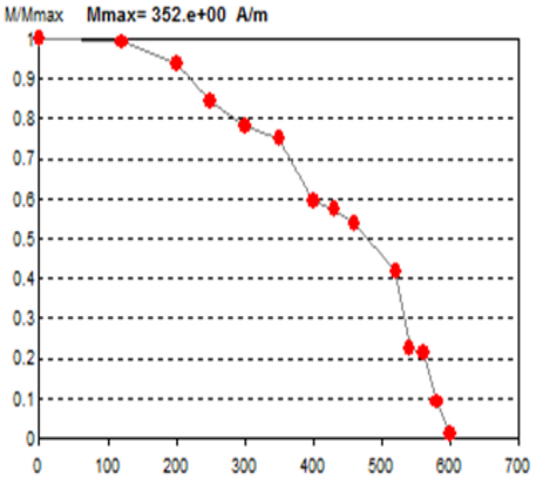

Temperature (˚c)

Alternating Field demagnetization

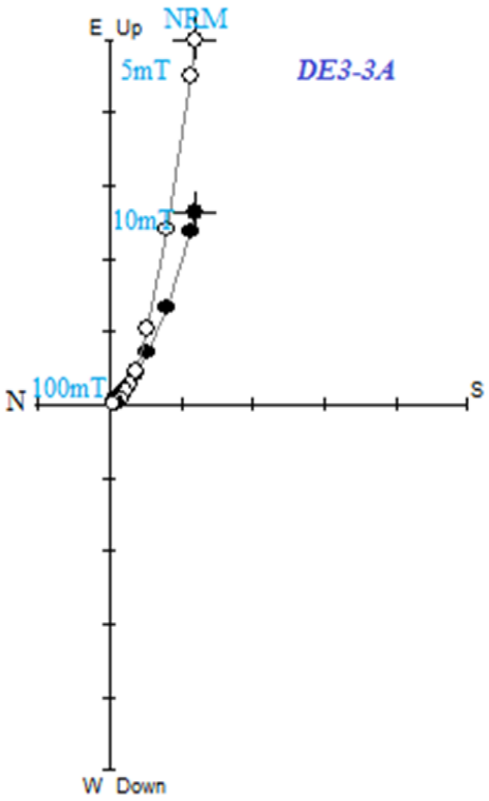

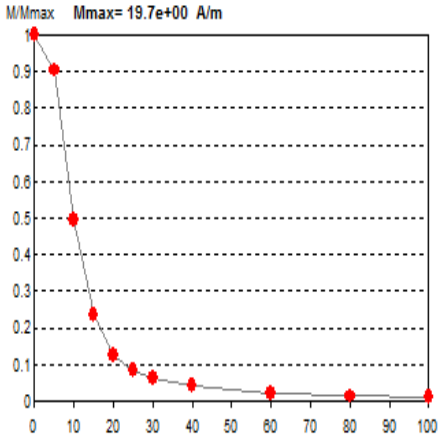

Field (mT)

b

Thermal demagnetization

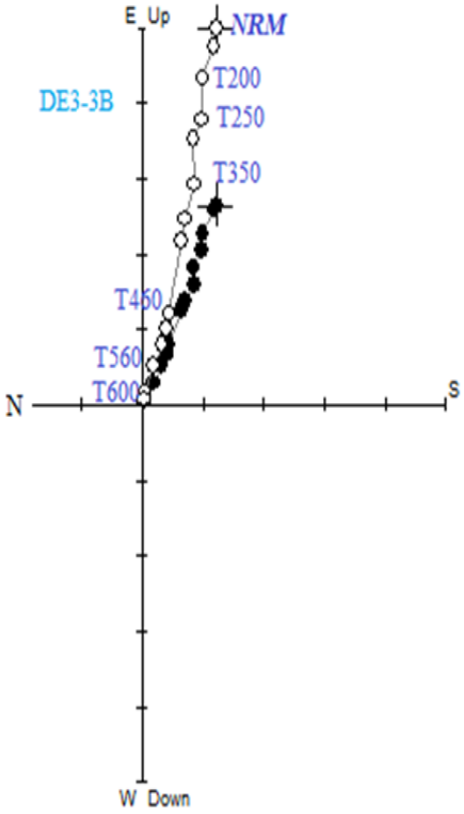

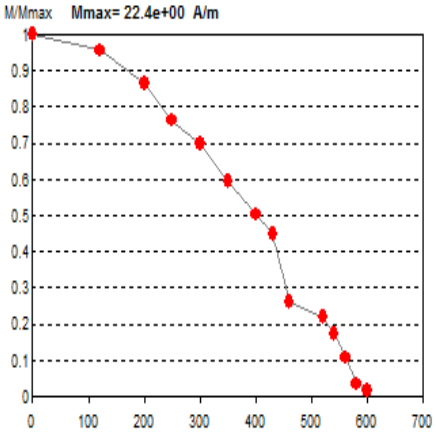

Temperature (˚c)

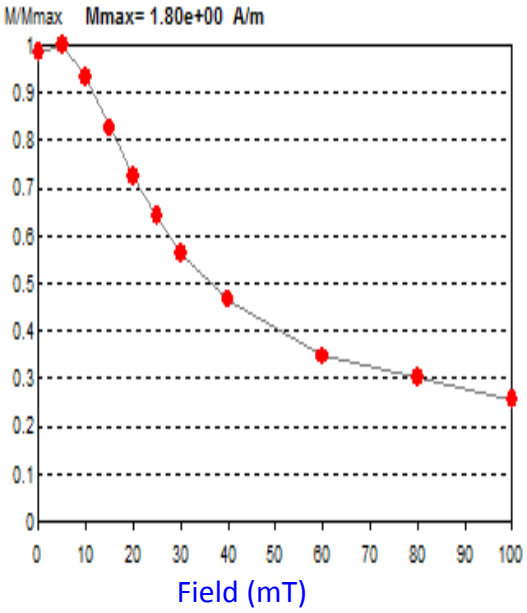

c

Alternating demagnetization

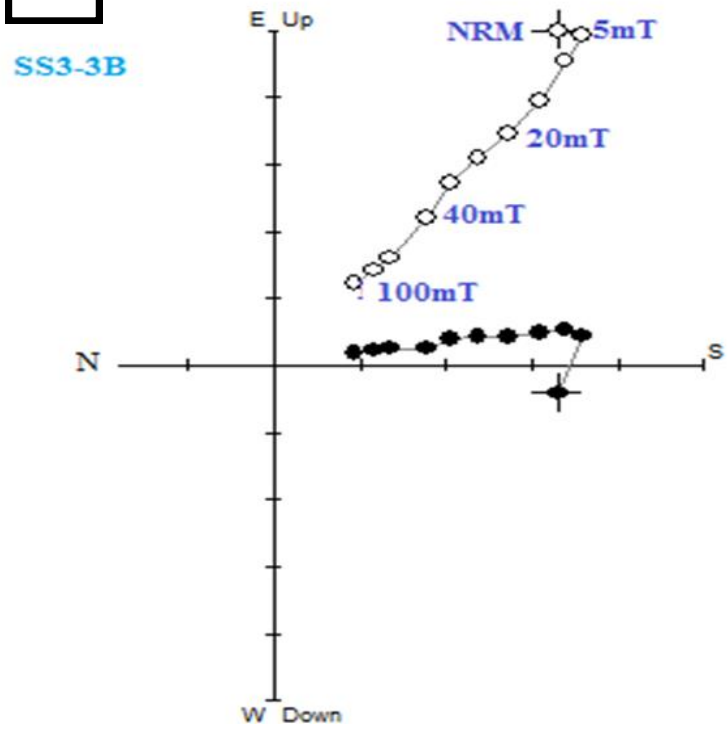

d

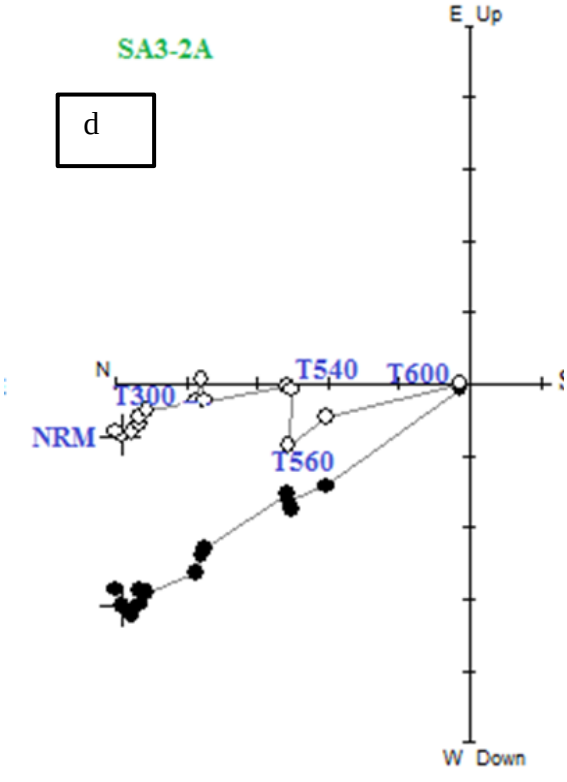

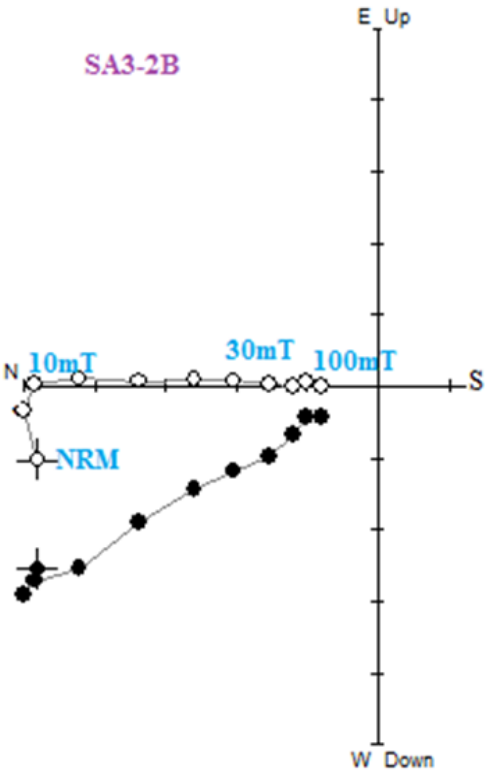

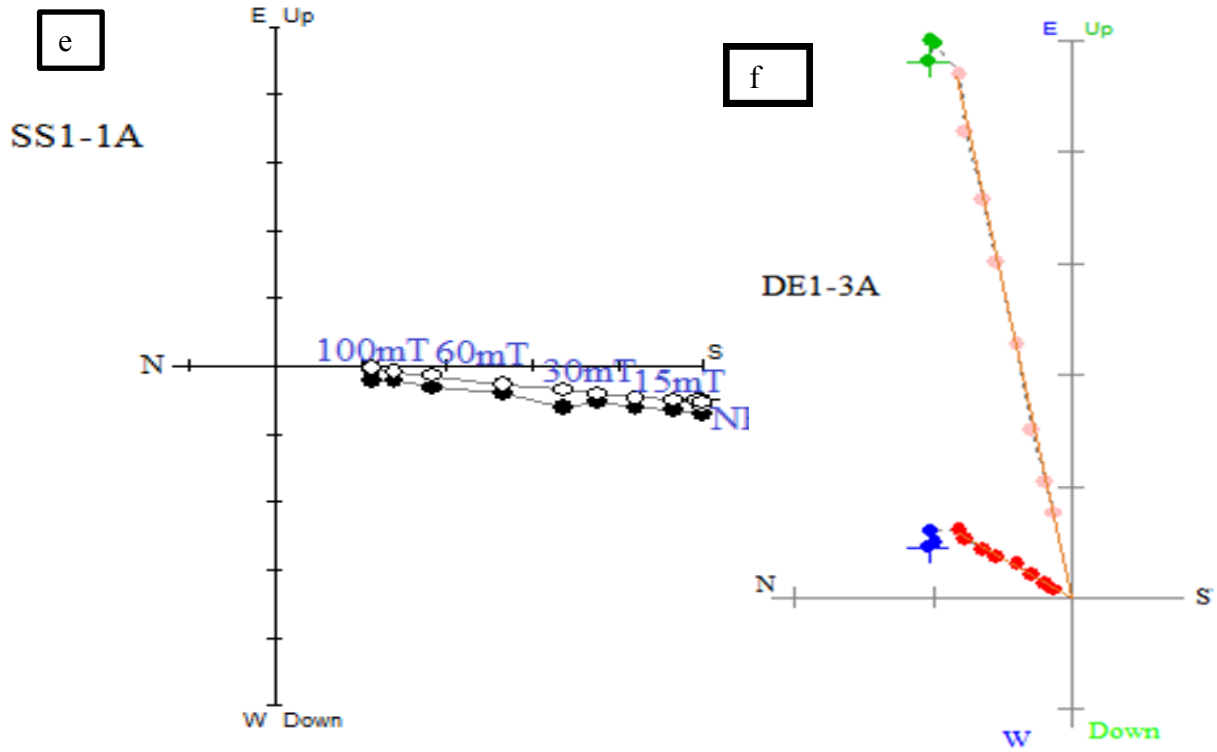

Figure 5.1.Vector component of demagnetization diagrams were done by TH demagnetization and AF demagnetization for typical twin specimens. Specimens shown on the same lines are the same core sample, solid circle symbol indicate the projection component in the horizontal plane (N-S verses E-W) and open circle symbol indicate the projection component in the vertical plane (N, E-Up to S, W-Down), display normal and reverse polarities from the measured representative paleomagnetic specimens. Whereas illustration the magnetic moment (M) of Alternating (AF) and Thermal demagnetization (TH) for typical specimens. (a) Shows Zijderveld (orthogonal vector) diagram summited to TH and AF demagnetization, which isolates ChRM to 20mT and 460°C respectively. (b) Orthogonal vector shows a trajectory toward the origin with no significant change in direction of NRM. (c) In this vector component AF demagnetization first cleaned 55% up to 40 mT, isolation ChRM cleaned 75% at 100mT. (d) vector component demagnetization diagram of overlapping components sample display low temperature up to about 300°C, intermediate components about 400°C up to 460°C and 540°C up to curie temperature the high temperature component. (e) This vector component shows reversed for representative paleomagnetic samples. (f) Example for orthogonal vector components which show a straight line segments directed towards the origin.

5.2. Rock magnetic analyses

The ferromagnetic minerals identification in a rock is used to determine a particular component of NRM (from progressive demagnetization and magnetization) with a particular rock magnetic mineral (identified from acquisition data and progressive TH demagnetization).The rock magnetic experiments have carried out for selected representative 9 specimens in order to characterize saturation magnetization and Curie temperature. The procedures used to identify rock magnetic minerals from magnetization (IM) and demagnetization (TH) data by Curie temperature and Coercivity spectrum analysis respectively. To identify the rock magnetic minerals is required for understanding acquisition of palemagnetic recording in rocks and at elevated temperatures, determine the composition.

5.2.1. IRM acquisition and measurements

Natural IRM can form as a secondary component of IRM by exposure to transient magnetic fields of lightning strikes.

The IRM acquisition by exposing of the specimen to a magnetizing field (H), using impulse magnetizer (IM-10), measurement of the result IRM using spinner magneto meter. The procedure in coercivity spectrum analysis is to induce isothermal remanent magnetization (IRM) by a magnetizing field (H), measure resulting IRM, then continuous acquisition by using a magnetizing field.

The field is produced by discharge of energy from the capacitor bank through a coil surrounding the sample cavity which the desired voltage corresponding to the field shown (figure 5.2.1a).

Then continuous acquisition by using the stronger magnetizing field with the following magnetizing steps were 32.5mT, 49.4mT, 66.6mT, 83.6mT, 168mT, 253mT, 337mT, 504mT, 666mT, 831mT, 994mT and 1154mT.

The saturation magnetization (Js) of ferromagnetic titanohematite ranging up to 480G whith microscopic coercive force, hc ≤300mT whereas saturation magnetization (Js) of titanohematite up to 2–3G with microscopic coercive force (hc) 1T.

When the Sample containing titanomagnetite acquires IRM in H 300mT, with no additional IRM is acquired in higher H, Sample containing hematite IRM is acquired up to 3T.

The IRM acquisition and associated measurement curve shown in (figure 5.2.1b, c, d, e, f, g and h) for the representative sample among 9 measured specimens for representative paleomagnetic site.

The investigated samples rise steeply at lower IRM fields from 0 to168mT and 0 to 253mT indicating magnetite contribution reach saturation and before 168mT no contribution of hematite (figure 5.2.1c and a, e respectively). Samples containing titanomagnetite rapidly acquire IRM steeply rise up to 253mT (80% magnetization) followed by gradual acquisition of additional IRM in strong H (figure 5.2. 1b).

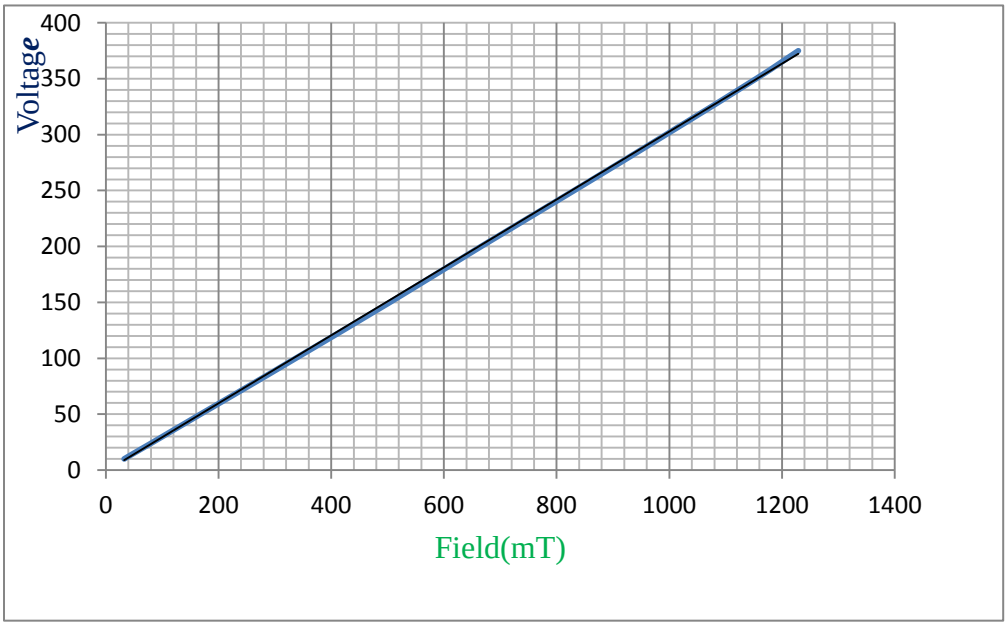

.

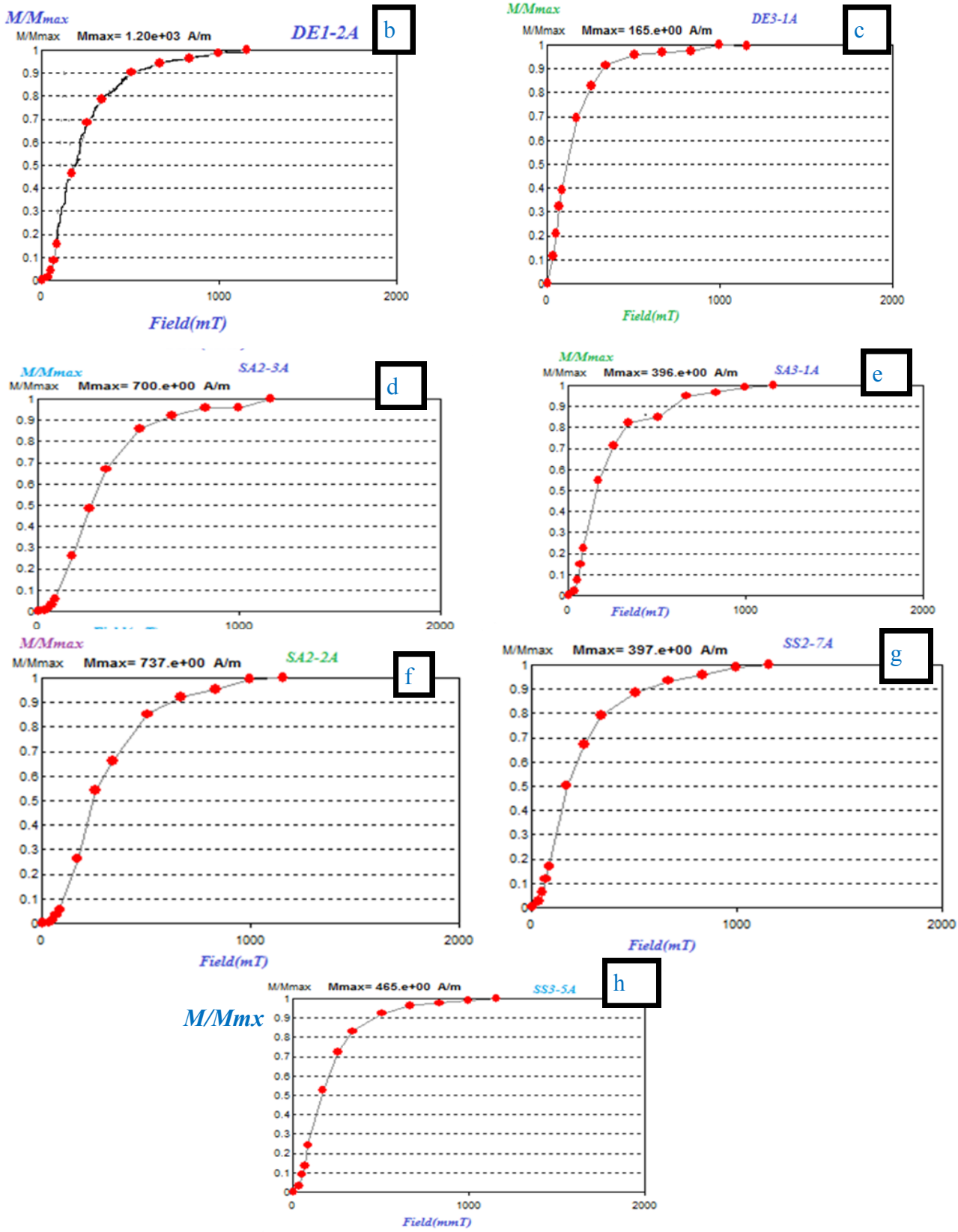
M/Mmax
M/Mmax Mmax= 1.20e+03 A/m
DE1-2A
b
Field(mT)
M/Mmax
M/Mmax Mmax= 165.e+00 A/m
DE3-1A
c
Field(mT)
M/Mmax
M/Mmax Mmax= 700.e+00 A/m
SA2-3A
d
M/Mmax
M/Mmax Mmax= 396.e+00 A/m
SA3-1A
e
Field(mT)
M/Mmax
M/Mmax Mmax= 737.e+00 A/m
SA2-2A
f
Field(mT)
M/Mmax Mmax= 397.e+00 A/m
SS2-7A
g
Field(mT)
M/Mmax Mmax= 465.e+00 A/m
SS3-5A
h
M/Mmx
Field(mmT)

Figure 5.2.1.Acquisition IRM of basalt which shows pattern of magnetization curves. (a) desired voltage which correspond the desired field, (b) The curve steeply rise up to 504mT with 90 % magnetization which contribute magnetite where as 10% is contribute hematite, 666mT to 1154mT. (c) In this curves all most the contribution of magnetite steep rise up to 337mT then reaches saturation 95%. (d, f, g, h) The magnetization curve smooth which shows the contribution of magnetite up to10% to 85%, and 15% is hematite but below 10% there is contribution of titanomaghemite as compare to the TH demagnetization magnetization (figure 5.2.1, 350°C -460°C).

5.2.2. Thermal demagnetization curves (TH)

The TH demagnetization laboratory was conducted for determine the composition of the NRM carrying magnetic minerals from collected representative paleomagnetic samples.

IRM decreases during TH demagnetization as blocking temperatures were reached. Major decreases in IRM during TH allow estimation of Curie temperatures because maximum blocking temperatures are less than the Curie temperature**.** A Curie temperature of 580°C is evident for magnetite, 680°C Curie temperature for hematite. Thermal demagnetization curve of a magnetic separate from basalt rock is illustrated in Figure 5.2.2A. The samples were heated up to a temperature of 640˚c. In (figure 5.2.2A. a, e and c) heating curve between 580°C to 620°C , 520°C to 600 °C for the representative sample of DE1-2A and DE3-1A respectively. These Curie temperature indicates the most ferromagnetic minerals carried out Ti-poor titanomagnetite for the representative samples were analyzed. Sample SA3-1A, SA2-2A, DE2-4A and SS2-7A showed different behavior with heating curve (figure 5.2.2A. b, d, e and f). In this curve observed between 540°C to 600°C and the second curve between 600°C and 640°C indicates due to Ti-poor magnetite and titanohematite respectively (figure 5.2.2A. b) and figure 5.2.2B. In (figure 5.2.2A. e) the first heating curve between and 200°C to 308°C probably due to the presence of titanomaghemite according (Yamamoto&Tsunakawa 2005; Mochizuki et al. 2011), the second curve 520°C to 580°C due to the presence of poor Ti- titanomagnetite or pure magnetite and the third heating curve observed between 600°C to 640°C due to low content of titanohematite. However, in (figure 5.2.2A. f) showed heating curve display between 400°C to 500°C explains due to the presence of maghemite (Larson and Walker, 1975).

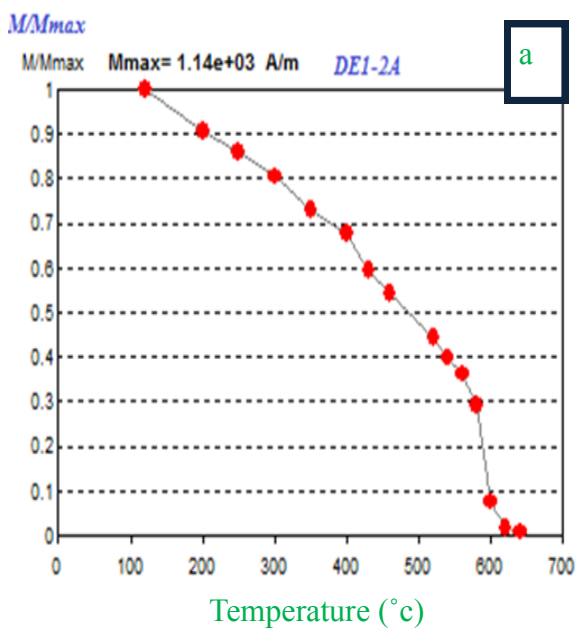
M/Mmax
M/Mmax Mmax= 1.14e+03 A/m
DE1-2A
a
Temperature (˚c)

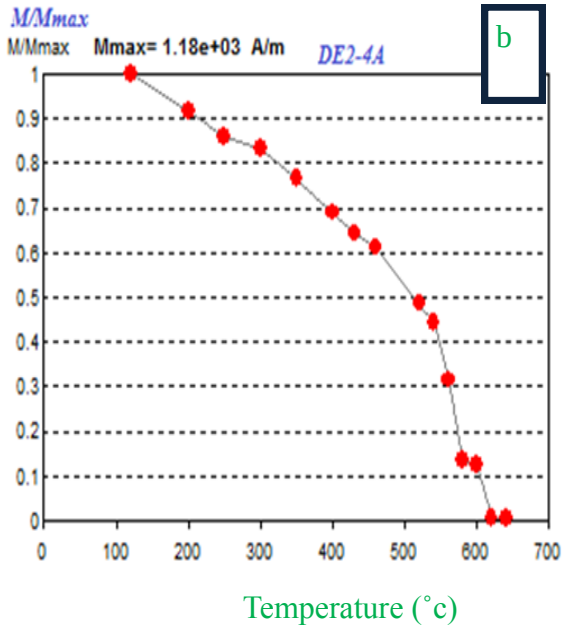
M/Mmax
M/Mmax Mmax= 1.18e+03 A/m
DE2-4A
b
Temperature (˚c)

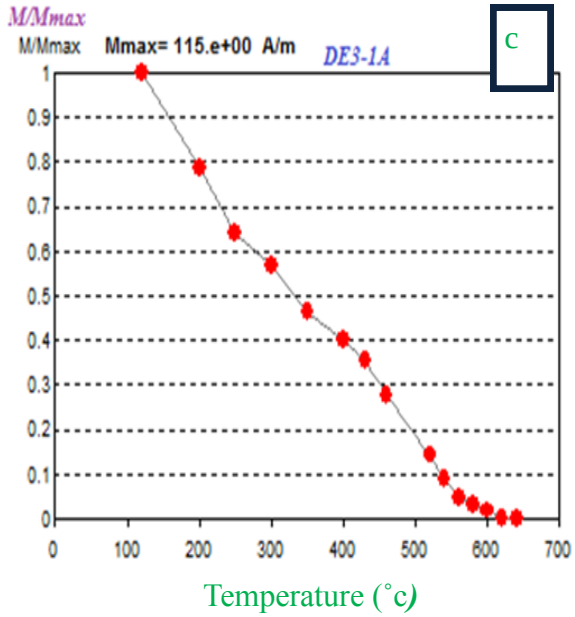
M/Mmax
M/Mmax Mmax= 115.e+00 A/m
DE3-1A
c
Temperature (˚c)

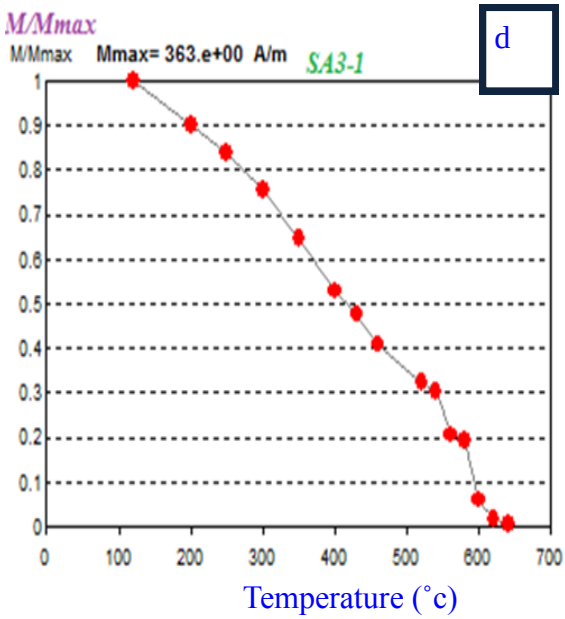
M/Mmax
M/Mmax Mmax= 363.e+00 A/m
SA3-1
d
Temperature (˚c)

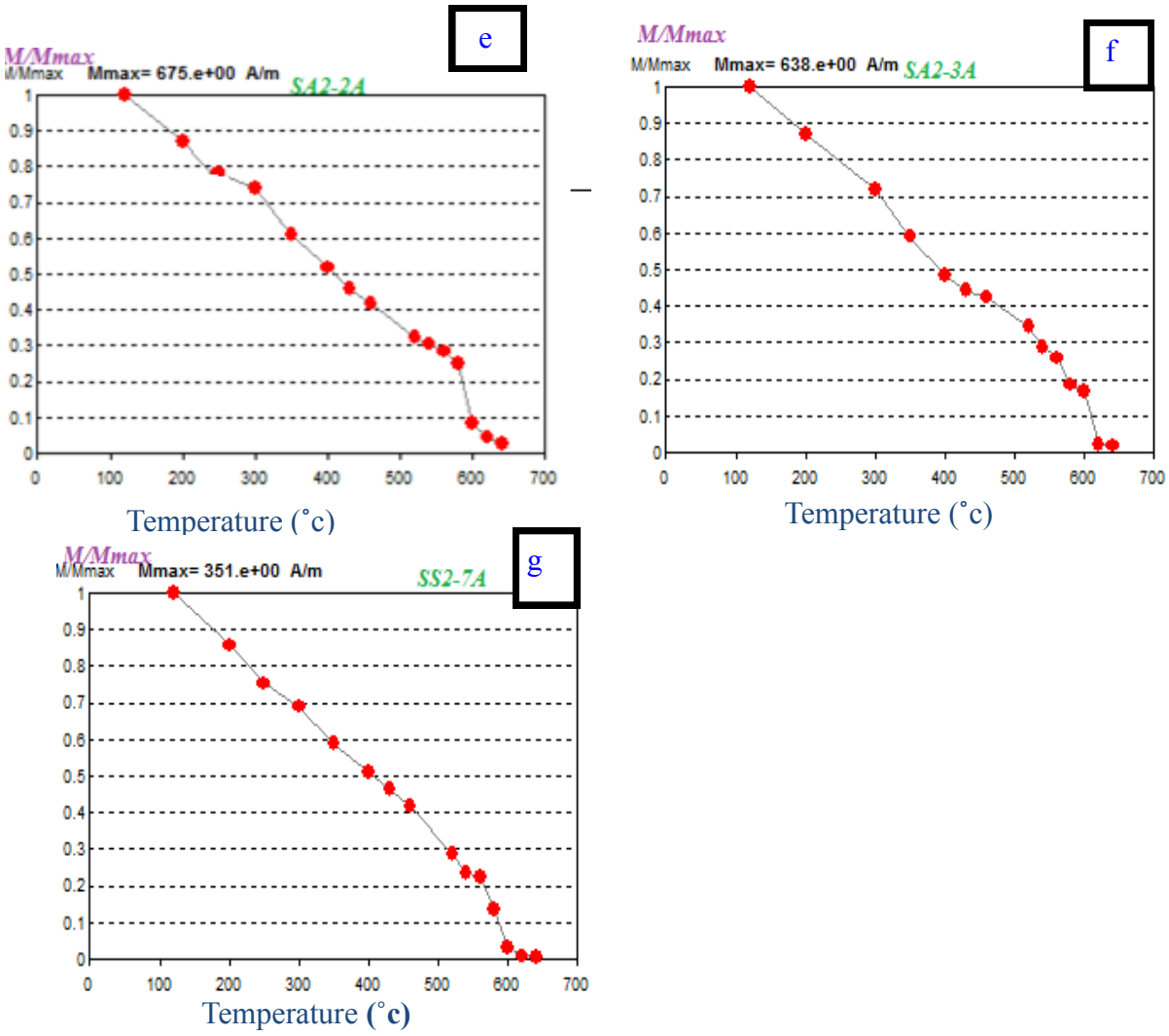

Figure 5.2.2A.Thermal demagnetization curves for representative samples and shows single or multiple heating curves.

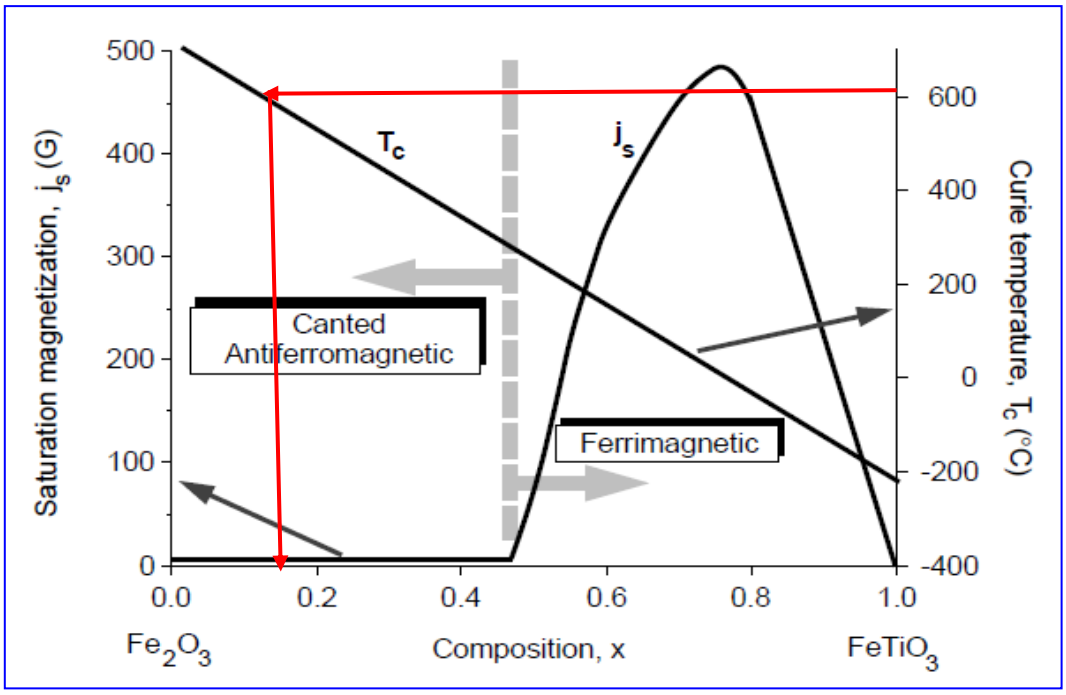

Figure 5.2.2B.Curie temperature for titanohematite series. Composition is indicated by parameter x; the left axis indicates saturation magnetization (js); the right axis indicates Curie temperature (TC). At Curie temperature of 620°C to 640°C the composition indicates approximately 0.15 which explains Ti- poor titanohematite (Nagata 1961).

5.3. Paleomagnetic Direction

By Paleomagnetism application detect displaced with respect to a paleomagnetic pole; determine displace of a crustal block with respect to vertical axis. The apparent polar wander (APW) paths of the continent explain how that continent has displaced with respect to the rotation axis. Each reference pole was determined by paleomagnetic analysis of rocks with dated age of the crustal block.

The paleomagnetic directions of the specimen remenant magnetization were removed at the final step of progressive demagnetization magnetization process.

The specimens low stability components removed by the AF demagnetization between 10mT-30mT with 85% to 65% demagnetization, in some specimens resisted up to 40mT-60mT with 65% to 50% demagnetization due to the presence of strong microscopic coercive force (figure 5.1.). In the case of TH demagnetization technique the low temperature component removed up to 300°C, intermediate temperature components up to 400°C and 430°C- 460°C of the overlapping components, higher un blocking temperature up to 540°C, highest un blocking temperature up to curie temperature (Kidane et al.,1999).

After progressive demagnetization, isolate the secondary component then determine ChRM direction by illustrating orthogonal vector components in order to identify the linear vector component which a straight line segments directed towards the origin (figure 5.1).

The directions of magnetization for the ChRM direction were determined by best fit lines ((PCA)Kirschvink (1980) for samples that showed stable end segments, whereas remagnetization circles were used to determine the best fitting great circles to determine lower MAD values according to Halls (1976, 1978). The maximum angular devotion (MAD) dominant specimens ChRM less than or equal to 3˚ and no sample had MAD>5˚.

5.3.1. Mean directions

Site mean directions were calculated by using Fischer statistics (Fischer, 1953) for stable line or straight line segment which directed to the origin. The procedures conducts to calculate mean direction of several paleomagnetic data were:

i. When the specimen was prepared more than one from the sample, then ChRM direction for the multiple specimens had been averaged.

ii. A Site mean ChRM direction was calculated from ChRM directions of paleomagnetic samples.

iii. A paleomagnetic investigation involves sites with a particular rock unites. After averaged ChRM direction then determine sit mean direction and paleomagnetic pole position of the rock unit (table 1).

The figure below shows the site mean declination directions together with expected declinations values were reported as line and arrow respectively (figure 5.3.1.). The pattern of declination counter clock wise vertical rotation in the study area. As Muluneh et al (2013) the observed paleomagnetic distribution site mean declination silsa area, similarly there is counter clock wise vertical rotation and as Kidane et al (2003) in the Unda-Gamarri (Central Afar) shows small magnitude counter clock wise vertical rotation.

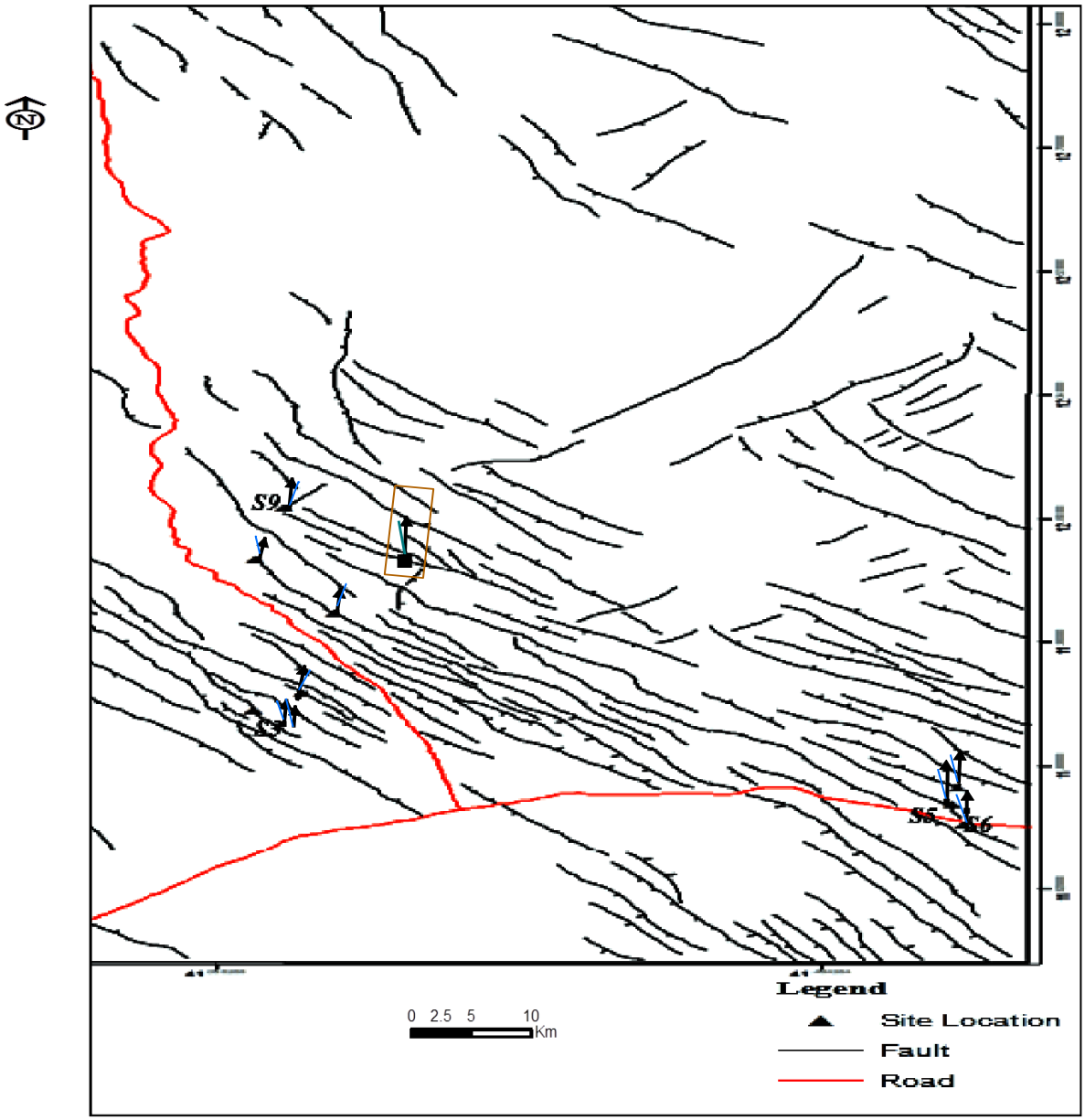

Figure 5.3.1.Map of the study area which shows the distribution of the paleomagnetic site mean direction, line describe the observed site mean; arrow shows the expected mean direction whereas the rectangle shows the overall site mean direction.

The individual site mean ChRM direction calculated for all the 9 paleomagnetic sites were reported table1 below.

Table 1 paleomagnetic site mean for all analyzed rocks ChRM direction from central Afar for 9 sites Dechotto, Saha and Silsa which are name indicated locality site of DE, SA and SS respectively. Then the overall paleomagnetic sites mean ChRM direction is reported.

Site Name	Latitude	Longitude	N	Ds	Is	K	α95
DE1	11.91	41.6	7	161.5	-18.8	77.5	6.9
DE2	11.92	41.6	4	160.2	-43.2	27.9	17.7
DE3	11.88	41.62	8	160.9	-17.5	74.8	6.4
SA1	12	41.2	4	193.1	6.4	182	6.8
SA2	11.98	41.15	5	355.6	0.1	78.5	8.7
SA3	11.98	41.15	4	341.5	6.9	73.8	10.8
SS1	12.07	41.25	5	191.2	14.9	113.3	7.2
SS2	12.13	41.2	7	162.1	-15.8	100.4	6.1
SS3	12.18	41.18	3	184.3	-29.1	67.8	15.1
Mean1			9	352.5	12.5	13.2	14.7
Mean2			7	352.3	5.6	17.7	14.8
Expected mean			26	359.7	16.4		5.7

Site mean; latitude and longitude were location coordinates in degree; N, number of samples; Ds and Is are declination and inclination of stratigraphic coordinates in degree; K, Fischer precision parameter; too large α95, 95% confidence interval, due to transitional direction which increase α95.

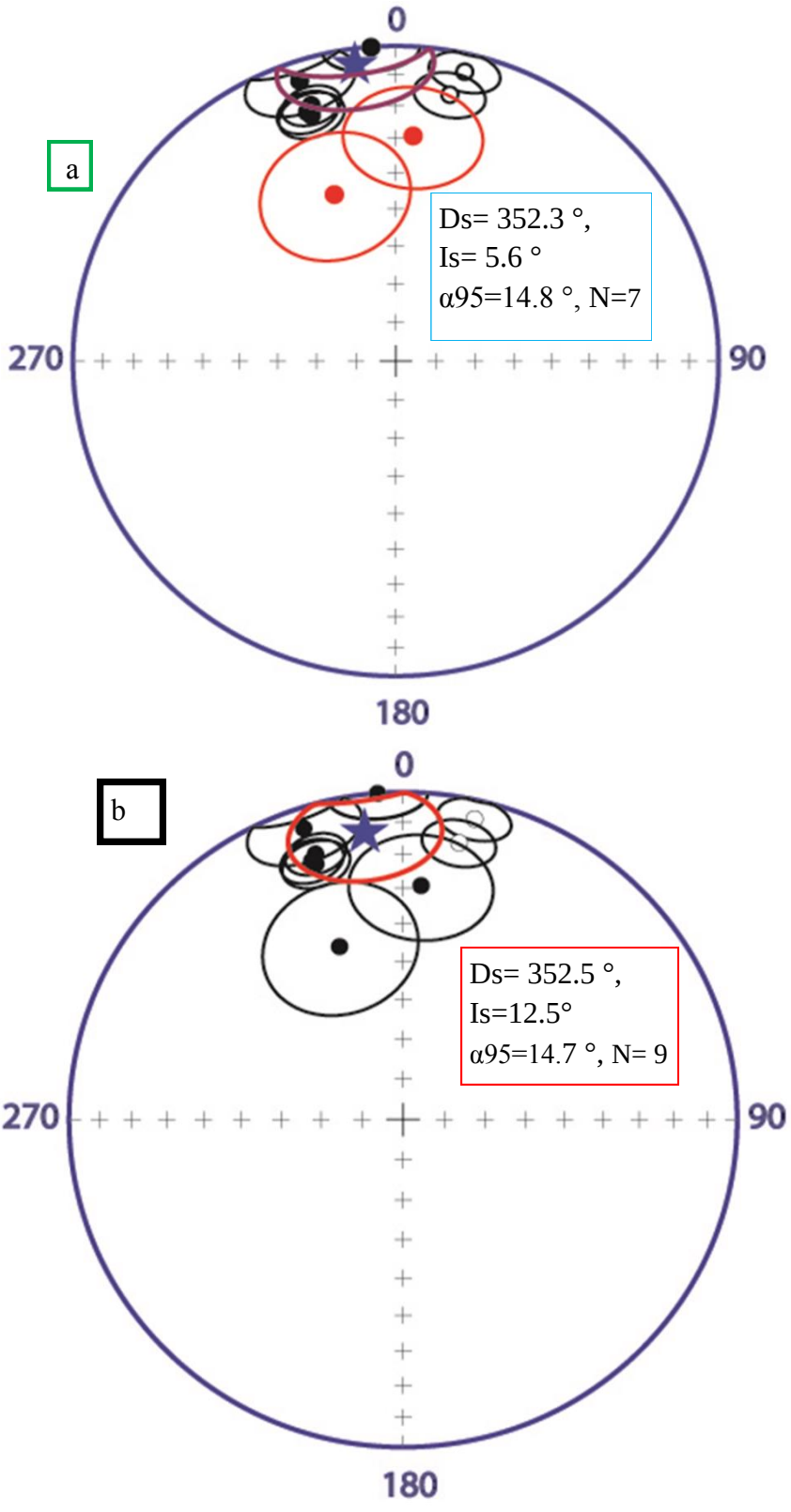
a
0
270
90
180
Ds= 352.3 °,
Is= 5.6 °
α95=14.8 °, N=7
b
0
270
90
180
Ds= 352.5 °,
Is=12.5°
α95=14.7 °, N= 9

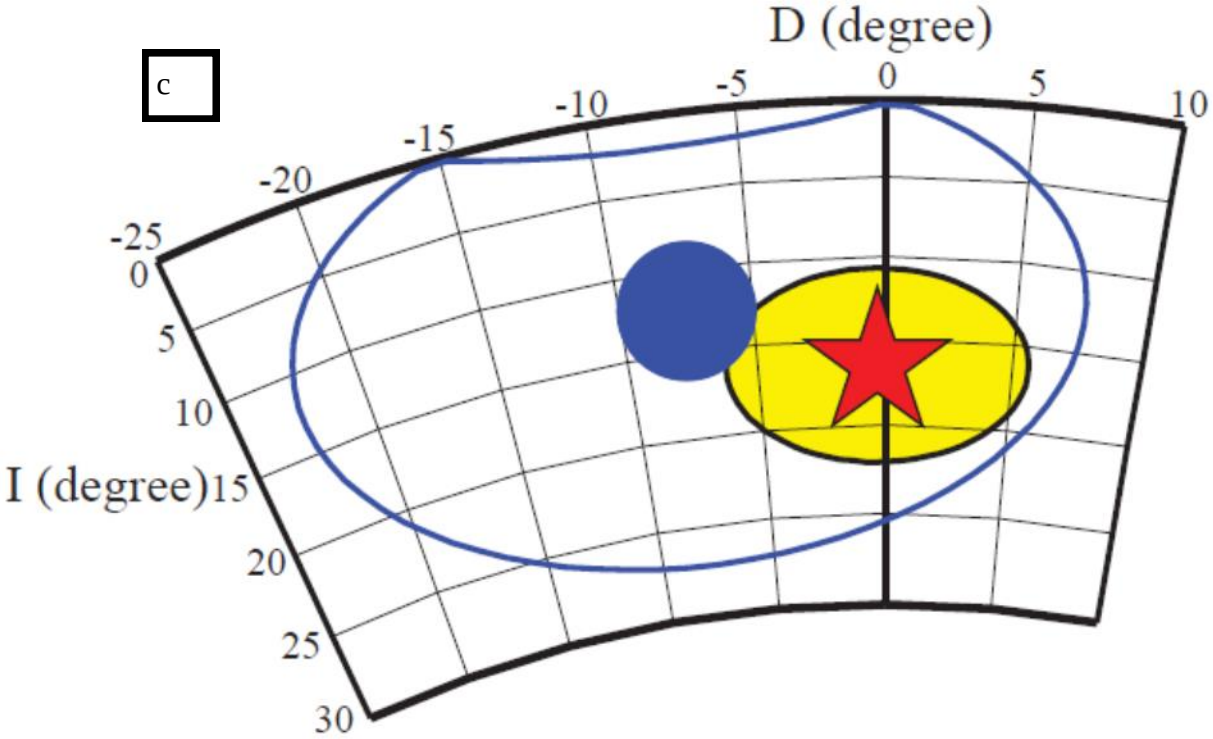

Figure 5.3.1.Paleomagnetic mean direction. (a) Stereographic projection of characteristic remenant magnetic direction from the site of basalt in the study area and site mean ChRM direction (blue star with 95% confidence interval (pink color)) which exclude 2 site mean**. (**b) Stereographic projection of ChRM direction for the overall Fisherman means direction (blue star with 95% confidence interval (red color)). Solid circle indicates for lower hemisphere and open circle for upper hemisphere NRM directions.

(c) The comparison of the observed overall mean direction (blue circle) and expected direction (red star symbol) the two directions are with in α95, 95% confidence interval of the calculated mean, the directions are not distinguish due to α95 large McFadden and McElhinny, 1964 statistically difficult to analyzed and they are not significant different due to small number of site (with 9 site of 55 samples and 87 specimens).

Table 2. shows the values of declination and inclination difference with expected and obserbed direction.

	D	*I*	*α95*	R±ΔR	*F*±Δ*F*
Expected Mean	359.7	16.4	5.7	-2.7±6.6	-0.7±6.3
Observed Mean	352.5	12.5	14.7	-7.2±6.2	3.9±3.2

The vertical-axis rotation R and the flattening of inclination F were calculated by the following equations:

$$R = D_o - D_X$$

$$F = I_x - I_O$$

The original method to calculate confidence limits to R and F was to treat the errors in the observed and expected directions as independent errors and calculated by the following equations (Demarest 1983).

$$\Delta R = 0.8\sqrt{\Delta D_o^2 + \Delta D_x^2}$$

$$\Delta F = 0.8\sqrt{\Delta I_o^2 + \Delta I_x^2}$$

The normal and reverse polarity indicate positive reversal test indicates that the ChRM directions are free from secondary NRM and isolate ChRM (McFadden and McElhinny, 1990), when the reversal polarities changed to their normal polarity part, then overall site mean is calculated with 2 normal polarity and 7 reverse polarity are showed and results are obtained for the Ds= 352.5°, Is = 12.5°, K= 13.2, α95= 14.7°, N= 9 and Ds= 352.3°, Is= 5.6°, α95=14.8°, K=17.7, N= 7.

5.4. Discussion

5.4.1.Tectonic Rotation

The expected average dipole field direction based on the Apparent Polar Wander Path reference curve for Africa (Besse & Courtillot ,2002, Kidane et al.,2003) is obtained (Ds= 359.7°, Is = 16.4°, α95 = 5.7°).

The paleomagnetic observation on the 9 site of Gulf basalt (dated between 0.6 and 1.1Ma Kidane et al., 1999 and Lahitte, 2000) inclination and declination difference of the all and reduced site with expected mean paleomagnetic directions; ΔD =-7.2°, ΔI =3.9° and ΔD=-2.7°, ΔI =-0.7°. These difference of declination and inclination with their un certainty explained by a rotation about a vertical axis (R±ΔR) and inclination flattening (F±ΔF) respectively. The vertical axis rotation of the overall site mean direction is: -7.2±6.2; inclination flattening is 3.9±3.2 (figure 5.3.2c and table 2) and the resulted value indicates there is block rotation with vertical axis counters clockwise rotation; this observed counterclockwise rotation cannot be due to the major overlap between the NW propagating Gulf of Aden Ridge and SE propagating Red Sea Rift but locally due to small rift propagation (figure 5.4.1). The age determinations in the studied area show that the time bracketed by the sampled basaltic rock units (0.03 Ma to 1.11 Ma: Lahitte et al., 2003), The dextral shear at the northern boundary of the major overlap and the new overlap develop a dextral shear on the existing NW-oriented fault blocks which causes counterclockwise by bookshelf faulting (Hofstetter and Beyth , 2003).The dextral normal faults trend of NW and SE and Dabbahu volcano explains sinisterly shear at the extremities of the major overlapping rifts (Rowland et al., 2007). The paleomagnetic indicate vertical axis counter clock wise rotation. The strain transfer model for the overlap zone between the two arms of the propagators in the Afar triple junction predicts insignificant but clockwise rotation in its northwestern sector (Manighetti, 1993). The paleomagnetic studies in the area indicate no significant rotation. However, it shows locally small vertical axis counter clock wise rotation due to the propagation of small Rifting (0.65Ma Lahitte et al., 2001) with the sense of sinisterly shear which affect to in the study area small vertical axis counter clock wise rotation (figure 5.4.1). Locally the blocks small displace towards left which shown below.

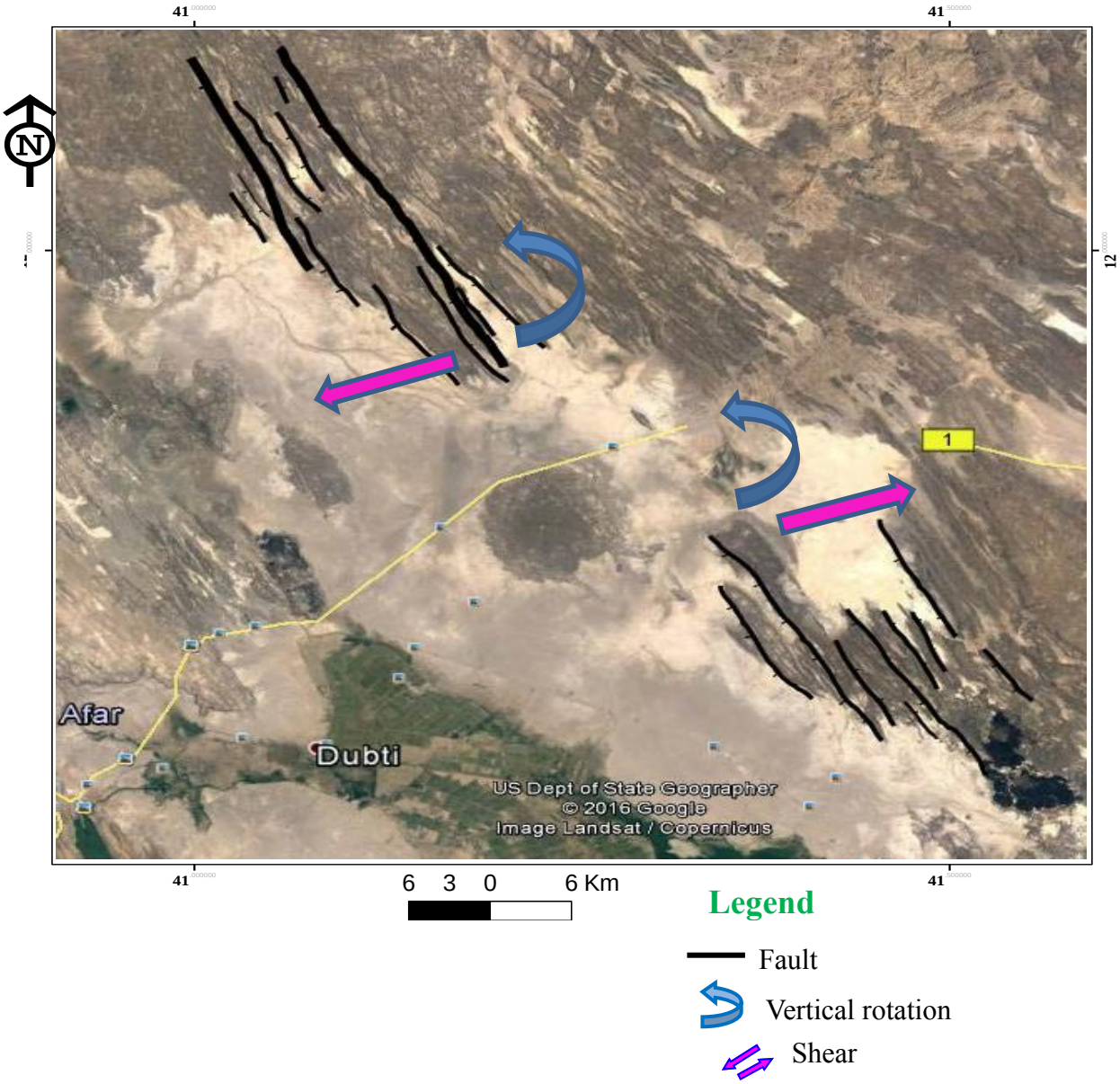

Figure 5.4.1.Tectonic rotation of the study area which locally shows sinisterly sense of shearing due to the propagation of small rifting, acts as counter clock wise block rotation.

5.4.2. Virtual Geomagnetic Polarity (VGP)

Pole position is calculated from a single observed mean direction of the geomagnetic field is termed as a virtual geomagnetic pole (VGP). The virtual geomagnetic pole position determines from calculated a single site-mean ChRM direction, then determine the mean of virtual geomagnetic pole. These pole position calculated from a single site-mean ChRM direction is a virtual geomagnetic pole. The mean of paleomagnetic pole is, λ= 80.9°, ϕ =277.8°, K = 22.8, α95 =11° is calculated from the set of VGP by Fischer statistics and treating each VGP as a point in stereographic projection for the 9 site considered. This result statically related to the value, λ =80.9°, ϕ = 221.9°, K= 14.4, α95 = 7.2° (Kidane et al., 1999) for stable part of Africa about ~2Ma of Gamarri Section. The study area sites mean VGP displayed in figure 5.4.2. The lava flow includes normal and reverse polarities in different sites and the VGP scatter indicates the paleosecular variation of the geomagnetic field.

Table 3 site mean virtual paleomagnetic pole (VGP) for all analyzed sites which explain the paleomagnetic pole and mean paleomagnetic pole of 9 sites.

Site name	**N**	**ϕ**	**λ**	**K**	**α95**
DE1	7	126.3	71.7	3.7	7.2
DE2	4	169.6	67.1	13.6	22
DE3	8	124.6	71	3.4	6.6
SA1	4	359.8	70	3.4	6.8
SA2	5	241.6	77.3	4.4	8.7
SA3	4	287.7	69.8	5.5	10.9
SS1	5	11.2	67.4	3.8	7.4
SS2	7	119.9	71.9	3.2	6.3
SS3	3	271.8	84.6	9.2	16.8
Mean VGP	9	277.8	80.9	22.8	11

Site name; N, number of samples; ϕ, pole longitude; λ, pole latitude; K, Fischer precision parameter; α95, 95% confidence interval.

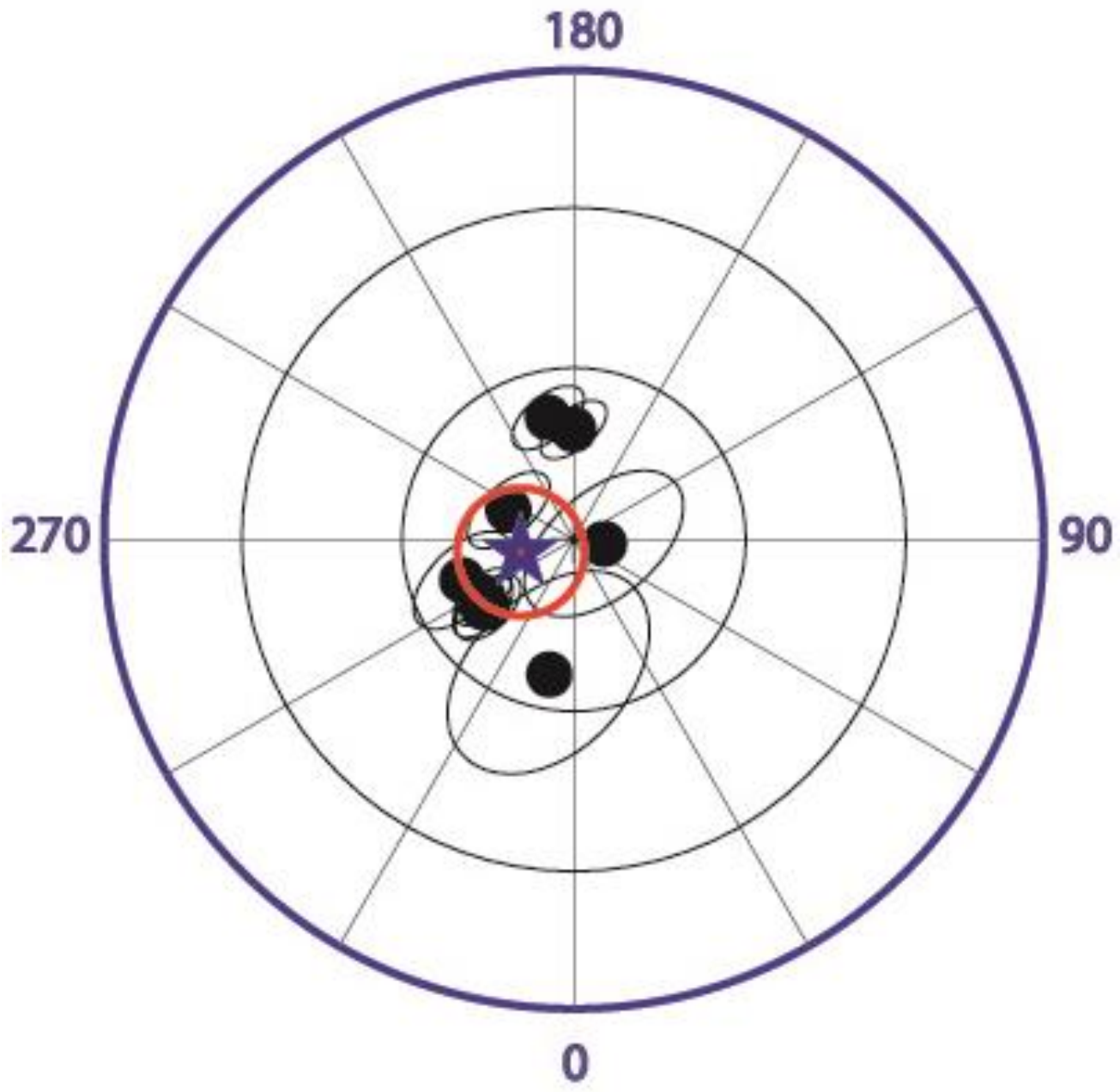

Figure5.4.2.Stereographic projection of virtual geographic polarity (VGP) of calculated mean pole, star symbol shows the mean VGP.

6. CONCLUSION AND RECOMMENDATION

6.1. Conclusion

This paleomagnetic investigation was done on 9 times independent lava flows (paleomagnetic sites). A total of 55 oriented core samples were collected from these sites. The core samples were oriented by using both magnetic and sun compass from the field. The samples were taken from basalt with the age of 0.03 to 1.1Ma (Gulf basalt) (Kidane et al., 1999 and Lahitte, 2000). The magnetic rock mineral studies indicate that the magnetic mineral carried high stability natural remenanet magnetizations were magnetite and Ti-poor titanomagnetite and low percentage of hematite saturated. In some samples secondary natural remenanet magnetization of maghemite and titanomaghemite minerals were saturated. These were determined by the Curie temperature and coercivity spectrum analysis with combination of thermal demagnetization and magnetization.

The high stability characteristic remenant magnetization isolated during AF demagnetization the field greater than 10mT up to 30mT and some specimens 40mT up to 60mT were as thermal demagnetization greater than 400°C.

A direction of magnetization was determined mostly by best fitted straight line in the Zijderveld diagram. The ChRM direction for all multiple specimens were averaged and the individual site mean ChRM direction calculated, then the overall site mean direction calculated.

The paleomagnetic mean flow direction from a total 9 flows, 7 flows are reverse polarity (2 flow normal polarity) of recent (Gulf) basalt, resulted over all mean direction: Ds= 352.5 °, Is= 12.5°, K= 13.2, $\alpha 95$=14.7 °, N= 9, were as obtained overall mean paleomagnetic direction is compared with expected direction (Ds= 359.7°, Is=16.4°, $\alpha 95$ = 5.7°) calculated from the Apparent Polar Wander Path reference curve for 1Ma / Mile- Gewane Ali Sabieh, (Kidane et al.,2003), Africa for 1Ma (Besse and Courtillot ,2002). The comparison shows a mean vertical axis rotation: R =-7.2±6.2; the inclination flatting: F=3.9±3.2. The mean paleomagnetic pole is calculated from the set of VGP, λ= 80.9°., ϕ =277.8°. , K = 22.8, $\alpha 95$ =11°. The paleomagnetic studies in these study area recommended, no significance rotation or locally indicate small counter clock wise vertical axis rotation due to the small young propagating rifting.

6.2 Recommendations

The ragged morphology and access of the area requires detailed study lithology unite and not reported (were as studied paleomagnetic technics were done).

The paleomagnetic results should be accompanied with chronology and microscopy techniques such as: optical microscopy, electron microprobe and SEM for future detail studies for rock magnetic analysis.

Due to few number of paleomagnetic site of collected sample, requires many paleomagnetic site with adequate time in order to further detail studies.

The paleomagnetic study of the triple junction in the Afar is required regional deformation in Northern Ethiopia rift prior to advanced modeling and the geology of the area is requires further detail study in this region.

Reference

1. Audin, L., 1999, Pe´ne´tration de la dorsale d'Aden dans la de´pression Afar entre 20 et 4 Ma, 318 p.
2. Acton, G., Tessema, A., Jackson, M., Bilham, R., 2000. The tectonic and geomagnetic significance of paleomagnetic observations from volcanic rocks from central Afar. Earth and Planetary Science Letters 180, 225–241.
3. Acton, G.D., Stein, S., Engeln, J.F., 1991. Block rotation and continental extension in Afar: a comparison to oceanic microplate systems. Tectonics 10, 501–526.
4. Barberi, F., Varet, J., 1977. Volcanism in Afar: small-scale plate tectonic implications, Bull. Geol. Soc. Amer., 88, 1251–1266.
5. Bellahsen, N., C. Faccenna, F. Funiciello, J. M. Daniel, and L. Jolivet (2003), why did Arabia separate from Africa? Insights from 3-D laboratory experiments, Earth Planet. Sci. Lett., 216(3), 365–381, doi: 10.1016/S0012-821X (03)00516-8.
6. Besse, J., and V. Courtillot (2002), Apparent and true polar wander and the geometry of the geomagnetic field in the last 200 million years, J. Geophys. Res., 107(B11), 2300, doi: 10.1029/2000JB000050.
7. Beyene, A. and Abdelsalam, M. (2005). Tectonics of the Afar Depression: A review and synthesis. J.African Earth Sci., 41, 41-59.
8. Butler, R.F., (1992). Paleomagnetisum: magnetic domains to geologic terrains. Oxford, Blackwell scientific publications, Ltd., 319.
9. Cochran, J.R., 1983. A model for development of Red Sea, Amer. Assoc. Petrol. Geol., 67, 41 69.
10. Corti, G., 2009. Continental rift evolution: from rift initiation of incipient break-up in the MER, east Africa.
11. Courtillot, V., Galdeano, A., Le Mouel, J.L., 1980. Propagation of an accreting plate boundary: discussion of a new aeromagnetic survey of the Republic of Djibouti. Earth and Planetary Science Letters 47, 144–160.
12. Courtillot, V., Achache, J., Landre, F., Bonhommet, N., Montigny, R., Feraud, G., 1984. Episodic spreading and rift propagation — new Paleomagnetic and geochronological data from the Afar nascent passive margin. Journal of Geophysical Research 89, 3315–3333.

13. Courtillot, V., R. Armijo, and P. Tapponnier, 1987 Kinematics of the Sinai triple junction and a two-phase model of Arabia– Africa rifting, in Continental Extensional Tectonics, 28, 559–573.
14. Courtillot, V., Jaupart, C., Manighetti, I., Tapponnier, P., Besse, J., 1999. On causal links between flood basalts and continental breakup. Earth and Planetary Science Letters 166, 177–185.
15. d'Acremont, E., S. Leroy, M. Maia, P. Gente, and J. Autin (2010), Volcanism, jump and propagation on the Sheba ridge, eastern Gulf of Aden: Segmentation evolution and implications for oceanic accretion processes, Geophys. J. Int., 180(2), 535–551 551, doi: 10.1111/ j.1365-246X.2009.04448.x.
16. Ebinger, C. J., & N. J. Hayward (1996), Soft plates and hot spots: Views from Afar, J. Geophys. Res., 101, 21,859– 21,876, doi: 10.1029/96JB02118.
17. Faccenna, C., T. W. Becker, L. Jolivet, and M. Keskin (2013), Mantle convection in the Middle East: Reconciling Afar upwelling, Arabia indentation and Aegean trench rollback, Earth Planet. Sci. Lett., 375, 254–269, doi:10.1016/j.epsl.2013.05.043.
18. Fisher, R.A., 1953. Dispersion on a sphere, Proc. R. Soc. A, 217, 295–305.
19. Hofmann, C., Courtillot, V., Féraud, G., Rochette, P., Yirgu, G., Ketefo, E., Pik, R., 1997. Timing of the Ethiopian flood basalt event and implications for plume birth and global change. Nature 389, 838–841.
20. Hofstetter, R.,& Beyth, M., (2003). The Afar Depression: interpretation of the 1960–2000 earthquakes, Geophys. J. Int., 155, 715–732.
21. Jacques, E., J. C. Ruegg, J. C. Lépine, P. Tapponnier, G. C. P. King, and A. Omar (1999). Relocation of M ≥ 2 events of the 1989 Dôbi seismic sequence in Afar: Evidence for earthquake migration, Geophys. J. Int. 138, 447–469.
22. Kidane, T., Carlut, J., Courtillot, V., Gallet, Y., Quidelleur, X., Gillot, P.Y., Haile, T., 1999. Paleomagnetic and geochronological identification of the Reunion subchron in Ethiopian Afar. Journal of Geophysical Research 104, 10405–10419.
23. Kidane, T., Courtillot, V., Manighetti, I., Audin, L., Lahitte, P., Quidelleur, X., Gillot, P.-Y., Gallet, Y., Carlut, J., Haile, T., 2003. New paleomagnetic and geochronologic results from Ethiopian Afar: block rotations linked to rift overlap and propagation and determination of 2 Ma reference pole for stable Africa. Journal of Geophysical Research 108, 1–32.

24. Lahitte, P., 2000. Le volcanisme Plio-Quaternaire lie´ aux me´canismes d'ouverture de la de´pression Afar, Ph.D. thesis, 250 pp., Univ. Paris XI, Orsay.
25. Lahitte, P., E. Coulié, N. Mercier, T. Kidane, and P.-Y. Gillot (2001), Chronologie K–Ar et TL du volcanisme aux extrémités sud du propagateur mer Rouge en Afar depuis 300 ka, C. R. Acad. Sci., Ser. II a: Sci. Terre Planets, 332(1), 13–20.
26. Lahitte, P., Kidane, Tesfaye, Courtillot, V., Bekele, A., Gillot, P.-Y., 2003b. New age constraints on the timing of volcanism in central Afar, and implications on emplacement and rifting. Journal of Geophysical Research 108 (B2). http://dx.doi.org/10.1029/ 2001JB001689, 2003.
27. Larson, E.E.,Walker, T.R., 1975. Development of chemical remanent magnetization during early stages of Red-Bed Formations in Late Cenozoic Sediments, Baja California. Geological Society of America Bulletin 86 (50506), 639–650.
28. Leroy, S., et al. (2012), from rifting to oceanic spreading in the Gulf of Aden: A synthesis, Arabian J. Geosci., 5(5), 859–901, doi: 10.1007/ s12517-011-0475-4.
29. Lister, G. S., and G. A. Davis (1989), the origin of metamorphic core complexes and detachment faults formed during Tertiary continental extension in the northern Colorado River region, USA, J. Struct. Geol., 11(1), 65–94.
30. Manighetti, I., 1993. Dynamique des syste`mes extensifs en Afar, Ph.D. thesis, 242 pp., Univ. Paris VI, Paris.
31. Manighetti, I., Tapponnier, P., Gillot, P., Jacques, Y E., Courtillot, V. ,Armijo, R., Ruegg, J. C, and King, G. (1998), Propagation of rifting along the Arabia-Somalia plate boundary: Into Afar, J. Geophys. Res., 103(B3), 4947–4974, doi: 10.1029/97JB02758.
32. Manighetti, I., Tapponnier, P., Courtillot, V., Gallet, Y., Jacques, E., Gillot, P.-Y., 2001. Strain transfer between disconnected, propagating rifts in Afar. Journal of Geophysical Research 106, 13,613–13,665.
33. McFadden, P.L., McElhinny, M.W., 1990. Classification of the reversal test in paleomagnetism. Geophysical Journal International 103, 725–729.
34. Mochizuki, N., Oda, H., Ishizuka, O., Yamazaki, T. and Tsunakawa, H., 2011. Palaeointensity variation across the Matuyama-Brunhes polarity transition: observations from lavas at Punaruu Valley, Tahiti, J. geophys. Res., 116, B06103, doi: 10.1029/2010JB008093.

35. Muluneh , A., Kidane, T., Rowland, T., Bachtadse,V.(2013), Counterclockwise block rotation linked to southward propagation and overlap of sub-aerial Red Sea Rift segments, Afar Depression: Insight from paleomagnetism, Tectonophysics 593, 111–120.
36. Nagata, T., 1961. Rock Magnetism, Maruzen Ltd., Tokyo, 350.
37. Pollar, D.D., and Aydin, A., 1988, progress in understanding jointing over the past century: Geological society of American Bulletin 100, 1181-1204.
38. Prévot, M., Grommé, S., 1975. Intensity of magnetization of subaerial and sub-marine basalts and its possible change with time. Geophysical Journal of the Royal Astronomical Society 40, 207–224.
39. Rowland, J.V., Baker, E., Ebinger, C.J., Keir, D., Kidane, T., Biggs, V., Hayward, N., Wright, T.J., 2007. Fault growth at a nascent slow-spreading ridge; 2005 Dabbahu rifting episode, Afar. Geophysical Journal International 171 doi: 10.1111/j.1365-246X.2007.03584.x.
40. Schilling,J.-G., Kingsley, R., Hanan, B. & McCully, B., 1992. Nd-Sr-Os isotopic variations along the Gulf of Aden: evidence for mantle-plume lithosphere interaction, J. geophys. Res., 97, 10 927–10 966.
41. Sigmundsson, F., 1992. Tectonic implications of the 1989 Afar earthquake sequence. Geophysical Research Letters 19, 877–880.
42. Stab, M., N. Bellahsen, R. Pik, X. Quidelleur, D. Ayalew, and S. Leroy (2015), Modes of rifting in magma-rich settings: Tectono-magmatic evolution of Central Afar, Tectonics, 35, doi:10.1002/2015TC003893.
43. Stuart, G.W., Bastow, I.D. & Ebinger, C.J., 2006. Crustal structure of the northern Main Ethiopian Rift from receiver function studies, in The Afar Volcanic Province within the East African Rift System, 253–267.
44. Tapponnier, P., Armijo, R., Manighetti, I., Courtillot, V., 1990. Bookshelf faulting and horizontal block rotations between overlapping rift zones in southern Afar. Geophysical Research Letters 17, 1–4.
45. Tiberi, C., Ebinger, C., Ballu, V., Stuart, G. & oluma, B., 2005. Inverse models of gravity data from the Red Sea – Aden – East African Rift triple junction zone, Geophys. J. Int., 163, 775–787.

46. Varet, J. (1978), Geology of central and southern Afar (Ethiopia and Djibouti Republic), map and report, 124 pp.

47. Wolfenden, E., C. Ebinger, G. Yirgu, A. Deino, and D. Ayalew (2004), Evolution of the northern Main Ethiopian rift: Birth of a triple junction,Earth Planet. Sci. Lett., 224(1–2), 213–228, doi:10.1016/j.epsl.2004.04.022.
48. Wolfenden, E., Ebinger, C., Yirgu, G., Renne, P., Kelley, S.P., 2005. Evolution of the southern Red Sea rift: Birth of a magmatic margin. Bull. Geolog. Soc. Am. 117, 846–864.
49. Yamamoto, Y. & Tsunakawa, H., 2005. Geomagnetic field intensity during the last 5 Myr: Tsunakawa-Shaw palaeointensities from volcanic rocks of the Society Islands, French Polynesia, Geophys. J. Int., 162, 79–114.
50. Zijderveld, J.D.A., 1967. A. C. demagnetization of rocks: analysis of results, in Methods in Palaeomagnetism, pp. 254–286, eds Collinson,D.W., Creer, K.M. and Runcorn, S.K., Elseiver.

Appendix

Appendix 1, Data for sun angle

Site Name	*Lat.*	*Lon.*
Date (dd/mm/yy)		
SA1	12°01.05'	41°12.48'
8/11/2016		

Sample	Time	AzSun	Az-Mag	AzGeo Decl
SA1-1			275	22
SA1-2	11:48	280	266	17
SA1-3	11:59	337	318	3
SA1-4			38	24
SA1-5			257	22

Site Name	*Lat.*	*Lon.*
Date (dd/mm/yy)		
SA2	11°59.03'	41°09.03'
8 /11/2016		

Sample	Time	Az. Sun	Az. Mag	Az. Geo Decl
SA2-1	15:29	47	85	43
SA2-2	15:30	37	103	44
SA2-3	15:36	52	111	28
SA2-4	15:41	44	98	23
SA2-5	15:44	54	99	26

Site Name	*Lat.*	*Lon.*
Date (dd/mm/yy)		
SA3	11°59.03'	41°09.03'
8 /11/2016		

Sample	Time	Az. Sun	Az. Mag	Az. Geo Decl
SA3-1	15:57	344	40	1
SA3-2	16:01	34	69	5
SA3-3	16:03	25	98	8
SA3-4	16:06	21	77	3
SA3-5	16:08	21	74	8
SA3-6	16:12	29	79	5

Site Name	*Lat.*	*Lon.*
Date (dd/mm/yy)		
DE1	11°54.8'	41°36.11'
9 /11/2016		

Sample	Time	Az. Sun	Az. Mag	Az. Geo Decl
DE1-1	11:53	10	356	8
DE1-2	12:03	10	9	15
DE1-3	12:08	356	357	5
DE1-4	12:12	0	357	-4
DE1-5	12:18	3	359	0
DE1-6	12:24	353	359	2

Site Name	*Lat.*	*Lon.*	*Date (dd/mm/yy)*
DE2	11°54.9'	41°36.04'	9 /11/2016

Sample	*Time*	AzSun	*AzMag*	*AzGeo Decl*
DE2-1	14:46	4	149	24
DE2-2	14:50	357	152	31
DE2-3	14:54	356	151	37
DE2-4	14:57	349	165	36
DE2-5	15:00	346	9	57
DE2-6	15:06	348	23	65
DE2-7	15:10	316	358	52

Site Name	*Lat.*	*Lon.*	*Date (dd/mm/yy)*
DE3	11°53.38'	41°37.45'	

Sam-ple	*Time*	AzSun	*AzMag*	*Az-Geo Decl*
DE3-1	17:04	13	85	-16
DE3-2	17:07	7	82	-15
DE3-3	17:10	3	85	-13
DE3-4	17:15	346	49	-10
DE3-5	17:18	342	41	-10
DE3-6	17:23	347	45	-6

Site Name	*Lat.*	*Lon.*	*Date*	*(dd/mm/yy)*
12°SS1	04.8'	41°15.16'	11 /11/2016	

Sample	*Time*	AzSun	*AzMag*	*AzGeo Decl*
SS1-1	10:17	127	89	-14
SS1-2	10:21	132	93	-9
SS1-3	10:23	133	95	5
SS1-4	10:27	176	137	18
SS1-5	10:32	177	136	26
SS1-6	10:38	169	133	10
SS1-7	1043	117	94	13

Site Name	*Lat.*	*Lon.*	*Date (dd/mm/yy)*
SS2	12°08.33'	41°12.5'	11 /11/2016

Sam-ple	*Tim e*	AzSu n	*Az-Mag*	*Az-Geo Decl*
SS2-1	5:52	54	50	17
SS2-2	5:55	50	46	23
SS2-3	6:01	39	43	13
SS2-4	6:04	45	44	31
SS2-5	6:08	54	59	28
SS2-6	6:10	42	44	32
SS2-7	6:13	52	55	18

Appendix 2. Data arranged for Paleomac software package

Site Name	Lat.	Lon.	Date (dd/mm/yy)
SS3	12°11.8'	41°11.12'	11 /11/2016

Sample	Time	AzSun	Az-Mag	AzGeo Decl
SS3-1	10:02	12	67	28
SS3-2	10:05	9	67	16
SS3-3	10:10	352	47	14
SS3-4	10:13	347	44	8
SS3-5	10:19	49	108	-4

DE1-1

Steps	X	Y	Z	M
0	2.93	1.05	-9.7	10.19
5	2.85	1.12	-10.04	10.5
10	2.92	1.35	-10.08	10.58
15	2.43	1.34	-9.49	9.883
20	2.27	1.18	-8.46	8.84
25	1.92	0.97	-7.21	7.52
30	1.63	0.82	-6.08	6.345
40	1.18	0.66	-4.59	4.785
60	0.85	0.46	-3.03	3.176
80	0.57	0.28	-2.1	2.196
100	4	1.66	-15.42	1.602

DE1-3A

Steps	X	Y	Z	M
0	1.56	1.34	-6.67	6.977
5	1.13	1.71	-7.33	7.611
10	0.81	2.21	-8.04	8.379
15	0.37	2.23	-7.69	8.012
20	0.4	2.13	-6.83	7.17
25	0.3	1.72	-5.72	5.981
30	0.26	1.57	-4.84	5.098
40	0.2	1.17	-3.54	3.735
60	0.13	0.81	-2.31	2.447
80	0.39	5.99	-15.99	1.708
100	0.24	4.31	-11.84	1.26

DE1-2A

Steps	X	Y	Z	M
0	-0.03	-3.24	4.89	58.67
5	0.01	-2.95	4.44	53.29
10	-0.14	-2.01	2.69	33.58
15	0.65	-10.2	11	14.98
20	0.84	-5.32	3.43	6.386
25	0.65	-3.13	0.64	3.264
30	0.71	-2.19	-0.21	2.309
40	6.34	-13	-7.5	1.631
60	4.43	-5.9	-9.1	1.172
80	3.53	-2.98	-8.25	0.9456
100	3.04	-1.67	-6.62	0.7472

DE1-4

Steps	X	Y	Z	M
0	0.9	-12	-5.41	131.6
5	1.11	-11.5	-5.01	125.6
10	0.75	-8.83	-3.79	96.41
15	0.05	-5.36	-2.6	59.55
20	0.36	-2.93	-1.77	34.37
25	1.96	-17.1	-12.03	21.01
30	2.22	-11.3	-9.09	14.7
40	-1.32	-5.51	-6.93	8.95
60	5.5	-5.43	-2.8	8.217
80	0.99	-2.17	-4.14	4.779
100	4.97	-11.3	-15.24	0.964

DE2-3A

Steps	X	Y	Z	M
0	-1.64	-0.14	-3.62	397.7
5	-1.53	-0.12	-3.27	361
10	-1.09	-0.04	-2.36	259.9
15	-6.44	0.02	-13.9	153.2
20	-2.98	0.42	-6.75	73.91
25	-1.33	0.4	-3.05	33.51
30	-6.42	4.08	-15.48	17.25
40	-2.29	2.62	-6.3	7.196
60	-0.89	1.69	-2.72	3.327
80	-5.73	13.24	-17.48	2.266
100	-3.7	10.19	-12.5	1.654

DE2-1A

Steps	X	Y	Z	M
0	-1.08	-0.55	-5.28	541.4
5	-0.98	-0.48	-4.88	500.3
10	-0.75	-0.44	-3.77	86.9
15	-0.52	-0.25	-2.53	259.9
20	-3.38	-1.57	-15.91	163.4
25	-1.79	-0.75	-9.28	94.78
30	-1.07	0.01	-5.59	56.89
40	-4.41	1.5	-19.34	19.9
60	-0.87	1.83	-4.5	4.93
80	-0.41	1.38	-2.27	2.687
100	-2.67	10.8	-15.63	1.919

DE2-4A

Steps	X	Y	Z	M
0	-0.91	-0.58	-3.09	327.3
5	-0.82	-0.58	-2.76	293.6
10	-6.08	-3.76	-19.54	208
15	-3.23	-1.69	-10.72	113.3
20	-1.57	-0.54	-5.15	54.12
25	-0.74	0.03	-2.27	23.85
30	-4.07	1.42	-12.46	13.18
40	-1.94	1.72	-5.8	6.349
60	-0.91	1.37	-2.8	3.247
80	-7.17	9.36	-18.58	2.201
100	-5.01	6.69	-14.47	1.672

DE2-5A

Steps	X	Y	Z	M
0	-1.47	-5.74	13.63	148.6
5	-2.01	-4.89	10.59	118.4
10	-1.05	-2.56	5.97	65.84
15	-0.73	-1.15	2.73	30.56
20	-3.94	-4.98	11.12	12.81
25	-2.9	-2.1	4.79	5.981
30	-2.14	-0.96	2.42	3.37
40	-15.33	-0.9	6.58	1.671
60	-9.43	3.88	-1.23	1.027
80	-6.32	3.91	-2.37	0.7799
100	-4.55	3.12	-2.34	0.5995

DE2-7B

Steps	X	Y	Z	M
0	-0.59	-0.66	2.32	248.5
5	-0.47	-0.61	2.09	222.6
10	-3.99	-3.96	14.74	157.8
15	-2.5	-3.01	9.3	100.9
20	-1.53	-1.62	5.05	55.22
25	-0.88	-0.77	2.39	26.55
30	-6.91	-6.08	17.56	19.83
40	-2.7	-1.99	4.17	5.353
60	-11.25	-4.12	0.24	1.198
80	-7.46	-1.86	-2.64	812.5
100	-7.36	-1.34	-1.58	765

DE3-1A

Steps	X	Y	Z	M
0	3.5	3.27	-10.38	11.44
5	2.86	3.55	-8.31	9.485
10	1.1	1.77	-2.97	3.632
15	5.6	12.04	-10.54	1.695
20	4.67	7.82	-7.23	1.163
25	3.9	6.28	-4.64	0.8732
30	3.07	5.1	-3.52	0.6916
40	2.27	4.01	-1.9	0.5011
60	1.46	2.42	-0.96	0.2989
80	2.41	2.23	-0.55	0.3331
100	6.26	12.69	-3.25	0.1452

DE3-2A

Steps	X	Y	Z	M
0	3.5	3.27	-10.38	11.44
5	2.86	3.55	-8.31	9.485
10	1.1	1.77	-2.97	3.632
15	5.6	12.04	-10.54	1.695
20	4.67	7.82	-7.23	1.163
25	3.9	6.28	-4.64	0.8732
30	3.07	5.1	-3.52	0.6916
40	2.27	4.01	-1.9	0.5011
60	1.46	2.42	-0.96	0.2989
80	2.41	2.23	-0.55	0.3331
100	6.26	12.69	-3.25	0.1452

DE3-3A

Steps	***X***	***Y***	***Z***	***M***
0	3.56	3.25	-11.8	12.74
5	3.3	3.34	-9.84	10.9
10	1.62	1.8	-4.12	4.775
15	9	9.87	-17.23	2.18
20	6.16	7.14	-9.66	1.35
25	4.86	5.75	-6.12	0.97
30	3.94	4.93	-4.39	0.7681
40	2.8	3.64	-2.54	0.5252
60	1.62	2.27	-1.21	0.3045
80	10.87	15.06	-6.7	0.1974
100	8.7	10.14	-4.54	0.1411

DE3-4A

Steps	***X***	***Y***	***Z***	***M***
0	4.52	4.85	-18.57	19.72
5	4.1	4.53	-16.73	17.81
10	2.34	3.11	-8.96	9.769
15	1.44	1.96	-3.97	4.652
20	9.79	13.36	-18.56	2.487
25	6.01	10.57	-10.93	1.635
30	5.41	8.36	-7.46	1.244
40	4.25	6.01	-3.76	0.8266
60	2.35	3.45	-1.61	0.4473
80	1.56	2.08	-0.96	0.2769
100	9.3	14.28	-6.09	0.181

DE3-6A

Steps	**X**	**Y**	**Z**	**M**
0	-1.35	4.67	15.96	166.9
5	-0.68	4.04	15.01	155.6
10	-0.48	2.93	10.38	108
15	-0.27	1.87	6.39	66.64
20	-0.11	1.16	3.7	38.79
25	-0.03	0.72	2.16	22.75
30	-0.07	5.07	13.42	14.34
40	0.2	2.71	6.07	6.646
60	0.36	1.33	2.12	2.523
80	3.1	9.31	11.28	1.495
100	2.76	7.26	7.43	1.075

SA1-4A

Steps	X	Y	Z	M
0	2.87	-2.93	-13.86	1.446
5	2.25	-2.27	-12.28	1.269
10	1.36	-2.52	-5.15	0.5892
15	1.19	-2.92	-1.62	0.3545
20	0.89	-2.94	-0.74	0.3156
25	0.99	-2.75	-0.35	0.2942
30	0.81	-2.55	-0.14	0.2676
40	-0.1	-2.18	-0.02	0.2183
60	3.89	-15.5	3.56	0.1641
80	1.77	-12	8.03	0.1452
100	2.06	-9.73	9.14	0.1351

SA1-5A

Steps	X	Y	Z	M
0	1.91	-3.14	0.16	0.3679
5	1.48	-2.85	0.44	0.3245
10	1.13	-2.65	0.92	0.3025
15	1.13	-2.65	0.92	0.3025
20	0.36	-2.93	-1.77	0.3437
25	1.96	-17.1	-12.03	21.01
30	2.22	-11.3	-9.09	14.7
40	-1.32	-5.51	-6.93	8.95
60	5.5	-5.43	-2.8	8.217
80	0.99	-2.17	-4.14	4.779
100	4.97	-11.3	-15.24	1.964

SA2-1A

Steps	X	Y	Z	M
0	-0.19	-3.45	0.06	3.453
5	-0.34	-3.42	0.01	3.432
10	-0.47	-3.33	0.01	3.362
15	-0.3	-3.21	0	3.221
20	-0.52	-3.03	0.02	3.074
25	-0.27	-2.78	0	2.795
30	-0.62	-2.71	-0.05	2.78
40	-0.41	-2.61	-0.08	2.645
60	-2.97	-18	-0.33	1.824
80	-2.34	-13.9	-0.16	1.407
100	-2.29	-6.44	0.15	0.684

SA2-2A

Steps	X	Y	Z	M
0	0.01	-3.04	0.34	3.063
5	-0.02	-3.01	0.31	3.03
10	-0.28	-2.94	0.28	2.966
15	-0.07	-2.8	0.25	2.813
20	-0.11	-2.59	0.26	2.607
25	-0.07	-2.36	0.21	2.369
30	-0.05	-2.12	0.18	2.125
40	-0.9	-17.1	1.71	1.722
60	-0.45	-10.3	1.45	1.041
80	-0.31	-6.35	1.1	0.645
100	-0.38	-4.3	0.66	0.437

SA2-5B

Steps	X	Y	Z	M
0	-1.42	-4.78	-0.99	5.08
5	-1.65	-4.87	-1.16	5.27
10	-1.1	-4.73	-1.11	4.98
15	-1.45	-4.28	-1.03	4.64
20	-1.24	-3.65	-0.9	3.96
25	-1.27	-3.01	-0.71	3.34
30	-0.82	-2.5	-0.6	2.70
40	-3.85	-17.6	-4.47	1.85
60	-3.67	-10.6	-2.69	1.16
80	-3.08	-7.26	-1.5	0.803
100	-1.22	-5.38	-0.86	0.558

SA3-1A

Steps	X	Y	Z	M
0	0.15	-0.68	2.02	2.14
5	-0.35	-1.89	2.69	3.31
10	-0.2	-2.16	2.52	3.32
15	-0.4	-1.76	2.05	2.74
20	-2.96	-13.6	15.75	2.10
25	-2.34	-10.7	12.57	1.66
30	-1.73	-8.79	10.34	1.37
40	-1.55	-6.71	7.83	1.04
60	-0.88	-4.34	5.07	0.673
80	-0.33	-3.24	3.82	0.502
100	-0.48	-2.48	3.19	0.407

SA3-2B

Steps	X	Y	Z	M
0	-0.36	-2.61	0.47	2.68
5	-0.46	-2.76	0.12	2.80
10	-0.38	-2.66	-0.05	2.69
15	-0.41	-2.34	-0.09	2.38
20	-2.67	-18.5	-0.6	1.87
25	-1.96	-14.2	-0.6	1.44
30	-1.74	-11.3	-0.54	1.14
40	-1.71	-8.64	-0.34	0.882
60	-0.93	-6.55	-0.13	0.662
80	-0.14	-5.28	-0.3	0.529
100	-0.52	-4.33	-0.07	0.436

SA3-3

Steps	X	Y	Z	M
0	-0.46	-3.03	1.3	3.33
5	-0.38	-3.21	0.9	3.35
10	-0.28	-2.76	0.61	2.84
15	-0.26	-2.04	0.37	2.09
20	-1.89	-16	2.83	1.63
25	-0.85	-13.7	2.43	1.40
30	-0.94	-12.2	2.21	1.24
40	-0.95	-10.3	1.73	1.05
60	-0.83	-8.35	1.43	0.852
80	-0.09	-6.85	1.24	0.696
100	-0.69	-6.11	0.99	0.623

SA3-4

Steps	X	Y	Z	M
0	-0.46	-2.84	1.24	3.14
5	-0.33	-3.1	0.74	3.20
10	-0.11	-2.68	0.46	2.72
15	-1.44	-19.6	2.85	1.99
20	-0.4	-15.2	2.3	1.54
25	-0.76	-12.8	1.67	1.30
30	-0.01	-11.4	1.57	1.15
40	-0.48	-9.8	1.2	0.988
60	0.25	-7.97	1.09	0.805
80	0.02	-6.79	0.92	0.685
100	0.04	-5.86	0.75	0.591

SS1-1A

Steps	X	Y	Z	M
0	-0.29	3.17	0.41	3.21
5	-0.28	3.22	0.47	3.27
10	-0.41	3.21	0.46	3.27
15	-0.37	2.99	0.43	3.05
20	-0.35	2.71	0.4	2.76
25	-0.3	2.42	0.35	2.47
30	-0.36	2.16	0.32	2.22
40	-2.37	17.07	2.38	1.74
60	-1.98	11.85	1.41	1.21
80	-1.31	8.97	0.9	0.911
100	-1.43	7.28	0.51	0.743

SS1-4A

Steps	X	Y	Z	M
0	0.62	2.01	3.49	4.07
5	0.69	2.1	3.52	4.16
10	0.58	1.97	3.42	3.99
15	0.55	1.76	3.07	3.58
20	0.48	1.55	2.63	3.09
25	0.4	1.26	2.22	2.58
30	3.59	10.82	19.31	2.24
40	2.85	8.37	14.75	1.72
60	2.01	5.8	9.39	1.12
80	1.25	3.75	6.47	0.758
100	0.91	3.17	4.88	0.589

SS1-5A

Steps	X	Y	Z	M
0	0.97	2.1	2.72	3.57
5	0.94	2.1	2.77	3.60
10	0.86	2.04	2.72	3.51
15	0.85	1.85	2.5	3.22
20	0.83	1.65	2.2	2.87
25	6.84	14.76	19.15	2.51
30	5.65	13	16.93	2.21
40	4.95	9.98	13.53	1.75
60	3.73	7.07	8.92	1.20
80	2.93	5.5	6.96	0.934
100	2.58	4.36	5.58	0.754

SS1-6A

Steps	X	Y	Z	M
0	0.35	2.21	3.13	3.85
5	0.46	2.2	3.21	3.92
10	0.3	2.17	3.14	3.83
15	0.2	2	2.94	3.56
20	0.39	1.76	2.64	3.19
25	0.2	1.55	2.3	2.78
30	0.18	1.37	2.04	2.46
40	1.64	11.38	16.1	1.98
60	1.09	7.68	11.37	1.38
80	0.98	5.83	8.6	1.04
100	0.59	4.87	6.96	0.852

SS2-1A

Steps	X	Y	Z	M
0	-3.43	19.23	-7.81	2.10
5	-0.38	2.09	-0.92	2.32
10	-3.18	19.89	-9.33	2.22
15	-3.04	17.86	-8.73	2.01
20	-3.42	16.28	-7.88	1.84
25	-3.26	15.12	-7.5	1.72
30	-3.04	14.21	-6.81	1.61
40	-2.67	12.94	-6.25	1.46
60	-2.04	11.49	-5.8	1.30
80	-2.17	10.56	-5.45	1.21
100	-2.09	9.31	-5.06	1.08

SS2-2A

Steps	X	Y	Z	M
0	-4.24	16.35	-6.28	1.8
5	-4.38	18.15	-8.34	2.05
10	-4.85	17.24	-9.09	2.01
15	-4.56	15.78	-8.36	1.84
20	-5.05	14.81	-7.83	1.75
25	-4.6	13.84	-7.64	1.65
30	-4.6	13.34	-7.56	1.60
40	-3.86	12.46	-7.03	1.48
60	-3.58	11.01	-6.58	1.33
80	-3.81	10.09	-5.62	1.22
100	-3.44	9.6	-5.21	1.15

SS2-4A

Steps	X	Y	Z	M
0	-0.89	2.29	-1.11	2.69
5	-1.14	2.42	-1.21	2.94
10	-1.06	2.35	-1.23	2.85
15	-1.01	2.19	-1.14	2.67
20	-0.82	2.01	-1.05	2.41
25	-8.14	17.99	-9.56	2.19
30	-7.48	16.74	-8.94	2.04
40	-6.01	14.22	-7.67	1.72
60	5.43	11.53	-5.94	1.41
80	-4.85	9.9	-5.26	1.22
100	-4.14	8.59	-5.04	1.08

SS2-6A

Steps	X	Y	Z	M
0	-8.81	15.59	-2.9	1.81
5	-9.73	18.9	-6.29	2.22
10	-1.13	2.33	-1.06	2.80
15	-1	2.42	-1.16	2.86
20	-1.05	2.28	-1.16	2.77
25	-0.94	2.08	-1.06	2.51
30	-7.87	18.71	-9.82	2.26
40	-6.81	15.51	-8.28	1.89
60	-6.13	12.06	-6.49	1.50
80	-4.76	10.34	-5.64	1.27
100	-3.94	9.54	-5.65	1.18

SS2-7A

Steps	X	Y	Z	M
0	-0.87	1.27	-1.32	2.03
5	-0.05	1.35	-0.7	1.52
10	-0.99	3.56	-1.41	3.96
15	-0.97	3.38	-1.31	3.75
20	-0.69	3.03	-1.19	3.32
25	-0.67	2.69	-1.06	2.97
30	-0.69	2.39	-0.9	2.64
40	-5.28	19.26	-7.17	2.12
60	-4.56	14.55	-5.86	1.63
80	-3.62	12.82	-5.25	1.43
100	-3.63	11.29	-4.25	1.26

SS3-1A

Steps	X	Y	Z	M
0	-5.79	13.2	-12.37	1.90
5	-2.57	14.99	-11.1	1.88
10	-2.61	14.35	-9.98	1.77
15	-2.1	12.81	-8.79	1.57
20	-2.42	11.29	-7.58	1.38
25	-1.16	9.92	-6.87	1.21
30	-1.73	8.87	-6.01	1.09
40	-1.53	7.33	-4.56	0.877
60	-1.33	5.97	-3.63	0.711
80	-0.93	4.92	-3.18	0.593
100	-0.87	4.09	-2.06	0.466

SS3-3B

Steps	X	Y	Z	M
0	-3.16	6.29	-16.27	1.77
5	-1.99	8.61	-15.71	1.80
10	-1.73	8.41	-14.47	1.68
15	-1.76	7.66	-12.64	1.49
20	-1.58	6.72	-11.07	1.31
25	-1.18	5.99	-9.83	1.16
30	-0.95	5.24	-8.65	1.02
40	-1.1	4.35	-7.09	0.839
60	-0.78	3.45	-5.16	0.626
80	-0.61	2.99	-4.55	0.547
100	-0.41	2.41	-3.87	0.458

SS3-4B

Steps	X	Y	Z	M
0	-1.48	1.38	-15.04	1.52
5	0.94	5.99	-12.51	1.39
10	1.53	6.89	-11.11	1.32
15	1.25	6.46	-10.25	1.22
20	3.69	6.04	-7.86	1.06
25	0.81	5.03	-7.47	0.904
30	0.19	3.23	-6.73	0.747
40	0.7	4.03	-6.24	0.746
60	1.41	4.41	-5.16	0.693
80	0.4	2.17	-3.2	0.389
100	0.24	1.77	-3.29	0.375

SS3-5A

Steps	X	Y	Z	M
0	-0.16	2.84	2.11	3.54
5	-0.11	2.38	0.88	2.54
10	-0.07	2.07	0.39	2.11
15	-0.67	8.15	2.34	0.851
20	-0.51	15.53	2.21	0.157
25	-0.01	6.7	0.89	0.676
30	-0.58	12.14	1.79	1.23
40	-0.2	10.19	1.71	1.03
60	-0.24	7.97	0.68	0.8
80	-0.29	6.94	0.56	0.697
100	-0.43	5.93	0.69	0.599

DE1-2B

Steps	X	Y	Z	M
NRM	1.25	1.54	-6.37	6.674
T120	1.36	1.6	-6.4	6.733
T200	1.39	1.72	-6.56	6.926
T250	1.05	1.84	-6.58	6.917
T300	1.24	1.49	-6.84	7.112
T350	1.33	1.8	-6.7	7.067
T400	1	1.72	-6.79	7.072
T430	1.2	1.82	-6.63	6.98
T460	1.03	1.66	-6.5	6.785
T520	0.89	1.71	-6.35	6.638
T540	0.89	1.72	-6.18	6.474
T560	0.79	1.87	-6.05	6.379
T580	0.63	1.6	-4.82	5.118
T600	0.54	1.49	-4.75	5.006

DE1-3B

Steps	X	Y	Z	M
NRM	2.47	0.92	-10.01	10.36
T120	2.76	1.49	-9.92	10.4
T200	2.64	1.38	-10.16	10.58
T250	2.71	1.61	-10.19	10.66
T300	2.72	1.37	-10.45	10.88
T350	2.61	1.54	-10.12	10.56
T400	2.36	1.72	-9.96	10.38
T430	2.34	1.34	-9.77	10.13
T460	2.34	1.41	-8.78	9.198
T520	2.19	1.58	-9.04	9.432
T540	2.25	1.87	-8.25	8.76
T560	2.09	1.53	-8.05	8.457
T580	1.48	0.95	-6.06	6.308
T600	1.36	0.79	-5.85	6.056

DE1-5

Steps	X	Y	Z	M
NRM	1.76	-7.71	3.19	8.531
T120	2.08	-7.63	3.23	8.542
T200	1.99	-7.56	2.84	8.315
T250	1.88	-7.1	2.39	7.72
T300	1.89	-6.77	2.23	7.377
T350	1.84	-6.3	1.73	6.786
T400	2.07	-5.77	1.04	6.214
T430	2.04	-4.88	0.04	5.293
T460	2.13	-4.16	-0.8	4.741
T520	2.22	-2.06	-2.28	3.787
T540	2.27	-2.02	-2.4	3.877
T560	1.48	-0.23	-2.47	2.888
T580	1.46	-0.33	-2.4	2.827
T600	1.38	-0.42	-2.3	2.714

DE1-6A

Steps	X	Y	Z	M
NRM	3.31	0.73	-7.49	8.223
T120	3.42	0.92	-7.55	8.343
T200	3.31	0.72	-7.77	8.471
T250	3.27	0.91	-7.81	8.511
T300	3.33	0.76	-7.47	8.218
T350	3.21	1.25	-7.7	8.44
T400	3.16	1.09	-7.8	8.487
T430	3.08	1.28	-7.63	8.324
T460	3.16	0.89	-7.63	8.304
T520	3.01	1.26	-7.23	7.935
T540	2.88	1.22	-7.12	7.777
T560	2.71	1.26	-6.78	7.409
T580	1.89	0.93	-4.88	5.316
T600	1.68	0.6	-4.76	5.083

DE2-2A

Steps	X	Y	Z	M
NRM	-0.8	-0.06	-5.88	593.2
T120	-0.71	0.06	-5.88	592.1
T200	-0.92	0	-5.68	575.2
T250	-0.88	-0.07	-5.49	556.3
T300	-0.91	-0.01	-5.23	530.9
T350	-0.64	0.12	-4.94	497.9
T400	-0.72	0.21	-4.62	467.6
T430	-0.65	0.05	-4.29	434.4
T460	-0.53	0.14	-4.01	404.3
T520	-0.46	0.1	-3.17	320.6
T540	-2.78	0.57	-15.13	154
T560	-1.87	0.49	-14.61	147.4
T580	-1.71	0.69	-13.44	135.7
T600	-2.42	0.38	-12.68	129.2

DE2-5B

Steps	X	Y	Z	M
NRM	-3.56	-8.47	16.61	189.8
T120	-3.72	-8.19	16.36	186.7
T200	-3.04	-7.07	14.09	160.6
T250	-0.09	-5.89	5.89	83.31
T300	-2.47	-4.9	10.04	114.4
T350	-2.06	-4.25	8.78	99.68
T400	-2.15	-3.58	7.56	86.39
T430	-1.68	-2.83	5.96	68.08
T460	-0.15	-2.1	2.88	35.71
T520	-1.31	-1.93	4.52	50.89
T540	-0.62	-1.03	2.4	26.88
T560	-0.57	-1	2.29	25.65
T580	-0.5	-0.83	2.02	22.43
T600	-2.65	-5	15.41	1.641

DE2-6

Steps	X	Y	Z	M
NRM	-0.86	-1	2.65	296.3
T120	-0.94	-1	2.62	296.1
T200	-0.77	-0.84	2.37	263.1
T250	-0.65	-0.78	2.25	247.2
T300	-0.62	-0.76	2.08	230
T350	-6.5	-7.19	19.37	216.6
T400	-5.6	-6.35	17.74	196.6
T430	-5.46	-6.08	16.13	180.8
T460	-4.87	-4.8	13.53	151.6
T520	-3.34	-3.07	8.99	100.7
T540	-2.28	-2.15	6.23	69.74
T560	-2.09	-2	5.98	66.46
T580	-2.74	-2.54	7.55	8.427
T600	-7	-5.97	19.55	2.161
T600	-7	-5.97	19.55	2.161

DE2-7A

Steps	X	Y	Z	M
NRM	-0.97	-1.25	3.14	0.3516
T120	-0.93	-1.16	3.16	0.3489
T200	-0.84	-1.09	2.99	0.3292
T250	-0.78	-0.97	2.7	0.2971
T300	-0.66	-0.88	2.52	275.4
T350	-0.63	-0.85	2.42	263.8
T400	-5.52	-7.07	18.88	209
T430	-5.44	-6.42	18.34	201.8
T460	-5.26	-6.27	17.06	189.2
T520	-4.35	-5.02	13.11	147
T540	-2.06	-2.68	7.05	78.2
T560	-2.08	-2.36	6.77	74.66
T580	-0.91	-1.01	2.9	31.99
T600	-1.14	-1.16	3.21	3.595

DE3-1B

Steps	X	Y	Z	M
NRM	3.89	4.19	-12.26	13.53
T120	3.83	4.46	-11.44	12.86
T200	3.1	4.1	-10.27	11.49
T250	2.6	3.46	-8.1	9.187
T300	2.43	3.02	-6.27	7.37
T350	2.1	2.79	-6.09	7.018
T400	1.71	2.22	-4.97	5.706
T430	1.28	1.73	-3.91	4.462
T460	1.36	1.57	-3.49	4.064
T520	9.34	10.98	-18.76	2.366
T540	7.13	9.21	-12.95	1.742
T560	4.65	6.25	-9.34	1.216
T580	2.05	2.91	-5.08	0.6203
T600	1.12	1.39	-2.2	0.2832

DE3-3B

Steps	X	Y	Z	M
NRM	0.52	0.56	-2.11	22.45
T120	0.52	0.54	-2.01	21.5
T200	4.42	4.6	-18.29	19.37
T250	4.08	4.48	-16.01	17.12
T300	3.52	3.85	-14.81	15.7
T350	3.19	3.81	-12.4	13.36
T400	2.81	3.18	-10.47	11.29
T430	2.64	2.88	-9.25	10.04
T460	1.77	1.96	-5.24	5.867
T520	1.48	1.73	-4.36	4.918
T540	1.16	1.41	-3.42	3.878
T560	0.6	0.8	-2.18	2.395
T580	2.27	1.88	-7.13	0.772
T600	1.21	1.29	-3.15	0.3615

DE3-5B

Steps	X	Y	Z	M
NRM	-0.26	4.01	10.59	113.3
T120	0.4	4.18	10.47	112.8
T200	-0.26	4.04	10.29	110.6
T250	-0.04	3.71	10.1	107.6
T300	3.66	0.02	9.55	102.2
T350	0.36	3.86	9.27	100.5
T400	-0.25	3.22	8.64	92.25
T430	-0.15	3.12	8.26	88.28
T460	0.07	3.09	7.89	84.77
T520	-0.42	2.34	6.61	70.24
T540	-0.07	2.16	5.9	62.84
T560	0.11	2.01	4.88	52.77
T580	-0.13	1.08	2.82	30.21
T600	-0.15	1.04	2.59	27.99

DE3-6B

Steps	X	Y	Z	M
NRM	0.31	1.27	10.45	10.53
T120	0.56	1.37	9.92	10.03
T200	0.36	0.69	7.42	7.464
T250	0.4	0.6	5.51	5.558
T300	0.22	0.47	4.88	4.905
T350	0.24	0.32	4.34	4.362
T400	0.19	0.31	3.53	3.552
T430	0.19	0.45	3.28	3.311
T460	0.27	0.28	2.99	3.014
T520	-0.21	1.64	6.34	0.6551
T540	0.71	0.94	5.96	0.6076
T560	1.22	0.76	6.99	0.7139
T580	-0.02	0.75	2.61	0.2718
T600	3.51	3.74	12.48	134.9

SA1-1A

Steps	X	Y	Z	M
NRM	-0.23	-4.51	-13.09	13.84
T120	-0.05	-4.98	-12.74	13.68
T200	0.7	-4.41	-11.87	12.69
T250	0.15	-4.16	-11.21	11.95
T300	0.09	-3.75	-10.42	11.08
T350	-0.22	-2.87	-9.27	9.707
T400	0.14	-3.04	-8.02	8.577
T430	-0.1	-2.79	-7.61	8.106
T460	-0.01	-2.36	-7.32	7.695
T520	0	-1.31	-3.99	4.203
T540	0.14	-1.29	-3.96	4.167
T560	-0.11	-1.27	-3.93	4.133
T580	-0.05	-1.21	-3.53	3.727
T600	0.05	-0.78	-1.64	1.82

SA1-2B

Steps	X	Y	Z	M
NRM	1.37	-7.5	-12.14	14.33
T120	1.61	-7.11	-12.3	14.29
T200	1.49	-6.63	-11.56	13.41
T250	1.83	-6.79	-10.53	12.66
T300	0.91	-6	-10.31	11.96
T350	1.18	-5.64	-8.55	10.31
T400	1	-4.69	-7.56	8.955
T430	0.83	-4.13	-6.73	7.943
T460	0.55	-4.07	-6.44	7.635
T520	0.73	-3.34	-5.56	6.526
T540	0.68	-2.92	-5.23	6.025
T560	0.61	-2.61	-4.57	5.293
T580	0.34	-1.4	-2.25	2.672
T600	0.19	-1.37	-2.13	2.541

SA1-3A

Steps	X	Y	Z	M
NRM	-4.36	8.28	-15.85	1.841
T120	-4.17	17.11	-15.8	2.366
T200	-2.91	16.35	-14.07	2.177
T250	-2.99	14.46	-14.16	2.046
T300	-1.93	12.53	-12.8	1.801
T350	-1.86	10.59	-10.92	1.533
T400	-1.01	9.15	-9.78	1.343
T430	-0.66	8.17	-9.84	1.281
T460	-0.42	5.83	-7.55	0.9549
T520	-3.31	2.9	0.68	0.4454
T540	-1.03	4.72	-5.68	0.7452
T560	-0.5	4.04	-5.11	0.6535
T580	-0.45	2.74	-3.83	0.4733
T600	-0.63	2.11	-3.43	0.4079

SA1-4B

Steps	X	Y	Z	M
NRM	1.27	-0.41	-9.13	0.9222
T120	1.63	-1.08	-9.07	0.9284
T200	2.06	-0.98	-8.3	0.8611
T250	1.52	-1.16	-7.35	0.7591
T300	1.22	-1.67	-6.96	0.7264
T350	1.46	-1.68	-5.48	0.5912
T400	0.99	-1.75	-4.74	0.5151
T430	1.13	-1.69	-4.04	0.4522
T460	0.47	-1.52	-3.98	0.4284
T520	0.29	-1.54	-2.4	0.2869
T540	0.66	-1.05	1.98	0.2337
T560	7.68	-10.97	-16.23	0.2104
T580	1.23	-4.63	-3.22	0.05774
T600	1.18	-4.1	-1.89	0.04663

SA1-5B

Steps	X	Y	Z	M
NRM	2.26	-3.19	0.07	0.3908
T120	2.39	-3.46	0.12	0.4207
T200	2.15	-3.29	0.4	0.3947
T250	2.32	-3.15	0.4	0.3932
T300	2.06	-3.26	0.57	0.3897
T350	1.74	-3.37	0.47	0.3819
T400	1.72	-3.19	-0.04	0.3624
T430	1.43	-2.71	0.9	0.3196
T460	1.58	-2.77	0.65	0.3253
T520	1.17	-2.34	0.73	0.2715
T540	1.29	-2.42	0.58	0.2803
T560	11.91	-19.67	5.91	0.2374
T580	6.9	-6.63	-1.76	0.09731
T600	0.71	-1.5	-2.84	0.3286

SA2-1B

Steps	X	Y	Z	M
NRM	-0.46	-2.72	-0.07	2.758
T120	-0.46	-2.75	-0.02	2.789
T200	-0.49	-2.68	-0.01	2.722
T250	-0.42	-2.59	-0.06	2.624
T300	-0.42	-2.4	0.01	2.438
T350	-0.43	-2.37	-0.02	2.406
T400	-5.51	-17.84	-2.28	1.88
T430	-5.21	-17.3	0.63	1.808
T460	-3.24	-14.42	-1.37	1.484
T520	-3.35	-13.64	-1.26	1.41
T540	-2.66	-13.1	-0.46	1.338
T560	-2.83	-10.75	-0.56	1.113
T580	-2.76	-9.61	3.41	1.056
T600	-1.1	-7.91	-0.49	0.8001

SA2-4A

Steps	X	Y	Z	M
NRM	-0.46	-4.4	-0.29	4.438
T120	-0.66	-4.44	-0.02	4.492
T200	-0.16	-4.35	-0.3	4.364
T250	-0.21	-4.29	-0.19	4.295
T300	-0.34	-4.18	-0.38	4.208
T350	-0.13	-3.76	-0.22	3.769
T400	-0.45	-2.87	-0.19	2.91
T430	-0.47	-2.63	-0.09	2.677
T460	-0.37	-2.45	0.22	2.483
T520	-0.21	-2.08	-0.02	2.086
T540	-1.21	-17.36	0.14	1.74
T560	-1.45	-15.61	2.8	1.593
T580	-1.52	-13.75	-0.49	1.384
T600	-2.12	-13.06	0.18	1.323

SA2-5A

Steps	X	Y	Z	M
NRM	-0.53	-5.36	-0.89	5.46
T120	-0.27	-5.47	-0.79	5.535
T200	-0.52	-5.37	-0.78	5.449
T250	-0.3	-5.27	-0.78	5.335
T300	-0.13	-5.1	-0.84	5.169
T350	-0.15	-4.34	-0.7	4.396
T400	-0.14	-3.75	-0.56	3.797
T430	-0.31	-3	-0.56	3.067
T460	-0.29	-2.82	-0.46	2.876
T520	-0.48	-2.56	-0.42	2.641
T540	-0.2	-2.33	-0.39	2.371
T560	-0.12	-2.18	-0.29	2.199
T580	-0.72	-16.76	-3.78	1.72
T600	-1.27	-14.76	-2.38	1.501

SA3-1B

Steps	X	Y	Z	M
NRM	0.22	-0.55	2.37	2.44
T120	0.23	-0.57	2.37	2.445
T200	0.1	-0.6	2.46	2.531
T250	-0.05	-1.02	2.61	2.805
T300	-0.12	-1.19	2.56	2.819
T350	-0.09	-1.15	2.09	2.389
T400	-0.18	-1.4	2.26	2.658
T430	-0.13	-1.33	2.07	2.466
T460	-0.18	-1.35	2.11	2.508
T520	-2.18	-11.24	16.78	2.032
T540	-2.2	-9.23	11.14	1.463
T560	-2.08	-8.85	13.06	1.591
T580	-0.63	-1.94	2.74	0.341
T600	-2.19	-2.58	7.96	0.8648

SA3-2A

Steps	X	Y	Z	M
NRM	-0.54	-2.56	0.28	2.632
T120	-0.42	-2.56	0.26	2.609
T200	-0.61	-2.52	0.25	2.603
T250	-0.56	-2.45	0.2	2.52
T300	-0.48	-2.42	0.16	2.47
T350	-0.5	-2.38	0.12	2.438
T400	-0.49	-2.05	0.07	2.107
T430	-3.91	-19.75	-0.64	2.014
T460	-3.66	-19.35	0.71	1.971
T520	-2.23	-13.29	-0.07	1.348
T540	-3.26	-13.32	0.06	1.371
T560	-3.01	-13.36	3.62	1.416
T580	-2.86	-10.82	1.82	1.134
T600	-0.38	-6.76	-0.68	0.06803

SA3-5A

Steps	X	Y	Z	M
NRM	-0.45	-3.45	1.31	3.714
T120	-0.11	-3.46	1.28	3.694
T200	-0.3	-3.47	1.24	3.695
T250	-0.5	-3.43	1.18	3.657
T300	-0.46	-3.37	1.07	3.565
T350	-0.45	-3.17	1.09	3.384
T400	-0.29	-3.01	0.92	3.16
T430	-0.27	-2.76	0.59	2.833
T460	-0.33	-2.7	0.54	2.771
T520	-0.38	-2.4	0.76	2.545
T540	-0.12	-2.14	0.5	2.199
T560	-2.2	-19.64	5.25	2.044
T580	-2.89	-16.38	3.75	1.705
T600	-0.41	-3.84	1.01	0.3986

SA3-6

Steps	X	Y	Z	M
NRM	-0.84	-4.55	1.52	4.872
T120	-0.7	-4.52	1.55	4.829
T200	-0.53	-4.52	1.45	4.775
T250	-0.6	-4.54	1.4	4.786
T300	-0.56	-4.5	1.03	4.647
T350	-0.38	-4.43	0.83	4.521
T400	-0.33	-3.89	0.35	3.915
T430	-0.21	-3.73	0.43	3.759
T460	-0.44	-3.52	0.33	3.564
T520	-0.28	-3.26	0.29	3.284
T540	-0.36	-3.03	0.27	3.066
T560	-0.29	2.837	0.24	2.837
T580	-0.21	-2.1	0.27	2.129
T600	-0.71	-7.58	0.58	0.7636

SS1-1B

Steps	X	Y	Z	M
NRM	-0.69	4.78	0.96	4.921
T120	-0.62	4.78	0.93	4.909
T200	-0.87	4.82	0.89	4.975
T250	-0.9	4.76	0.91	4.929
T300	-0.72	4.67	0.99	4.824
T350	-0.65	3.55	0.84	3.71
T400	-0.42	3.22	0.71	3.323
T430	-0.34	2.87	0.61	2.951
T460	-0.36	2.68	0.64	2.775
T520	-0.32	2.13	0.5	2.215
T540	-0.32	1.99	0.58	2.094
T560	-1.84	11.09	1.78	1.138
T580	-1.82	10.21	1.86	1.053
T600	-2.33	9.3	2.35	0.9871

SS1-3A

Steps	X	Y	Z	M
NRM	-0.54	4.62	1.86	5.005
T120	-0.5	4.67	1.81	5.037
T200	-0.75	4.61	1.78	4.999
T250	-0.71	4.67	1.43	4.937
T300	-0.86	4.12	1.82	4.59
T350	-0.56	3.29	1.34	3.594
T400	-0.28	3.07	1.36	3.373
T430	-0.49	2.94	1.09	3.174
T460	-0.4	2.67	1.06	2.901
T520	-0.39	2.06	0.86	2.262
T540	-1.47	18.78	8.12	2.051
T560	-1.74	17.52	7.24	1.904
T580	-2.02	10.82	5.93	1.25
T600	-1.35	10.08	4.52	1.113

SS1-4B

Steps	X	Y	Z	M
NRM	0.17	1.64	3.26	3.653
T120	0.2	1.74	3.25	3.69
T200	0.13	1.74	3.22	3.662
T250	0.19	1.63	3.18	3.573
T300	0.16	1.49	3.13	3.472
T350	0.33	1.33	2.63	2.97
T400	0.21	0.95	2.1	2.311
T430	1.47	8.12	17.46	1.931
T460	1.02	8.83	16.69	1.891
T520	0.79	5.88	12.18	1.355
T540	0.42	4.64	14.06	1.481
T560	1.44	4.74	11.75	1.275
T580	1.37	3.97	9.49	1.037
T600	0.82	4.19	8.92	0.9888

SS1-5B

Steps	X	Y	Z	M
NRM	0.64	1.81	2.92	3.495
T120	0.71	1.77	2.95	3.51
T200	0.67	1.89	2.93	3.549
T250	0.71	1.79	2.77	3.374
T300	0.68	1.78	2.8	3.389
T350	0.59	1.55	2.35	2.874
T400	0.49	1.25	2.06	2.456
T430	3.9	11.41	18.41	2.201
T460	5.28	11.59	19.65	2.342
T520	1.95	7.67	12.95	1.518
T540	2.54	6.86	11.68	1.378
T560	1.94	4.29	7.34	0.8718
T580	3.34	5.16	3.19	0.06927
T600	2.25	5.34	7.39	0.09394

SS1-7B

Steps	X	Y	Z	M
NRM	-0.69	3.06	0.59	3.191
T120	-0.47	3.09	0.6	3.183
T200	-0.71	3.01	0.58	3.144
T250	-0.5	3.05	0.62	3.151
T300	-0.5	2.93	0.59	3.025
T350	-0.54	2.2	0.51	2.316
T400	-0.31	2.05	0.41	2.115
T430	-4.99	19.3	1.84	2.002
T460	-2.52	17.77	4.36	1.847
T520	-3.94	14.81	2.54	1.553
T540	-2.96	13.43	4.82	1.457
T560	-0.54	2.3	0.62	0.2445
T580	-3.79	11.69	6.25	0.1379
T600	-0.64	2.03	0.15	0.2129

SS1-7B

Steps	X	Y	Z	M
NRM	-0.69	3.06	0.59	3.191
T120	-0.47	3.09	0.6	3.183
T200	-0.71	3.01	0.58	3.144
T250	-0.5	3.05	0.62	3.151
T300	-0.5	2.93	0.59	3.025
T350	-0.54	2.2	0.51	2.316
T400	-0.31	2.05	0.41	2.115
T430	-4.99	19.3	1.84	2.002
T460	-2.52	17.77	4.36	1.847
T520	-3.94	14.81	2.54	1.553
T540	-2.96	13.43	4.82	1.457
T560	-0.54	2.3	0.62	0.2445
T580	-3.79	11.69	6.25	0.1379
T600	-0.64	2.03	0.15	0.2129

SS2-1B

Steps	X	Y	Z	M
NRM	-0.43	2.12	-0.78	2.298
T120	-0.72	2.17	-0.81	2.424
T200	-0.49	2.37	-0.95	2.599
T250	-0.67	2.32	-0.82	2.549
T300	-0.58	2.23	-0.81	2.446
T350	-0.51	2.63	-2.06	3.374
T400	-0.33	2.21	-1.94	2.959
T430	-2.68	19.53	-5.46	2.046
T460	-3.12	18.82	-10.17	2.162
T520	-2.46	13.61	-9.54	1.68
T540	-1.87	13.52	-7.75	1.569
T560	-3.11	7.83	-1.89	0.8636
T580	-0.9	7.37	-5.65	0.9332
T600	-1.33	8.87	-3.59	0.09664

SS2-2B

Steps	X	Y	Z	M
NRM	-3.22	19.2	6.2	2.043
T120	-3.95	19.52	-7.65	2.134
T200	-0.57	2	-0.82	2.235
T250	-3.49	19.56	-7.24	2.114
T300	-0.59	2.08	-0.79	2.297
T350	-0.1	2.11	-0.25	2.125
T400	-6.92	18.3	-9.24	2.164
T430	-4.33	16.24	-7.75	1.85
T460	0.58	16.8	-2.45	1.699
T520	-0.81	8.25	-10.67	1.351
T540	-0.8	8.16	-7.51	1.112
T560	-1.37	8.11	-6.14	1.027
T580	-0.91	4.05	-2.37	0.477
T600	-0.75	3.58	-2.23	0.4287

SS2-3

Steps	X	Y	Z	M
NRM	-3.44	11.28	-5.73	1.311
T120	-3.39	11.22	-6.02	1.318
T200	-2.83	11.3	-7.5	1.386
T250	-3.33	12.55	-7.66	1.507
T300	-3.06	12.51	-6.53	1.444
T350	-3.08	12.75	-9.12	1.598
T400	-2.46	10.08	6.56	1.228
T430	-3.32	10.37	-7.86	1.343
T460	-1.49	10.48	-6.19	1.226
T520	-0.34	9.94	-18.3	2.083
T540	0.26	3.53	-3.31	0.4846
T560	-0.18	6.86	-7.33	1.004
T580	-1.27	3.79	-2.81	0.4885
T600	-0.77	3.48	-1.84	0.4009

SS2-4B

Steps	X	Y	Z	M
NRM	-0.78	2.24	-0.86	2.526
T120	-0.75	2.27	-0.92	2.56
T200	-0.95	2.37	-1.04	2.755
T250	-0.92	2.34	-0.96	2.693
T300	-0.77	2.41	-0.96	2.705
T350	-0.75	2.09	-0.87	2.381
T400	-7.4	19.25	-10.14	2.298
T430	-0.68	1.99	-1.12	2.386
T460	-6.62	18.1	-9.68	2.157
T520	-5.27	16.08	-10.64	1.998
T540	-4.35	12.8	-6.8	1.513
T560	-3.91	11.19	-1.63	1.196
T580	-6.05	16.29	-2.18	0.1751
T600	-6.37	14.07	-2.78	0.157

SS2-5A

Steps	X	Y	Z	M
NRM	-0.57	2.33	-0.6	2.469
T120	-0.62	2.3	-0.67	2.477
T200	-0.67	2.34	-0.75	2.544
T250	-0.44	2.31	-0.66	2.44
T300	-0.36	2.3	-0.73	2.444
T350	-0.45	2.16	-0.67	2.304
T400	-4.72	19.68	-5.87	2.107
T430	-2.99	18.39	-6.06	1.959
T460	-3.95	17.92	-5.06	1.903
T520	-2.22	15.84	-6.28	1.719
T540	-3.56	14.11	-5.19	1.545
T560	-2.64	11.21	-4.43	1.234
T580	-1.64	8.64	-4.21	0.975
T600	-2.02	7.73	-3.7	0.8804

SS2-6B

Steps	X	Y	Z	M
NRM	-0.57	2.33	-0.6	2.469
T120	-0.62	2.3	-0.67	2.477
T200	-0.67	2.34	-0.75	2.544
T250	-0.44	2.31	-0.66	2.44
T300	-0.36	2.3	-0.73	2.444
T350	-0.45	2.16	-0.67	2.304
T400	-4.72	19.68	-5.87	2.107
T430	-2.99	18.39	-6.06	1.959
T460	-3.95	17.92	-5.06	1.903
T520	-2.22	15.84	-6.28	1.719
T540	-3.56	14.11	-5.19	1.545
T560	-2.64	11.21	-4.43	1.234
T580	-1.64	8.64	-4.21	0.975
T600	-2.02	7.73	-3.7	0.8804

SS2-7B

Steps	X	Y	Z	M
NRM	-8.21	18.28	-7.16	2.128
T120	-8.63	18.58	-7.57	2.184
T200	-9.2	19.71	-9.49	2.373
T250	-9.58	19.61	-11.08	2.448
T300	-7.27	19.73	-9.59	2.311
T350	-7.63	19.47	-9.49	2.296
T400	-6.88	18.59	-8.39	2.152
T430	-5.39	17.81	-8.35	2.039
T460	-6.15	15.77	-6.38	1.809
T520	-4.2	12.75	-4.68	1.422
T540	-3.91	11.23	-4.49	1.271
T560	-1.21	4.12	-1.48	0.4541
T580	-1.83	4.53	-3.77	0.617
T600	-2	4.86	-1.3	0.5417

SS3- 1B

Steps	X	Y	Z	M
NRM	-5.88	13.67	-12.99	1.975
T120	-4.98	13.56	-13.13	1.952
T200	-5.14	14.9	-12.93	2.038
T250	-5.41	14.3	-13.11	2.01
T300	-4.8	14.48	-12.8	1.992
T350	-3.82	13.52	-9.96	1.722
T400	-3.34	11.75	-8.11	1.467
T430	-2.14	10.59	-7.46	1.313
T460	-2.5	9.62	-7.9	1.269
T520	-2.73	9.5	-4.86	1.101
T540	-2.42	9.07	-6.46	1.14
T560	-2.3	5.49	-3.95	0.7142
T580	-1.91	4.62	-3.89	0.6335
T600	-1.13	3.96	-3.01	0.5105

SS3- 2A

Steps	X	Y	Z	M
NRM	-5.38	12.36	-17.26	2.19
T120	-5.03	13.51	-17.16	2.242
T200	4.25	13.48	-17.61	2.258
T250	-4.35	14.38	-16.9	2.261
T300	-5.05	13.73	-16.69	2.219
T350	-3.68	14.66	-14.85	2.119
T400	-1.8	13.38	-13.04	1.877
T430	-0.16	1.36	-2.03	2.45
T460	-2.02	11.55	-16.45	2.02
T520	-1.61	11.2	-11.67	1.625
T540	-1.94	10.38	-10.47	1.487
T560	-1.34	8.5	-8.44	1.206
T580	-1.73	7.27	-5.59	0.9331
T600	-0.5	2.97	-2.53	0.3933

SS3- 3A

Steps	X	Y	Z	M
NRM	-2.38	6.96	-11.58	1.372
T120	-2.37	7.66	-12.66	1.498
T200	-3.53	8.3	-12.53	1.544
T250	-3.14	8.66	-12.85	1.581
T300	-2.91	8.34	-12.46	1.527
T350	-1.33	8.47	-12.22	1.493
T400	-1.83	7.3	-10.89	1.323
T430	-1.54	7.19	-13.32	1.522
T460	-2.85	10.01	-7.82	1.302
T520	-0.84	7.87	-9.29	1.22
T540	-1.33	6.07	-8.78	1.075
T560	-0.91	6.09	-7.98	1.008
T580	-0.69	1.24	3.28	0.3578
T600	-0.5	2.03	-3.07	0.372

SS3- 4A

Steps	X	Y	Z	M
NRM	-1.22	2.65	-17.99	1.822
T120	-1.11	3.65	-18.15	1.854
T200	-0.51	4.72	-16.32	1.7
T250	-0.46	4.39	-16.61	1.718
T300	-0.71	5.73	-18.71	1.958
T350	-0.06	5.02	-14.49	1.534
T400	0.53	5.13	-14.89	1.576
T430	-0.01	4.9	-12.12	1.308
T460	0.18	4.21	-9.58	1.047
T520	0.34	4.18	-9.04	0.9968
T540	-0.3	3.61	-8.51	0.9245
T560	-0.97	0.94	-7.41	0.7535
T580	-0.36	0.88	-2.78	0.2937
T600	-9.17	10.08	-15.95	0.2098

DE1-2A

Steps	X	Y	Z	M
NRM	0.38	3.76	-11.91	1.25
32.5	-16.93	-0.93	-1.36	17.01
49.4	-4.91	0.51	-0.09	49.4
66.6	-10.37	0.34	-0.15	103.8
83.6	-18.52	2.34	-0.45	186.7
168	-5.56	0.22	0.08	556.5
253	-8.15	1	-0.14	821.5
337	-9.41	0.59	0.16	942.8
504	-10.61	2.24	-0.11	1085
666	-11.3	0.6	0.06	1131
831	-11.56	0.41	0.25	1157
994	-11.84	-0.12	0.5	1185
1154	-11.64	-2.88	-0.45	1200

DE2-4A

Steps	X	Y	Z	M
NRM	-4.18	7.98	-14.59	1.714
32.5	-19.58	-0.28	-4.31	20.05
49.4	-5.95	-0.28	-1.06	60.55
66.6	-12.54	-0.28	-2.13	127.2
83.6	-2	0.31	-0.42	207.1
168	-6.33	0.06	-0.87	639.4
253	-8.86	-0.28	-1.3	895.4
337	-10.39	0.42	-1.5	1050
504	-11.46	1.08	-1.49	1160
666	-11.93	1.3	-1.68	1212
831	-12.1	1.52	-1.61	1230
994	-12.17	-1.3	-1.59	1235
1154	-10.33	1.33	-0.67	1240

DE3-1A

Steps	X	Y	Z	M
0	13.57	4.8	-2.58	0.1462
32.5	-19.13	0.73	-1.41	19.19
49.4	-3.39	0.07	-0.58	34.38
66.6	-5.3	0.07	-0.39	53.11
83.6	-6.4	0.56	-0.41	64.38
168	-11.4	0.5	-0.85	114.5
253	-13.68	-0.09	-0.7	137
337	-15.06	-0.46	-0.83	150.9
504	-15.82	0.05	-0.78	158.4
666	-15.91	0.92	-1.08	159.7
831	-16.06	0.45	-0.92	160.9
994	-16.42	1.61	-0.41	165
1154	-16.36	1.05	-0.76	164.1

SA2-2A

Steps	X	Y	Z	M
NRM	-0.61	-4.33	0.73	0.4432
32.5	-2.45	-0.67	-0.19	2.547
49.4	-9.05	-0.31	-0.86	9.094
66.6	-2.46	0.01	-0.22	24.68
83.6	-4.07	0.05	-0.37	40.89
168	-19.25	0.83	-1.78	193.5
253	-3.96	0.43	-0.34	399.9
337	-4.85	0.34	-0.38	487.4
504	-6.22	0.72	-0.51	628.1
666	-6.75	0.54	-0.55	679
831	-6.9	1.27	-0.58	704.4
994	-7.22	1.16	-0.47	732.5
1154	-7.27	1.06	-0.61	737.4

SA2-3A

Steps	X	Y	Z	M
0	-1.82	-4.55	-0.35	0.4915
32.5	-2.61	-0.7	-0.45	2.736
49.4	-8.92	1.17	-1.19	9.073
66.6	-2.08	-0.01	-0.28	21.01
83.6	-3.86	0.36	-0.5	39.04
168	-18.1	1.97	-2.23	183.4
253	-3.36	0.09	-0.38	338.6
337	-4.64	-0.37	-0.52	468.4
504	-5.85	1.19	-0.62	600
666	-6.33	0.99	-0.75	645.5
831	-6.65	0.6	-0.65	670.6
994	-6.67	0.42	-0.67	671.7
1154	-6.94	0.23	-0.85	700

SA3-1A

Steps	X	Y	Z	M
0	-0.43	-2.5	3.24	0.4113
32.5	-8.91	1.27	-0.28	9.001
49.4	-2.93	-0.17	-0.2	29.37
66.6	-5.82	0.41	-0.5	58.53
83.6	-8.85	-0.23	-0.58	88.69
168	-2.16	0.17	-0.15	217.2
253	-2.79	-0.39	-0.17	282.3
337	-3.24	0.18	-0.28	325.8
504	-3.35	0.19	-0.18	336
666	-3.75	-0.02	-0.34	376.2
831	-3.82	-0.01	-0.29	383.4
994	-3.92	0.05	-0.28	393.5
1154	-3.93	0.38	-0.33	395.9

SS1-6A

Steps	X	Y	Z	M
0	-0.36	4.15	7.37	0.8463
32.5	-7.42	-0.39	-0.11	7.428
49.4	-2.47	-0.36	-0.19	25.08
66.6	-4.03	-0.46	-0.3	40.65
83.6	-6.71	-0.44	-0.45	67.43
168	-18.85	-1.68	-1.6	189.9
253	-2.74	0.13	-0.16	274.7
337	-3.32	0.14	-0.23	332.7
504	-3.87	0.2	-0.25	388.8
666	-4.1	-0.23	-0.32	411.4
831	-4.22	-0.33	-0.32	424.6
994	-4.36	-0.7	-0.23	442.2
1154	-4.3	-0.91	-0.35	443.8

SS2-7A

Steps	X	Y	Z	M
0	-2.94	11.82	-4.02	1.283
32.5	-9.49	1.63	-1.65	9.766
49.4	-2.39	0.08	-0.4	24.28
66.6	-4.5	0.17	-1.08	46.32
83.6	-6.63	0.18	-0.96	67.03
168	-19.75	0.83	-2.37	199.1
253	-2.64	0.24	-0.31	266.5
337	-3.11	-0.16	-0.36	313.1
504	-3.49	0.09	-0.4	351.3
666	-3.67	0.22	-0.48	370.6
831	-3.78	0.18	-0.42	380.9
994	-3.91	-0.13	-0.39	393.6
1154	-3.94	0.08	-0.45	396.5

SS3-5A

Steps	X	Y	Z	M
NRM	-0.15	5.95	0.75	0.5994
32.5	-14.67	0.81	-1.07	14.73
49.4	-4.12	-0.69	-0.42	41.97
66.6	-6.25	-1	-0.66	63.6
83.6	-11.13	-1.49	-1.22	113
168	-2.42	0.23	-0.25	243.9
253	-3.3	-0.5	-0.38	336.2
337	-3.82	-0.43	-0.37	385.8
504	-4.27	-0.1	-0.43	0.4288
666	-4.45	0.01	-0.42	0.4469
831	-4.52	0.21	-0.39	0.4545
994	-4.58	-0.09	-0.44	0.4605
1154	-4.53	-0.91	-0.49	464.5

DE1-2A

Steps	X	Y	Z	M
NRM	-11.84	-0.12	0.5	1185
T120	-11	-2.93	-0.45	1139
T200	-10.11	-2.09	-0.42	1034
T250	-9.53	-2.29	-0.44	981.1
T300	-8.96	-1.95	-0.4	918.3
T350	-8.18	-1.49	-0.36	831.9
T400	-7.62	-1.26	-0.4	773
T430	-6.71	-0.89	-0.21	677.1
T460	-6.07	-1.11	-0.29	617.3
T520	-4.95	-0.92	-0.22	504.3
T540	-4.42	-0.98	-0.25	453
T560	-4.04	-0.81	-0.21	412.7
T580	-3.25	-0.62	-0.13	330.9
T600	-8.43	-1.45	-0.44	85.69
T620	-19.26	-4.62	-0.52	19.81
T640	-8.29	-1.82	-0.38	8.495

DE2-4A

Steps	X	Y	Z	M
NRM	-12.17	-1.3	-1.59	1235
T120	-11.64	1.41	-1.48	1182
T200	-10.72	1.02	-1.39	1086
T250	-9.91	1.8	-1.32	1016
T300	-9.64	1.61	-1.37	986.5
T350	-8.83	1.78	-1	906.3
T400	-7.96	1.43	-1.03	815.7
T430	-7.38	1.62	-0.86	760.3
T460	-7.07	1.13	-0.97	722.7
T520	-5.58	1.16	-0.76	574.9
T540	-5.14	0.79	-0.68	524.4
T560	-3.67	0.5	-0.49	373.5
T580	-15.73	2.41	-2.19	160.6
T600	-14.53	2.51	-1.96	148.7
T620	-8.06	0.88	-1.02	8.17
T640	-7.5	1.15	-1	7.654

DE3-1A

Steps	X	Y	Z	M
NRM	-16.42	1.61	-0.41	165
T120	-11.42	0.64	-0.55	114.5
T200	-9	0.29	-0.54	90.24
T250	-7.33	0.43	-0.48	73.62
T300	-6.47	0.5	-0.38	64.96
T350	-5.29	0.05	-0.33	53.02
T400	-4.55	0.4	-0.28	45.81
T430	-4.04	0.03	-0.19	40.47
T460	-3.14	0.25	-0.16	31.53
T520	-16.16	2.46	-0.35	16.35
T540	-10.14	-0.09	-0.79	10.17
T560	-5.29	-0.31	-0.42	5.311
T580	-3.27	0.95	-0.11	3.406
T600	-2.1	-0.3	-0.18	2.129
T620	-13.49	-1.88	4.11	0.1423
T640	-10.94	6.14	-3.86	0.1313

SA2-2A

Steps	X	Y	Z	M
NRM	-7.22	1.16	-0.47	732.5
T120	-6.68	0.68	-0.66	674.9
T200	-5.79	0.83	-0.51	587.4
T250	-5.2	0.8	-0.5	528.8
T300	-4.91	0.8	-0.44	499.5
T350	-4.07	0.47	-0.39	411.9
T400	-3.46	0.41	-0.33	350
T430	-3.07	0.31	-0.28	309.4
T460	-2.77	0.37	-0.28	280.4
T520	-2.14	0.31	-0.21	217.2
T540	-2.03	0.26	-0.19	205.2
T560	-18.83	2.9	-1.87	191.4
T580	-16.55	2.36	-1.59	167.9
T600	-5.61	0.47	-0.51	56.48
T620	-2.91	0.43	-0.29	29.58
T640	-17.65	2.72	-1.92	17.97

SA2-3

Steps	X	Y	Z	M
NRM	-6.67	0.42	-0.67	671.7
T120	-6.3	0.5	-0.86	637.8
T200	-5.49	0.37	-0.7	554.6
T250	-5.06	0.06	-0.69	510.4
T300	-4.53	0.17	-0.64	458.1
T350	-3.73	0.2	-0.48	376.2
T400	-3.06	0.07	-0.45	308.9
T430	-2.79	0.04	-0.4	281.6
T460	-2.67	0.16	-0.41	270.8
T520	-2.18	0.08	-0.3	219.8
T540	-18.06	0.23	-2.52	182.4
T560	-16.33	0.24	-2.21	164.8
T580	-11.66	0.44	-1.77	118
T600	-10.55	0.51	-1.48	106.6
T620	-14.08	0.46	-2.05	14.24
T640	-11.79	0.68	-1.73	11.93

SA3-1A

Steps	X	Y	Z	M
NRM	-3.92	0.05	-0.28	393.5
T120	-3.61	0.18	-0.33	363.2
T200	-3.26	0.04	-0.31	327.4
T250	-3.03	-0.08	-0.31	304.3
T300	-2.72	0.31	-0.23	274.3
T350	-2.32	0.25	-0.19	234
T400	-19.09	1.5	-1.58	192.1
T430	-17.17	1.18	-1.71	172.9
T460	-14.73	1.05	-1.5	148.4
T520	-11.62	1.28	-1.04	117.4
T540	-10.88	0.85	-1.09	109.7
T560	-7.42	0.64	-0.8	74.86
T580	-6.92	0.38	-0.7	69.65
T600	-2.15	0.24	-0.14	21.65
T620	-5.58	0.13	-0.59	5.616
T640	-2.25	0.06	-0.25	2.267

SS1-6A

Steps	X	Y	Z	M
NRM	-4.36	-0.7	-0.23	442.2
T120	-3.88	-0.63	-0.37	395
T200	-3.26	-0.56	-0.33	332.4
T250	-2.83	-0.57	-0.29	289.9
T300	-2.5	-0.51	-0.24	255.9
T350	-19.29	-4.58	-2.01	199.3
T400	-15.54	-3.39	-1.61	159.9
T430	-14.09	-3.17	-1.55	145.3
T460	-12.77	-2.94	-1.43	131.8
T520	-9.39	-1.56	-0.97	95.71
T540	-8.71	-1.96	-0.97	89.76
T560	-6.49	-1.35	-0.77	66.75
T580	-5.35	-0.96	-0.53	54.56
T600	-2.75	-0.43	-0.33	28
T620	-2.44	-0.4	-0.23	2.482
T640	-2.23	-0.27	-0.24	2.259

SS2-7A

Steps	X	Y	Z	M
NRM	-3.91	-0.13	-0.39	393.6
T120	-3.48	0.12	-0.43	350.5
T200	-2.98	0.17	-0.38	301.3
T250	-2.62	0.11	-0.34	264.6
T300	-2.4	0.1	-0.3	242
T350	-2.04	0.18	-0.27	206.9
T400	-17.73	1.41	-2.32	179.4
T430	-16.09	1.22	-2.29	163
T460	-14.38	1.33	-2.08	145.9
T520	-9.91	0.91	-1.57	100.8
T540	-8.17	0.62	-1.24	82.91
T560	-7.8	0.49	-1.19	79.02
T580	-4.72	0.36	-0.7	47.89
T600	0	-1.1	-0.22	11.21
T620	-2.97	0.24	-0.28	2.994
T640	-13.08	1.76	-1.68	1.33

	SS3– 5A			
Steps	X	Y	Z	M
NRM	-4.58	-0.09	-0.44	460.5
T120	-4.19	-0.68	-0.45	427.2
T200	-3.9	-0.65	-0.42	398.1
T250	-3.6	-0.65	-0.42	368.6
T300	-3.38	-0.56	-0.33	344.6
T350	-3.06	-0.59	-0.31	312.9
T400	-2.78	-0.55	-0.27	284.8
T430	-2.61	-0.38	-0.26	265.1
T460	-2.35	-0.28	-0.23	237.8
T520	-17.83	-3.35	-1.74	182.2
T540	-12.22	-2.45	-1.31	125.3
T560	-8.41	-1.53	-0.81	85.82
T580	-4.09	-0.85	-0.45	41.98
T600	-13.58	-3.59	-1.25	14.1
T620	-7.43	-1.73	-0.69	7.662
T640	-5.58	-1.18	-0.63	5.733

Appendix 3, Structural data for stereographic projection

Strike (degree)	Dip amount (degree)	Dip direction
315	45	NE
310	50	NE
317	43	NE
285	15	NE
280	10	SW
300	30	SW
305	50	SW
290	20	SW
155	65	SW
156	64	SW
305	35	SW
220	50	NE
310	50	NE
278	8	NE
286	16	NE
296	26	NE
283	13	SW
292	22	SW
240	30	SE
287	17	SW
296	26	SW
289	19	SW
302	32	NE
307	37	NE
290	20	NE
318	42	SW

ACKNOWLEDGEMENT

I grateful to my advisor, Prof. Tesfaye Kidane, for a clear and precise training in the field

Sampling, sample treatment and data analysis back in the laboratory as well as data interpretation and for his continuous support passing throughout the study.

I am also grateful to my co-advisor Dr. Ameha Atnafu for training in the field sampling, collecting samples, sample treatment and other activities.

I thank Addis Ababa University, School of Earth Science for funding part of this work and for letting me use the facility of paleomagnetic laboratory for free.

I thank the Afar Consortium security without them the fieldwork was impossible.

I would like to thank Dr. Balemal Atnafu, Dr. Beniyam Tesfaw, Ato Yemane, Ato Hale Yesus and all staff members of School of Earth Science for providing the necessary materials for this study.

I am very much grateful to my family; Dad, Mom, Wetet and Melkam whenever I need you.